

A Thesis Submitted for the Degree of PhD at the University of Warwick

Permanent WRAP URL:

<http://wrap.warwick.ac.uk/78770>

Copyright and reuse:

This thesis is made available online and is protected by original copyright.

Please scroll down to view the document itself.

Please refer to the repository record for this item for information to help you to cite it.

Our policy information is available from the repository home page.

For more information, please contact the WRAP Team at: wrap@warwick.ac.uk

**INVESTIGATIONS OF OPTICALLY
ACTIVE POLYMERIC CHIRAL
STATIONARY PHASES**

by

Elizabeth Jane Kelly

A thesis submitted in partial fulfilment of the
requirements for the degree of Doctor of Philosophy
at the University of Warwick

Department of Chemistry,
University of Warwick.

October 1997

IMAGING SERVICES NORTH

Boston Spa, Wetherby
West Yorkshire, LS23 7BQ
www.bl.uk

**MISSING PAGES ARE
UNAVAILABLE**

CONTENTS

	Page
ACKNOWLEDGEMENTS	1
DECLARATION	2
SUMMARY	3
ABBREVIATIONS	4
CHAPTER 1 INTRODUCTION	8
1.0 IMPLICATION OF CHIRALITY	9
1.0.1 Measuring enantiomeric purity	11
1.0.2 The Theory of Chromatography	14
1.1 EQUATIONS USED TO DESCRIBE CHROMATOGRAPHY	16
1.2 HIGH PERFORMANCE LIQUID CHROMATOGRAPHY	19
1.2.1 The modern HPLC system	20
1.2.2 Silica as a stationary phase	20
1.3 POROUS GRAPHITIC CARBON AS A STATIONARY PHASE	22
1.3.1 Method of production	23
1.3.2 Characterisation of PGC	23
1.4 CHIRAL SEPARATIONS IN HPLC	26
1.4.1 Chiral Stationary Phases (CSP) for HPLC	27
1.4.2 Synthetic polymers as chiral stationary phases	33
1.4.3 Bound protein phases	35
1.5 POLYSACCHARIDES AND THEIR USE IN CSP	36
1.5.1 Polysaccharide phenylcarbamates	38
1.5.2 Use of porous graphitic carbon in liquid chromatography	42

1.5.3	Solvent considerations	44
1.6	SUMMARY	45
CHAPTER 2	APPLICATION OF POROUS GRAPHITIC CARBON (PGC) AS A SUPPORT FOR CELLULOSE TRIS (3,5-DIMETHYLPHENYL CARBAMATE)	47
2.0.1	Optimum cellulose type	47
2.1	OPTIMUM LOADING OF CDMPC ON PGC	52
2.1.1	Optimum coating method	52
2.1.2	Interpretation of Results from Figure 2.1.1	54
2.1.3	Investigation of the surface character of Column 1 and Column 2 phases by laser light scattering	56
2.1.4	Investigation of surface character of Column 1 and Column 2 phases by scanning electron microscopy (SEM)	57
2.2	THE USE OF ACIDIC AND BASIC MOBILE PHASE ADDITIVES	60
2.2.1	Acidic mobile phase additives	61
2.2.2	Effect of TFA on peak widths, retention and resolution	61
2.2.3	The effect of changing concentration of DEA on column performance	64
2.3	PROBLEM COMPOUNDS ON PGC	68
2.4	CONCLUSIONS	70
CHAPTER 3	THE SYNTHESIS OF POLY-L-LEUCINE AND ITS ANALYSIS BY MALDI-TOF AND ESI MASS SPECTROMETRY	72
3.1	THE LITERATURE REVIEW OF POLY-AMINO ACIDS AND THEIR APPLICATION TO ENANTIOMERIC ORGANIC SYNTHESIS	76
3.2	THE EFFECTS OF STRUCTURAL VARIATIONS IN POLYPEPTIDE CATALYSTS	78

3.3	APPLICATION OF THE WORK OF JULIA AND COLONNA INDUSTRIAL PROCESSES	80
3.4	SYNTHESIS OF POLY-L-LEUCINE	83
3.4.1	Initiation by water	84
3.4.2	Initiation by amine	85
3.4.3	Synthesis of poly-L-leucine from L-leucine	86
3.4.4	Problems with the analysis of Poly-L-leucine	88
3.5	ANALYSIS OF POLY-L-LEUCINE BY MALDI-TOF AND ESI MASS SPECTROMETRY	89
3.5.1	MALDI-TOF Mass Spectrometry	89
3.5.2	Sample preparation	91
3.6	ANALYSIS OF POLY-L-LEUCINE BY MALDI-TOF MASS SPECTROMETRY	93
3.7	ANALYSIS USING ELECTROSPRAY IONISATION MASS SPECTROMETRY (ESI)	99
3.8	CONCLUSIONS	102
	CHAPTER 4 CHARACTERISATION OF STRUCTURAL CONFORMATION AND CONTROL OF MOLECULAR WEIGHT PROFILE OF POLY-L-LEUCINE	103
4.1	SOLID PHASE PEPTIDE SYNTHESIS (SPPS)	104
4.1.1	Protection chemistry	106
4.1.2	Polymeric Support	107
4.1.2	Coupling procedure	109
4.2	THE SYNTHESIS OF POLY-L-LEU ₁₅	114
4.2.1	Analysis of H.Leu ₁₅ .OH synthesised by coupling of penta-peptide	115

4.2.2	Analysis of sequential synthesis by MALDI-TOF	116
4.3	CHARACTERISATION OF THE STRUCTURAL CONFORMATION OF POLY-L-LEUCINE	116
4.3.1	α -helical secondary structure of poly-L-leucine	117
4.3.2	The structure of leucine and its implication for the helix propensity	119
4.3.3	Implication of the polymeric structure	119
4.4	ANALYSING THE SECONDARY STRUCTURE OF POLY-L-LEUCINE	120
4.4.1	Circular dichroism of H.Leu ₁₅ .OH	120
4.4.2	X-ray powder diffraction of poly-L-leucine	121
4.5	CONTROL OF MOLECULAR WEIGHT PROFILE OF POLY-L-LEUCINE	123
4.6	MEASUREMENT OF MOLECULAR WEIGHT PROFILE OF POLY-L-LEUCINE	124
4.6.1	Viscometry	125
4.7	CONCLUSIONS	127
CHAPTER 5	THE APPLICATION OF POLY-L-LEUCINE TO CHIRAL HPLC	128
5.0	APPLICATION OF POLY-L-LEUCINE TO CHIRAL LIQUID CHROMATOGRAPHY OF DIPEPTIDES	128
5.1	CHOICE OF ANALYTES	129
5.2	PREPARATION OF PGC COATED WITH POLY-L-LEUCINE	131
5.2.1	Optimum coating level of PGC coated with poly-L-leucine phases	131
5.3	ORDER OF ELUTION DISPLAYED BY POLY-L-LEUCINE PHASES	132

5.4	COMPARISON OF POLY-L-LEUCINE TYPES	134
5.4.1	Unexpected separation of <i>trans</i> -stilbene oxide	135
5.4.2	Explanation of differences between Columns B and C	137
5.5	THE EFFECT OF MOLECULAR WEIGHT ON THE ENANTIOSELECTIVITY OF POLY-L-LEUCINE PHASES	137
5.5.1	The application of H.Leu ₁₅ .OH to chromatography	137
5.5.2	The application of a continuously extracted poly-L-leucine to chromatography	138
5.6	PRODUCTION OF OPTIMUM COLUMN	139
5.6.1	Separation of <i>bis</i> -phenyl-oxiranyl methanone	141
5.7	UNSUCCESSFUL CHROMATOGRAPHY	143
5.8	PROPOSED MECHANISM OF ENANTIORECOGNITION OF POLY-L-LEUCINE	144
5.9	CONCLUSIONS	146
CHAPTER 6	EXPERIMENTAL	148
6.0	SOLVENTS AND CHEMICALS	148
6.1	SYNTHESIS OF CDMPC	149
6.2	ELEMENTAL ANALYSIS	150
6.3	PREPARATION OF CDMPC-COATED PHASES	151
6.3.1	Preparation of CDMPC-coated APS phase	152
6.3.2	Preparation of CDMPC-coated PGC phases	152
6.3.3	Packing procedure	152
6.4	GEL PERMEATION CHROMATOGRAPHY (GPC)	153
6.5	DETERMINATION OF PARTICLE SIZE	154

6.6	CHROMATOGRAPHIC EVALUATION OF CDMPC-COATED PHASES	155
6.7	SYNTHESIS OF POLY-L-LEUCINE	155
6.7.1	Synthesis of <i>N</i> -carboxy anhydride L-leucine (NCA L-leucine)	156
6.7.2	Polymerisation of L-leucine NCA using the humidity cabinet	156
6.7.3	Polymerisation of L-leucine NCA <i>via</i> amine initiation	157
6.7.4	Polymerisation of L-leucine	157
6.7.5	Continuous extraction of poly-L-leucine	158
6.8	SOLID PHASE SYNTHESIS OF H.LEU ₁₅ .OH	158
6.8.1	Functionalisation of the resin	159
6.8.2	Washing procedure	159
6.8.3	Equipment used in SPPS	160
6.8.4	Ultra-violet monitoring of Fmoc residue	161
6.8.5	Loading profile of sequential SPPS of H.Leu ₁₅ .OH	162
6.8.6	Deprotection of tethered peptide to produce free amine residue	163
6.8.7	Kaiser test	163
6.8.8	Standard coupling step	163
6.8.9	Problem coupling steps	164
6.8.10	Cleavage of the peptide from the resin	165
6.9	SYNTHESIS OF H.LEU ₁₅ .OH USING PENTA-PEPTIDE COUPLING	166
6.9.1	Synthesis of penta-peptide	166
6.9.2	Cleavage of the penta-peptide from the resin	166

6.9.3	Thin layer chromatography (TLC) of Fmoc.leu ₅ .OH	167
6.9.4	Analysis of Fmoc.leu ₅ .OH by reversed-phase HPLC	167
6.9.5	Coupling of penta-peptides	168
6.9.6	Fmoc assay of block coupling synthesis of H.Leu ₁₅ .OH	169
6.6.7	Preparation of H.Leu ₁₅ .OH from the resin	169
6.6.8	Circular dichroism	169
6.7	PREPARATION OF POLY-L-LEUCINE COATED PGC	170
6.7.1	Microanalysis of PGC-Poly-L-leucine phases	171
6.7.2	Synthesis of racemic epoxides	172
6.7.3	Synthesis of bis-(3-phenyl-oxiranyl)-methanone	173

List of Figures

		Page
Figure 1.0	The enantiomers of thalidomide	10
Figure 1.0.1	Typical chiral shift reagent	13
Figure 1.0.2	Injection of sample into chromatographic system	14
Figure 1.0.3	Separation of a mixture	15
Figure 1.1	Typical chromatogram of 2 analytes	16
Figure 1.2.1	Diagram of a HPLC system	20
Figure 1.2.2	Surface functionality of silica	21
Figure 1.3.2	Porous structure of PGC	24
Figure 1.3.3	2-dimensional structure of graphitic - PGC	25
Figure 1.4.0	The three point interaction rule	28
Figure 1.4.1	tetranitrol-9-fluorenylideneaminoxypropionic acid, TAPA	29
Figure 1.4.2	Early Pirkle phases	31
Figure 1.4.3	Chiral stationary phases based on bound cyclodextrin	33
Figure 1.4.3	Poly(triphenylmethyl methacrylate)	34
Figure 1.4.4	Helical structure forced by the presence of the triphenyl group	34
Figure 1.4.5	<i>trans</i> -Stilbene oxide	35
Figure 1.5.0	Cellulose	36
Figure 1.5.1	Cellulose tris(phenylcarbamate) derivatives	39
Figure 1.5.2	Interaction of analyte with the urethane linkage in carbamate group	39
Figure 1.5.3	Commercially available chiral stationary phases produces by Daicel	40

Figure 1.5.4	Chiral selector and anchor group	43
Figure 2.0.2	Comparison of separation of benzoin methyl ether	49
Figure 2.0.3	Comparison of separations of alprenolol	49
Figure 2.0.4	Comparison of separations of 2-phenoxy propionic acid	50
Figure 2.1.3	A schematic of laser light scattering particle size instrument	56
Figure 2.1.5	SEM of batch coated particles	59
Figure 2.1.6	SEM of single-step coated particles	59
Figure 2.2.2	The effect of TFA on capacity factors	62
Figure 2.2.3	The effect of TFA on peak width	63
Figure 2.2.4	The effect of TFA on α value	64
Figure 2.3.0	The effect of changing the concentration of DEA on k_{average} and α	65
Figure 2.3.1	Separation of Flavanone enantiomers on PGC and silica based phases	68
Figure 2.3.2	Problem compounds on PGC	69
Figure 3.0.1	Chiral ligand exchange combinations	73
Figure 3.0.2	Enantioselective synthesis followed by kinetic resolution	74
Figure 3.0.3	Titanium complex implicated in Katsuki-Sharpless epoxidation	74
Figure 3.1.0	Relationship of secondary structure to optical isomer produced	76
Figure 3.1.1	Asymmetric epoxidation of chalcone in a triphase system with poly-S-alanine	77
Figure 3.1.2	Structural variation of analyte	77
Figure 3.1.3	Unsuccessful analytes	78
Figure 3.2.0	Structural variation in polypeptide catalyst	79
Figure 3.2.1	Random copolymer polypeptide catalysts	80

Figure 3.3.1	Leukotriene antagonist, SK & F 104353	81
Figure 3.3.2	Step 2 in synthesis of SK & F 104353	82
Figure 3.3.3	Unexpected synthesis	82
Figure 3.4.0	Synthesis of L-leucine-N-carboxy anhydride	83
Figure 3.4.1	Homopolymerisation of L-leucine-NCA in a humidity cabinet	84
Figure 3.4.2	Free peptide synthesised by water initiation	85
Figure 3.4.3	Ethylenediamine initiated polymerisation of L-leucine NCA	86
Figure 3.4.4	Proposed active species in polymerisation on L-leucine	87
Figure 3.4.5	Proposed mechanism of initiation by complex in Figure 3.4.4	87
Figure 3.5.1	Schematic of Kratos III MALDI-TOF	91
Figure 3.5.2	α -cyano-4-hydroxy cinnamic acid (ACCA)	92
Figure 3.5.3	Dihydroxybenzoic acid(DHB)	92
Figure 3.6.1	Poly-L-leucine from L-leucine NCA (Water initiation)	94
Figure 3.6.2	MALDI-TOF of amine initiated poly-L-leucine	95
Figure 3.6.3	Proposed termination mechanism of amine initiated polymerisation of L-leucine NCA	96
Figure 3.6.4	Proposed structure of amine-initiated poly-L-leucine	96
Figure 3.6.5	MALDI-TOF of poly-L-leucine synthesised from L-leucine using triphenyl phosphite and N-methyl pyrrolidine	97
Figure 3.7.0	Schematic of the “Quattro II” electrospray source	100
Figure 3.7.1	ESI mass spectrum of amine initiated poly-L-leucine	101

Figure 4.1.0	Schematic of stepwise solid-phase peptide synthesis of linear peptides	106
Figure 4.1.0	N ^α -9-fluorenylmethoxycarbonyl (Fmoc) protecting group	107
Figure 4.1.1	Barlos resin	108
Figure 4.1.2	Active ester coupling reagents	109
Figure 4.1.3	Formation of the active ester using HOBt	110
Figure 4.1.4	Kaiser test	112
Figure 4.1.5	UV assay of Fmoc protecting group	113
Figure 4.1.6	Formula to determine loading in sequential SPPS	114
Figure 4.2.1	ESI mass spectrum of H.Leu ₅ .OH	115
Figure 4.2.2	ESI mass spectrum of H.Leu ₁₅ .OH synthesised by penta-peptide coupling	115
Figure 4.2.3	MALDI-TOF of sequential synthesis of Fmoc.Leu ₁₅ .OH	116
Figure 4.4.1	CD of H.Leu ₁₅ .OH	120
Figure 4.4.3	Amine initiated poly-L-leucine	122
Figure 4.4.4	Poly-L-leucine from humidity cabinet	122
Figure 4.5	MALDI-TOF showing poly-L-leucine before and after continuous extraction	124
Figure 5.1.1	Chalcone- α,β -epoxide on blank PGC	130
Figure 5.1.2	Chalcone- α,β -epoxide on poly-L-leucine coated PGC	130
Figure 5.1.3	Chalcone- α,β -epoxide	131
Figure 5.3.2	Cyanine dye NK-2012	133
Figure 5.4.1	<i>trans</i> -Stilbene oxide	136
Figure 5.4.2	Comparison of different poly-L-leucine samples using <i>trans</i> -stilbene oxide	136

Figure 5.6.2	Mixture of enantiomers	141
Figure 5.6.3	Resolution of <i>bis</i> -phenyl-oxiranyl methanone on column E	142
Figure 5.6.4	Assignment of peaks in the resolution of <i>bis</i> -phenyl-oxiranyl methanone	143
Figure 6.8.3	Glassware used in SPPS	161
Figure 6.6.4	Schematic describing gradient elution for Fmoc.leu ₅ .OH	168
Figure 6.6.6	Fmoc assay of block coupling synthesis of H.Leu ₅ .OH	169

LIST OF TABLES

Table 1.3.0	Comparison of carbon type phases	22
Table 2.0	SEC data for Avicel and Sigmacel derivatives	48
Table 2.0.1	SEC analysis of Sigmacel Type 101	51
Table 2.1	Comparison of batch and single step coating methods	53
Table 2.1.1	Plate Height results for Columns 1 and 2	55
Table 2.1.4	Comparison of single-step and batch methods of coating by laser light scattering	57
Table 2.2	The effect of TFA on the chromatographic behaviour of acidic analytes	61
Table 2.3.1	The effect of DEA concentration on retention and resolution characteristics	66
Table 3.6.5	MALDI-TOF characteristics of amine initiated poly-L-leucine	97
Table 3.6.7	Multiple series observed in Figure 3.5.8	98
Table 4.3.1	Helix propensity (<i>s</i> values) values for several amino acids	118
Table 5.2.1	Coating level of poly-L-leucine on PGC	131
Table 5.3.1	Isomers used to test order of elution.	132
Table 5.4.0	Comparison of different poly-L-leucine samples	135

Table 5.5.2	Continuous extraction polymer column - column E	136
Table 5.6.1	Successful chromatography on 250mm column	140
Table 5.7.1	Unsuccessful analytes for poly-L-leucine column F	141
Table 6.1	Yields of the synthesis of CDMPC	150
Table 6.2	C, H and N results for CDMPC	150
Table 6.3	Quantities used for the preparation of CDMPC phases	152
Table 6.4	Results from laser light scattering	154
Table 6.8.2	Standard washing procedure	160
Table 6.8.4	UV monitor for Fmoc residue	161

LIST OF EQUATIONS

Equation 1.0	Calculation of capacity factors	17
Equation 1.1	Calculation of separation factor, α .	17
Equation 1.2	Calculation of Resolution, R_s .	18
Equation 1.3	Calculation of Plate number, N	18
Equation 1.4	Calculation of Plate height, H	19
Equation 4.4.1	Relative viscometry, η_{rel}	126
Equation 4.4.2	Specific viscometry, η_{sp}	127
Equation 4.4.3	Reduced viscometry, η_{red} .	127
Equation 6.8.4.1	Assay of Fmoc derivatisation	164

LIST OF GRAPHS

Graph 4.6	Reduced viscosity of Poly-L-leucine samples	127
Graph 6.2.1	Conversion of cellulose by 3,5-dimethyl phenyl isocyanate	153

ACKNOWLEDGEMENTS

I would like to thank the following people and institutions for their help with
the work discussed within this thesis

Professor David Crout and Dr David Haddleton
for their supervision and continued encouragement

**

Professor Stephen Matlin
for giving me the initial opportunity to pursue this research

**

Dr Sally Grieb
for her continued help, ideas and valued friendship

**

Mr Paul Ross, Hypersil
for his help and encouragement

**

Dr Brian Ridge and Miss Michelle Palmer
for their patience and dedication

**

The University of Warwick and Hypersil
for financial support

**

To Mum, Dad and Caz
for all your love and everything you do for me

**

To Al
for everything, especially letting me loose with Zippy and Patchy

**

To all my friends
for lots of laughs and good times throughout my time at Warwick

DECLARATION

The observations and recommendations described in this thesis are those of the author, except where acknowledgement has been made to results and ideas previously published. The work was undertaken at the Department of Chemistry, University of Warwick, between October 1st 1994 and September 30th 1997, and has not previously been submitted for a degree at any institution.

SUMMARY

This thesis describes the application of optically active helical polymers to chiral stationary phases for high performance liquid chromatography. The use of porous graphitic carbon as a support for these phases is examined and its implication for the nature of the separation.

In the first case 3,5-dimethylphenyl carbamate (CDMPC) was studied. This work continued the study by Grieb and Matlin. The use of porous graphitic carbon as a support for this polymer was examined. PGC is produced by Hypersil under the name Hypercarb. It is a porous carbon phase with virtually no surface functionalities. It was confirmed that a 25% w/w loading of CDMPC produced using a batch coating method produced the optimum phase. The nature of the cellulose used to synthesise the CDMPC was also studied by gel permeation chromatography. It was found that Avicel cellulose (Merck) gave the best results.

CDMPC has certain characteristics which make it an effective phase, these are; a) α -helical secondary structure and b) optical activity within the monomer unit. We decided to examine other polymers which possess these characteristics, in particular poly-L-leucine. It is believed that this polymer has an α -helical secondary structure and in its synthesis L-leucine is used as a single pure isomer. This polymer has been shown to be effective as an asymmetric organic catalyst.

Poly-L-leucine was synthesised using condensation polymerisation with three methods of initiation using both L-leucine and *N*-carboxy anhydride L-leucine as monomers. *N*-carboxy anhydride L-leucine was initiated by ethylenediamine in solution and water *via* a humidity cabinet. L-leucine was polymerised using triphenyl phosphite, lithium chloride and *N*-methyl pyrrolidine. Poly-L-leucine containing a maximum of fifteen residues was synthesised using solid phase peptide synthesis techniques.

These polymers were examined using MALDI-TOF and ESI mass spectrometry. The polymers synthesised from *N*-carboxy anhydride L-leucine were examined using viscometry. Comparing these results it was considered that the molecular weight of the water-initiated polymer was greater. This polymer was further modified by continuous extraction to remove lower molecular weight fragments. All of these polymers were coated onto the surface of PGC by evaporation. It was shown that a 20% w/w loading level was optimum for this type of phase. The optimum phase was found to be made from the water initiated polymer after continuous extraction.

This phase was shown to be capable of the resolution of a variety of racemic epoxides.

LIST OF ABBREVIATIONS

in alphabetical order

α	selectivity
Å	Angstrom
ACCA	α -cyano-4-hydroxy cinnamic acid
ALP	alpreneolol
APS	aminopropylated silica
BME	benzoin methyl ether
°C	degrees centigrade
CD	circular dichroism
CDMPC	cellulose tris(3,5-dimethylphenyl carbamate)
C, H and N	carbon, hydrogen and nitrogen (microanalysis)
CSA	chiral solvating agent
CSP	chiral stationary phase
CSR	chiral shift reagent
CTB	cellulose tribenzoate
CTPC	cellulose triphenyl carbamate
Da	Dalton mass units
DEA	diethylamine
DHB	2,5-dihydroxybenzoic acid
DIEA	diisopropylethyl amine
DMF	dimethylformamate

<i>et al.</i>	with co-workers
ESI-MS	electrospray ionisation mass spectrometry
FLAV	flavanone
g	gram
GC	gas chromatography
GPC	gel permeation chromatography
HAPyU	<i>O</i> -(7-aza-benzotriazole-1-yl)-1,1,3,-bis(tetramethylene) uronium hexafluorophosphate
HBTU	(1H-benzotriazole-1-yl)-1,1,3,-tetramethyluronium hexafluorophosphate
HCl	hydrochloric acid
HOBt	hydroxybenzotriazole
HPLC	high performance liquid chromatography
H.Leu _x .OH	peptide produced using solid phase peptide synthesis containing x number of leucine residues
i.d.	internal diameter
IR	infra-red
<i>k</i>	capacity factor
LC	liquid chromatography
MALDI-TOF-MS	matrix assisted laser ionisation/desorption time-of-flight mass spectrometry
μm	micrometers
m	metres
mm	millimetres

mmol	millimoles
MA	mandelic acid
MCTA	microcrystalline cellulose triacetate
mg	milligrams
MHz	mega-hertz
mL/min	millilitres per minute
M_n	number average molecular mass
M_p	melting point
M_w	weight average molecular mass
N	plate number
nm	nanometres
NMR	nuclear magnetic resonance
PA	phenethyl alcohol
PDI	polydispersity
PGC	porous graphitic carbon
psi.	pounds per square inch
R_s	resolution
SEM	scanning electron microscopy
t_0	retention time of unretained analyte or flow marker
TFA	trifluoroacetic acid
TLC	thin layer chromatography
TSO	<i>trans</i> -Stilbene oxide
UK	United Kingdom
UV	ultra-violet detection

v/v

volume for volume

% w/w

percentage weight for weight

L-ZGP

N-carboxybenzoylglycyl *L*-proline

CHAPTER 1

INTRODUCTION

“I call any geometrical figure or any group of points, *chiral*, and say it has *chirality*, if its image in a plane mirror, ideally realised, cannot be brought to coincide with itself.” LORD KELVIN 1893.

In making this definition of chirality Lord Kelvin was defining a natural phenomenon that is expressed at all levels of life. The most obvious example is our hands, the left and right hands being non-superimposable mirror images of one another. However, chirality exists not only on the macro level but also on the molecular level. It is this molecular chirality which is of particular interest and importance.¹⁻²

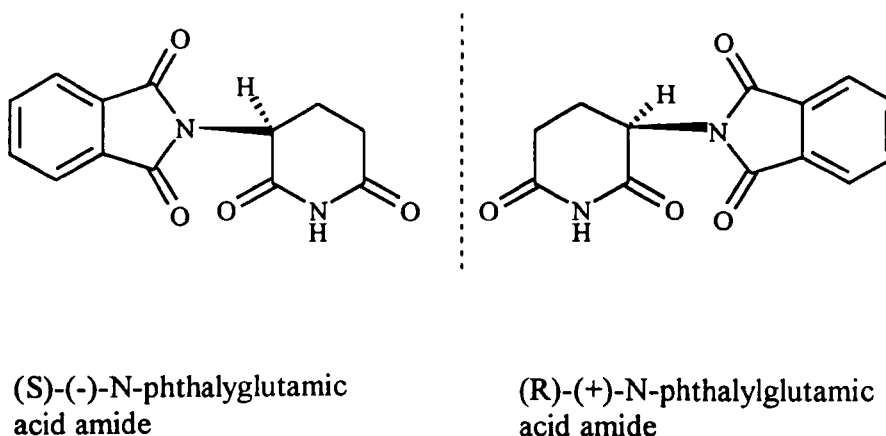
Chirality is a dominant factor in all biological structure and function.³⁻⁴ Therefore, if chirality is overlooked or misjudged the consequences may be disastrous. This was most visibly demonstrated through the thalidomide tragedy⁵ (Section 1.2). It is largely due to the adverse effects of thalidomide and the ever increasing

understanding of molecular structure and function, that the need to explore and control chirality and its implications has grown rapidly over recent years.

1.0 IMPLICATION OF CHIRALITY

Chirality plays a major part in all biosynthetic pathways and metabolism. This is generally termed biodiscrimination. Optical isomers have identical chemical and physical properties in a symmetrical environment. However, it is when a chiral compound interacts with an asymmetric environment that its chirality becomes a dominant factor. It is usual that *in vivo* only one isomer is tolerated. This has produced a largely chiral environment with many receptors relying on some level of chirality to function. One of the first descriptions of biodiscrimination was given in 1886 by Puitti.⁷ Puitti reported the isolation of dextrorotatory asparagine. When he compared its taste to that of the naturally occurring levorotatory asparagine he found the non-natural enantiomer to have a sweet taste while the natural enantiomer was tasteless. To the extent that stereoisomers such as asparagine interact with chiral receptors *in vivo*, biodiscrimination is a diastereomeric form of discrimination. There are many examples of enantiomers that display markedly differing behaviour.⁸ This was most tragically demonstrated in the 1960s with the use of the pharmaceutical agent, thalidomide (Fig. 1.0). Thalidomide, in its racemic form, was prescribed to expectant mothers as a sedative and anti-nausea preparation to ease the symptoms of morning sickness. In 1979 it was discovered that the (S)-(-) enantiomer was teratogenic. This caused serious abnormalities in the developing foetus which led in particular to characteristic malformation of the limbs.⁹ The use of thalidomide highlighted just how sensitive biological function is to chirality.

Figure 1.0 The enantiomers of thalidomide



Other examples of optical enantiomers which are therapeutically beneficial include (S)-(-)-3-(3,4-dihydroxyphenyl)-alanine which is commonly known as L-DOPA and is a naturally occurring neurotransmitter which has been found to be active in the treatment of Parkinson's disease.¹⁰ Morphine is widely used as a pain killer however, it is only the (-)-morphine enantiomer which possess this analgesic activity.¹¹ The active isomer is termed the eutomer while the inactive isomer is known as the distomer. The ratio between the eutomer and distomer, the eudismic ratio, is a measure of the stereoselectivity which exists in the biological system under examination.

Generally, four types of behaviour are observed for enantiomers which are biologically active and these have to be considered thoroughly in the pharmaceutical development of a compound,

- the desired effect is entirely due to one enantiomer and the other is entirely without activity
- the enantiomers have identical pharmacological activities

- the pharmacological activity of the enantiomers is qualitatively identical but quantitatively different
- the pharmacological activity of the enantiomers is both qualitatively and quantitatively different

The effect of chirality is prominent not only in the development of pharmaceuticals but also in agrochemicals and food and drink additives. In agrochemicals the synthesis of the single active isomer is more economical and minimises any toxic effects which might be exerted by the final product. As discussed previously it is known that many isomers possess different tastes or odours depending on their chirality. This is utilised by the food and drink industry as well as in perfumery. The (R)-isomer of aspartame, which is a low calorie sweetener marketed under the brand name Nutrasweet, is very sweet while the L,L-(-)-isomer is bitter.¹² Racemisation of the isomer therefore, is a problem as it will alter the flavour and aroma of the food or drink in which it is contained. A need exists, especially in the pharmaceutical industry, to have the ability to assess accurately the enantiomeric purity of a compound. The analysis of a mixture of enantiomers would provide valuable information on the ratio of the enantiomers present. This information is often needed before any purification or separation of the enantiomers can be attempted.

1.0.1 Measuring enantiomeric purity

A measure of optical purity can be obtained by following two distinct methodologies which involve the analysis of the intact mixture or the prior separation of the mixture into its constituent isomers.

Analysis of a mixture

Polarimetry uses one of the basic characteristics of optical isomers, that is the ability to rotate the plane of plane-polarised light. Plane-polarised light has one vibrational plane which contains two oppositely circularly polarised vectors.

When polarised light passes through a solution of the non-racemic mixture the two vectors interact differently with the chiral environment and this causes the plane of the light to rotate. The expression of this rotation for a sample of known concentration at known temperature is the measure of optical rotation. Optical rotation is qualified as being either levo (-) or dextro (+) rotatory depending on the direction of the rotation.

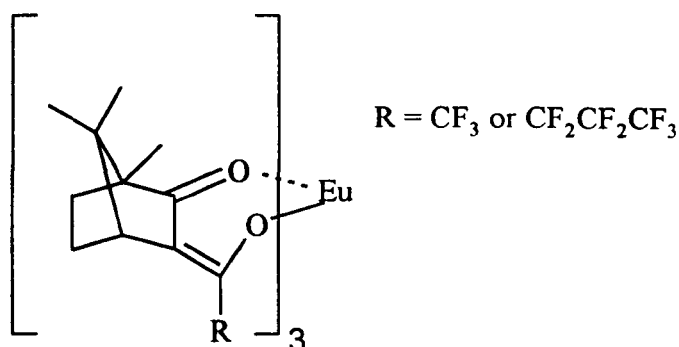
To quantify the optical purity of the sample a comparison is necessary between the sample and a standard of known optical purity, essentially a single optical isomer. This is often not readily available.

Nuclear Magnetic Resonance (NMR) can be used to identify differences between diastereomeric environments. The interaction therefore of the mixture of enantiomers with another isomer would produce a sample suitable for analysis by ^1H NMR. Burlingame and Pirkle¹³ synthesised a series of chiral trifluoromethyl aryl carbinols, which they described as chiral solvating agents (CSA). The complexation of an enantiomer by a CSA produces a change in the chemical shift of the observed resonances relative to that of its mirror image form. The size of this shift depends on the strength of the binding in the diastereomeric complex which is formed. Two signals for every resonance are therefore observed, one from each diastereomer. These signals can be integrated to give the ratio of enantiomers contained in the sample and therefore a measure of enantiomeric

purity. CSA do not have to be optically pure as this would only affect the size of the splitting and not the integration.

An alternative method for the analysis of optical isomers by NMR is to use a chiral shift reagent (CSR). CSR are based on optically active paramagnetic metal complexes, the metal centre is usually taken from the lanthanide series¹⁴ (Fig. 1.0.1).

Figure 1.0.1 Typical chiral shift reagent



A CSR reagent reversibly co-ordinates to both enantiomers and the influence of the local magnetic field of the metal ion spreads out the spectrum. The co-ordination of the CSR to the respective enantiomers differs due to the binding constants for the individual complexes. It is this difference in the binding constants which gives differing movement in the spectra of each enantiomer.

The shift in the resonances allows the signals to be integrated and to provide a ratio of the enantiomers contained in the original sample.

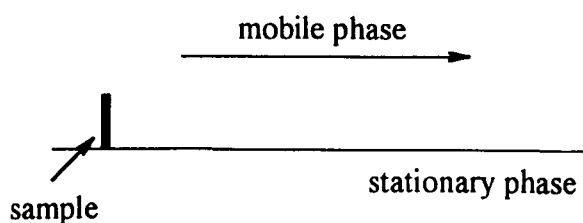
Methods involving separation

With the development of liquid chromatography by Mikhail Tswett in 1903 a subtle approach to the separation of a mixture into its component parts became available. Tswett¹⁵ was a botanist who studied natural plant pigments in particular. He demonstrated the separation of α and β carotene on an inulin column which was eluted by ligroin. However, as this work was originally published in Russian it was not widely read. This technique was reproduced in the 1930s by Kuhn and Lederer¹⁶, and it was this publication which began the wider study and use of liquid chromatography. Before undertaking a study on the application of liquid chromatography to the resolution of optical isomers it is worth discussing the theory of chromatography and the development of modern techniques, in particular high performance liquid chromatography.

1.0.2 The Theory of Chromatography

Chromatography requires two phases, a fluid mobile phase which is required to flow over the surface of a fixed stationary phase. The sample is introduced in to the mobile phase at one end of the system (Fig. 1.0.2).

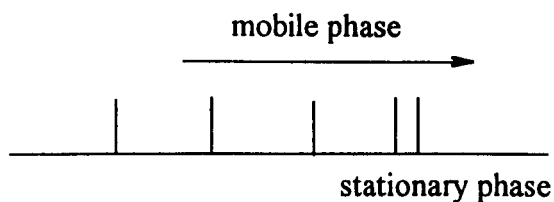
Figure 1.0.2 Injection of sample into chromatographic system



As the sample is carried along in the mobile phase it undergoes some form of interaction with the stationary phase. The nature of the interaction may be due to forces including van der Waals and polar interactions, the passage of the sample

relative to the mobile phase is therefore hindered. The sample therefore becomes distributed between the two phases in a dynamic equilibrium (Fig. 1.0.3). In size exclusion chromatography interaction with the stationary phase is not desirable and it is the mass transfer of the analyte within the porous structure of the stationary phase which determines separation.

Figure 1.0.3 Separation of a mixture



The strength of the interaction of the sample with the stationary phase depends on the physicochemical nature of the sample molecules. Chromatography occurs because different chemical entities display different distribution coefficients (K) between the two phases. The rate of migration of each entity therefore will be different, the mixture will become separated into bands which each travel through the system at different speeds. The fluid which carries the analyte can be either a liquid or a gas and although gas chromatography is an established and widely used technique, however it is liquid chromatography which is of particular interest to this thesis.

Twsett employed a polar packing material and a non-polar mobile phase. This combination is therefore known as normal phase chromatography. It is typified by the use of a silica stationary phase and a majority hexane with a small percentage alcohol mobile phase. When the polarities are reversed, reversed-phase chromatography is observed. The use of reversed-phase systems allows the

analyst to examine polar analytes which would not be available in normal phase.

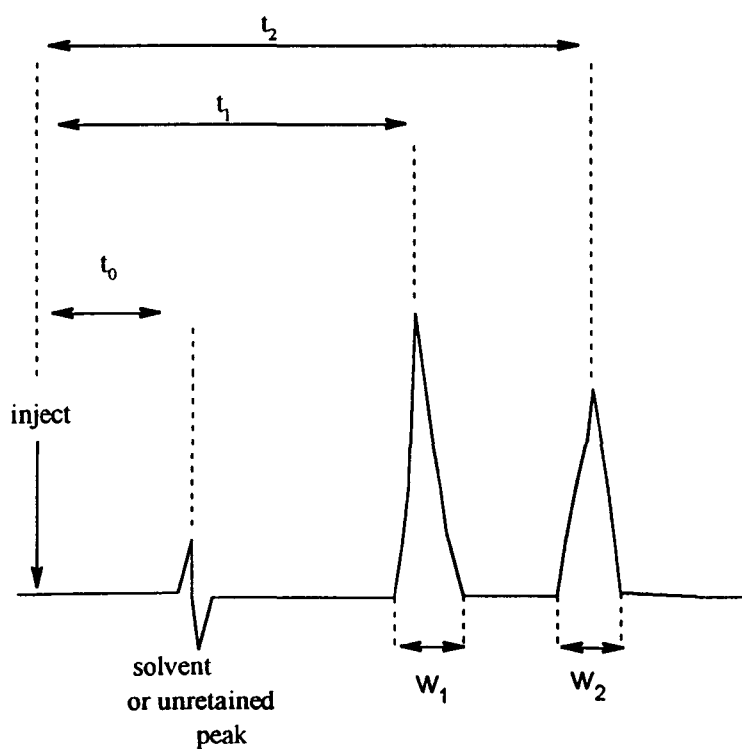
This technique is very widely used and is typified by the use of octadecyl modified silica stationary phase with an aqueous based mobile phase.

1.1 Equations used to describe chromatography

A number of equations exist for the calculation of the separation and retention characteristics as well as the overall performance of the column. A typical chromatogram is shown in

Figure 1.1.

Figure 1.1 Typical chromatogram of 2 analytes



The quantities t_0 , t_1 and t_2 are the absolute retention times of three solutes, t_0 represents an unretained analyte or a solvent flow marker. They can be measured in time, volume of solvent or distance on the chart recorder. These retention

times can vary with column length or mobile phase flow rate and therefore, do not provide a reproducible measure of an analytes retention. It is therefore, necessary to use capacity factors, k (Equation 1.0).

Equation 1.0 Calculation of capacity factors

$$k = \frac{t_R - t_0}{t_0}$$

where k = capacity factor, t_R = retention time of analyte, t_0 = solvent flow marker

Capacity values are usually between 1 -10, if the values are too low the peaks are not sufficiently retained while if the k values are too high the analysis time may be too long. The capacity factors of the two retained analytes can be used to calculate the selectivity or separation factor, α , of the two peaks relative to one another (Equation 1.1). By convention this equation is written so $\alpha \geq 1$.

Equation of 1.1 Calculation of separation factor, α .

$$\alpha = \frac{k_2}{k_1} = \frac{t_{R2} - t_0}{t_{R1} - t_0}$$

where α = separation factor, k_1 = capacity factor of first eluting analyte, k_2 =

capacity factor of second eluting analyte, t_{R1} = retention time of first eluting

analyte, t_{R2} = retention time of second eluting analyte, t_0 = solvent flow marker

This separation of one component from one another is described by the resolution factor, R_s . This factor does take in to account the peak widths generated by the column (Equation 1.2).

Equation 1.2 Calculation of Resolution, R_s .

$$R_s = \frac{t_{R2} - t_{R1}}{0.5 (w_1 + w_2)}$$

where R_s = resolution, t_{R1} = retention time of first eluting analyte, t_{R2} = retention time of second eluting analyte, w_1 = width of first eluting analyte at baseline, w_2 = width of second eluting analyte at baseline

Overall column performance can be calculated to take into account both retention and peak shape characteristics. Column performance is measured using plate number or plate height which are terms derived from distillation (Equations 1.3 and 1.4). Of the two measurements plate height is generally used as it is a measure per unit length of column and can therefore, be used to compare different column lengths.

Equation 1.3 Calculation of Plate number, N

$$N = 16 \left[\frac{t_R}{w} \right]^2$$

where N = plate number, t_R = retention time of peak, w = width of peak at baseline

Equation 1.4 Calculation of Plate height, H

$$H = \frac{L}{N}$$

where L = column length, N = plate number

The equations shown here will be used to calculate all separation and resolution values for the columns discussed later.

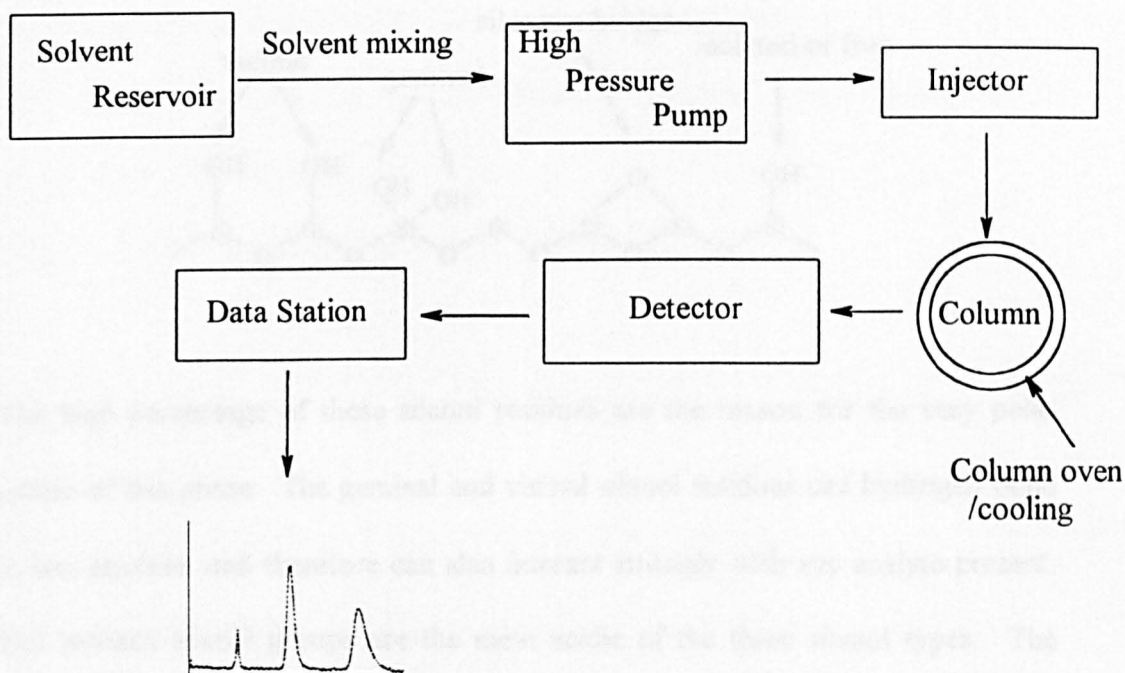
1.2 HIGH PERFORMANCE LIQUID CHROMATOGRAPHY

In 1969 J.J Kirkland and L.R Snyder¹⁷ described High Performance Liquid Chromatography (HPLC) for the first time. This technique overcame many of the problems that were inherent in classical liquid chromatography of the type first described by Tswett. Previously an open glass column was filled with the stationary phase of choice which was then eluted under gravity. This technique suffered in particular from, poor reproducibility, low resolution and long run times. Detection was tedious as samples were collected in fractions and analysed individually. This decreased the sensitivity of the technique because when the analyte was present in a fraction it was extremely dilute. With the development of in-line detection this problem was largely overcome. Detectors such as ultra-violet diode arrays, fluorescence detectors and mass spectrometers provide sensitive and accurate analysis of the separation. The introduction of high pressure pumps and stainless steel columns allowed the system to be run at increased pressure which greatly decreased run times and improved peak shape.

1.2.1 The modern HPLC system

This diagram (Fig. 1.2.1) describes the basic configuration of a modern HPLC system.

Figure 1.2.1 Diagram of a HPLC system

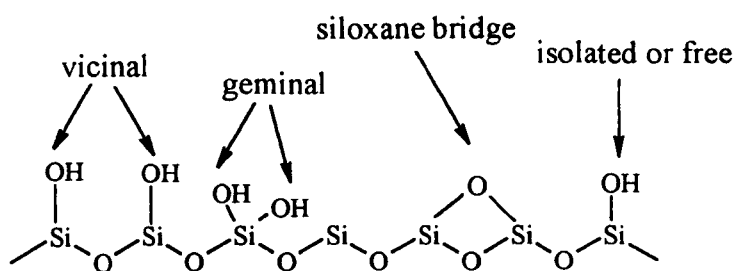


As well as varying the solvents between aqueous and organic phases it is also important to be able to change the content of the column. This is the most important part of the HPLC system; there are many packing materials available which offer a very wide range of polar or non-polar and achiral or chiral environments. The most popular packing material is silica. Silica is often used on its own as a packing or as a base for coating and bonded phases.

1.2.2 Silica as a stationary phase

The silica which is produced as a chromatographic packing is amorphous. It is usually produced as porous particles of controlled dimensions.¹⁸ The surface functionality is dominated by the presence of silanol residues. These are present in three forms (Fig 1.2.2).

Figure 1.2.2 Surface functionality of silica



The high percentage of these silanol residues are the reason for the very polar nature of this phase. The geminal and vicinal silanol residues can hydrogen bond to one another, and therefore can also interact strongly with any analyte present. The isolated silanol groups are the most acidic of the three silanol types. The concentration of isolated silanol groups can be controlled in manufacture. The higher the concentration the more hydrophilic the nature of the silica.

As mentioned previously the dimensions of the silica particle can be controlled. These dimensions include particle size, pore size, pore volume and surface area. These dimensions are varied by each manufacturer to try to produce a phase with desirable characteristics which are tailored for specific applications.

Silica however, has limited stability to the full pH range, especially high pH.

The presence of hydroxyl ions cause dissolution of the silica packing material.

Also the presence of the silanol functionality on the surface of silica provides a site for non-selective interaction. Also, the silanol groups do offer a site for covalent attachment of other chemical entities such as C_{18} chains. Stationary phases are

available which do not have such limitations. One such group is the carbon based phases.

1.3 POROUS GRAPHITIC CARBON AS A STATIONARY PHASE

There are three types of carbon phases which have been investigated as chromatographic supports;

Table 1.3.0²⁰ Comparison of carbon type phases

Type	Characteristics	Usefulness in liquid chromatography
Active charcoal/carbon	High surface area Microporous Heterogeneous surface	Poor - extreme peak tailing
Graphitised carbon black	Low surface area Very mechanically fragile Heterogeneous surface	Good - however poor peak shape in HPLC
Porous graphitised carbon	Moderate surface area Wide pores Mechanically robust Homogenous surface	Very good - phase has high capacity

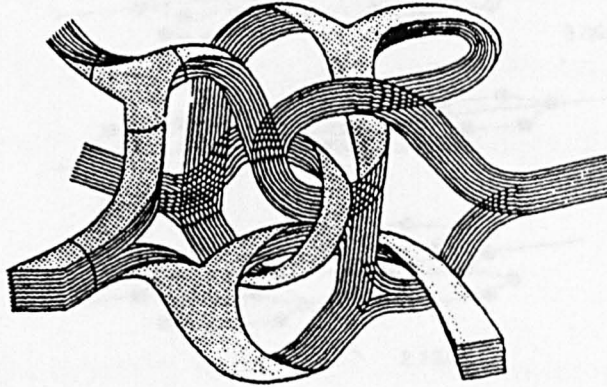
1.3.1 Method of production

In 1982 Knox *et al.*¹⁹ described the production of a new carbon phase which they called porous graphitic carbon (PGC). PGC was produced using a template of well-bonded silica gel of high porosity. It is this template which governs the final dimensions of the PGC particle. Initially the template was produced with 7 μm particle size with specific surface area of 50 m^2/g and pore volume of 1.4 cm^3/g . The template was then impregnated with a melt of phenol / hexamine in a 6:1 weight ratio. The impregnated material was then heated gradually to 150 $^{\circ}\text{C}$ to form a phenol-formaldehyde resin with the porous structure of the template. This material was then heated in a oxygen-free atmosphere in a specially designed rotary oven. During this process 50 % of the weight of the polymer was lost and the density was increased to 2 g/cm^3 . The material is then treated with hot aqueous potassium hydroxide which dissolves the silica template. The remaining material was porous glassy carbon which was heated to 2500 $^{\circ}\text{C}$ in an oxygen-free atmosphere to produce porous graphitic carbon.

1.3.2 Characterisation of PGC

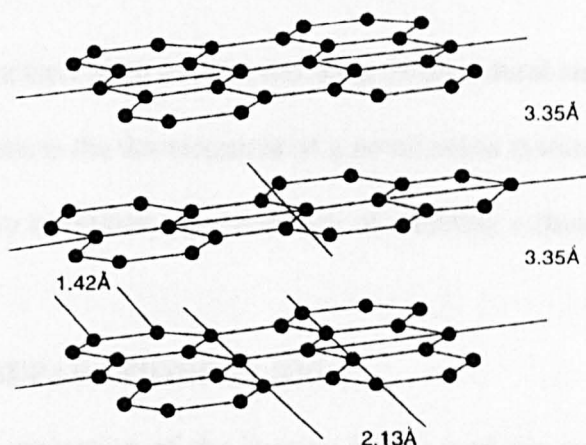
PGC has a porosity of 75 % and the particles are constructed from sheets of hexagonally arranged carbon atoms with sp^2 hybridisation. This layered structure is typical of a 2-dimensional graphite. The sheets of benzene rings are separated by 3.35 \AA and the spacing of the carbon atoms within these sheets is very close to that in large polycyclic molecules such as anthracene. Within the sheets of carbon valency is fully satisfied. Therefore, there is little or no functionality present on the surface of PGC. These sheets of carbon are twisted together to form the random porous structure of the PGC particles (Fig. 1.3.2)

Figure 1.3.2 Porous structure of PGC



The spacing between the graphitic layers is typical for a 3-dimensional graphite. However, unlike 3-dimensional graphite, PGC displays no ordering of the atoms between the layers. There is no relationship between one layer and its neighbour above or below. PGC is therefore a 2-dimensional graphite, or a turbostratic carbon (Fig. 1.3.3). It is believed that this lack of ordering between the layers underlies the high degree of mechanical strength which is displayed by PGC.

Figure 1.3.3 2-dimensional structure of graphitic - PGC



It has been suggested that carbon atoms at the edge of these sheets do not have a fully satisfied valency and can support functionality.²⁰ These functionalities are derived by exposure to the atmosphere and are therefore hydroxyl, carbonyl, carboxylic acid or amino groups. It is estimated that these surface functions compose less than 1% of the total mass of the material. Their influence on chromatography therefore, although feasible, is minimal.

PGC offers many desirable properties and has therefore become a successful commercial product. PGC is produced by Hypersil and is sold under the trade name Hypercarb.²⁰

These properties can be summarised as;

- use with non-polar and polar solvents
- homogenous surface with no surface functionality
- unique retention mechanism
- stereoselective surface allows the separation of geometric isomers
- stable to a wide pH range

- resistant to solvent swelling or shrinkage

Both PGC and silica have been used as the support for achiral and chiral CSP. As the topic of this thesis is the development of a novel chiral stationary phase for HPLC it is necessary to review other methods of effecting a chiral separation.

1.4 CHIRAL SEPARATIONS IN HPLC

Methods involving separation of the isomers before analysis can be divided into direct and indirect methods.

Indirect methods for the separation of optical isomers rely on the formation of a diastereomer of each isomer before separation. If each isomer is covalently bonded to a pure single isomer then the diastereomers formed are no longer mirror images, and will have different physicochemical properties. This allows the diastereoisomers to be separated. The enantiomers can be recovered by removing the derivatising agent.

Indirect methods do however have disadvantages:

- the derivatising agent has to be enantiomerically pure and is therefore likely to be costly or require synthesis
- the derivatising agent has to be easy to remove in such a way that it does not react with the analyte or alter its chirality.

Direct methods rely on a chiral selector, an optically active compound, which is either present in the mobile phase or immobilised as a stationary phase. This approach therefore, does not require any derivatisation of the analyte.

Chiral mobile phase additives

Many racemic mixtures have been separated on achiral columns using mobile phase additives such as camphorsulphonic acid ²¹ and perhaps the most widely used additives, cyclodextrins.²² This technique allows less expensive columns such as silica, C₁₈ and PGC to be used. A wide variety of mobile phase additives are available. The additives however, as with derivatising agents, are single enantiomers and may be costly or require synthesis. The use of mobile phase additives also may limit the detection method or *vice versa*. These disadvantages however, mean that the use of chiral stationary phases dominates the field of chiral HPLC.

1.4.1 Chiral Stationary Phases (CSP) for HPLC

All of these techniques rely on the ability of the chiral selector to form a transient diastereomeric complex with the analyte enantiomers. The differing stability of these complexes leads to different retention times. The enantiomer that forms the less stable complex will be eluted first.

In 1952 Dalgliesh ²³ used paper chromatography to study the separation of amino acid enantiomers. Although he was not the first to report this separation he did correctly attribute it to the optically active molecules that made up the paper. He proposed some requirements for enantiorecognition to happen,²⁴

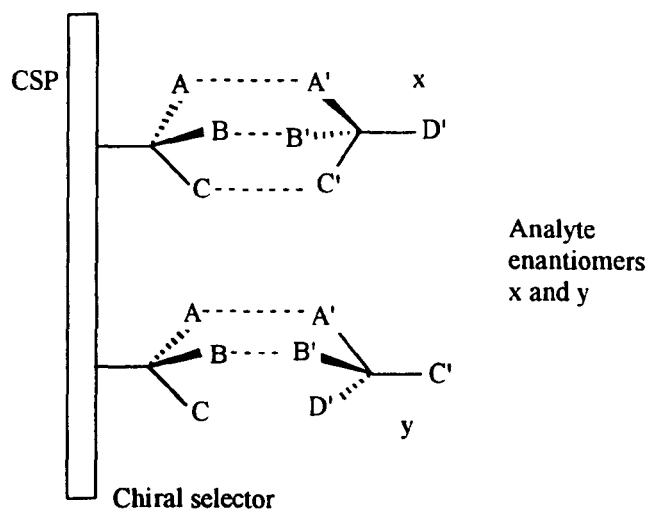
- three points of attachment are required for stereochemical specificity in adsorption
- the amino, carboxylic acid and side chain in the amino acid participate in the molecular interactions through hydrogen bonding or steric repulsions

Dalgliesh's work was not unique and had been preceded by work by Karagounis *et al.*²⁵ and Henderson *et al.*²⁶ who had demonstrated the separation of enantiomers on columns of powdered D- and L-quartz and lactose. These papers suggested the necessity of structural requirements for asymmetric recognition.

Pirkle *et al.*²⁷ have explored the 'three point rule' which is believed to be necessary for enantioselectivity to occur. Pirkle suggests that, "Chiral recognition requires a minimum of three simultaneous interactions between the CSP and at least one of the enantiomers, with at least one of these interactions being stereochemically dependent."

This is demonstrated in Figure 1.4.0,

Figure 1.4.0 The three point interaction rule



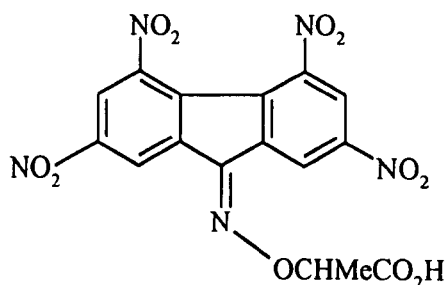
For simplicity HPLC-CSP are generally divided into 6 types;

Ligand exchange chromatography (Type 1) involves the formation of a reversible metal complex by the co-ordination of substrates that act as ligands.

This technique was first demonstrated in LC by Davankov *et al.*²⁸ who used a resin packing of styrene-divinylbenzene to which amino acid residues were bonded. The resin was saturated by Cu(II) ions which formed a bis-amino acid copper complex. Commercial columns of this type are available including Chiralpak W from Diacel Industries Ltd.

Charge transfer packing (Type 2) were first described by Gil-Av *et al.*²⁹, who wanted to separate helicene enantiomers. This was particularly hard as helicenes contain neither acidic nor basic functions to assist with chiral recognition. They effected this separation by bonding a chiral charge-transfer acceptor, tetranitrol-9-fluorenylideneaminoxypropionic acid (TAPA) (Fig. 1.4.1) to aminopropylated silica.

Figure 1.4.1 tetranitrol-9-fluorenylideneaminoxypropionic acid, TAPA



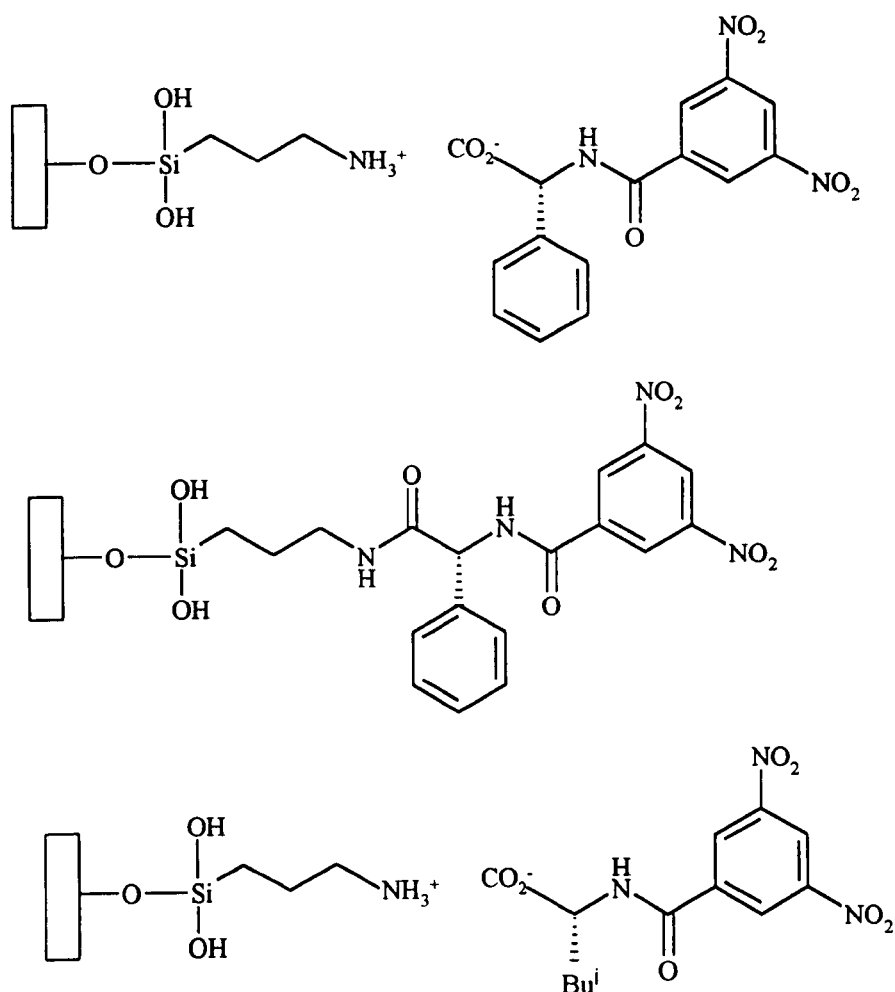
Asymmetric strand packings (Type 3) are often also called 'multiple interaction' or 'brush-type' phases. They consist of relatively simple organic molecules, with one or two asymmetric centres, which are chemically bonded to another support, usually silica. The organic molecules which act as the chiral selector are usually well defined and often contain one of the following functions near the chiral centre:

- a π -acidic or π -basic aromatic group which is capable of donor-acceptor interactions
- a polar hydrogen donor/acceptor
- a dipolar bond which is suitable for dipole-dipole interaction
- a bulky non-polar groups for steric repulsion, van der Waals interactions or conformational control

It is within this group of chiral stationary phases that the application of the three point interaction theory is most readily observed.

This type of phase was first described by Pirkle *et al.*³⁰ in the 1970s. After initial successful studies Pirkle produced a range of dinitrobenzene modified phases, which are shown in Figure 1.4.2.

Figure 1.4.2 Early Pirkle phases ³¹⁻³²



Pirkle suggested that there were two possible mechanisms of recognition: intercalative and nonintercalative.

Intercalative interactions involve the penetration of the chiral units of the phase by analyte which has been selected by the CSP. The mechanism depends on dipole stacking and hydrogen bonding. If the analyte has a long alkyl chain attached and this chain is orientated into the phase this may interfere with the specificity. This mechanism therefore, is promoted by producing a phase with a long anchor chain between the chiral selector and the base of the phase.

Nonintercalative interactions are characterised in particular by side-by-side dipole stacking and hydrogen bonding. This was suggested as there was an observed order in elution for different analytes or anchor chain length.

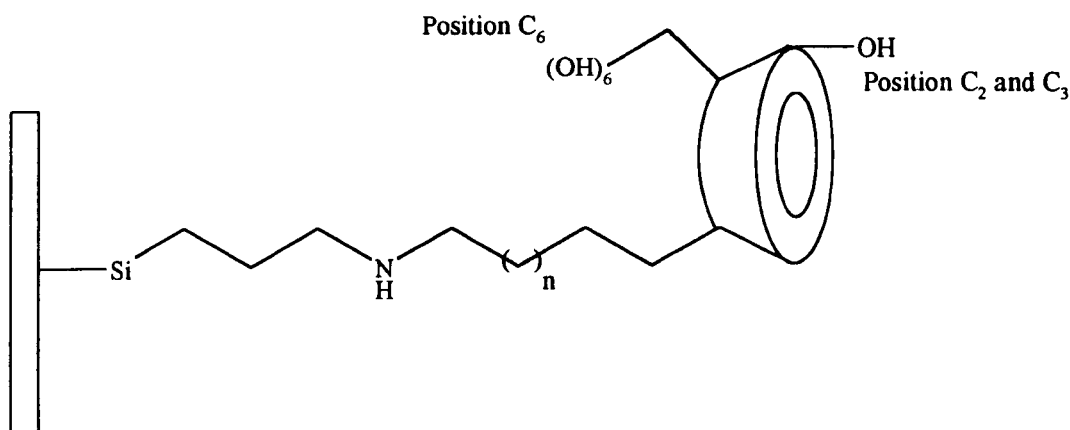
This theory led to phases which contained the same chiral selector molecule which is bound at different sites. This changes the orientation of the chiral selector relative to the base of the phase. Such phases can be designed to be extremely selective for specific analytes.

A wide variety of such asymmetric strand phases has since been designed and include acylated dimethylnaphthyl-alkylamine or *N*-naphthylamino acids. The use of bonded macrocyclic ligands has also produced some interesting phases including antibiotics such as vancomycin and teicoplanin. Such phases are multimodal and can be rapidly switched between normal and reversed-phase operation.

Chiral cavity packings (Type 4) were first described by Cram *et al.* who described the use of chiral crown ether bound to silica gel.³³

The use of cyclodextrins had also made an impact in this area.³⁴ Cyclodextrins are cyclic oligomers of D-glucose containing 6-8 units. Cyclodextrins assume a cylindrical shape. They contain 30-40 asymmetric centres. The molecule is overall hydrophilic. However, the cylindrical cavity is relatively hydrophobic owing to the lack of hydroxyl groups. It is possible, therefore, to separate a variety of water insoluble compounds as they can fit into the chiral hydrophobic cavity depending on the chirality and structure in general of the analyte. If the inclusion complexes which are formed differ in energy of formation then the cyclodextrin will discriminate between the enantiomers present (Fig. 1.4.3).

Figure 1.4.3 Chiral stationary phases based on bound cyclodextrin



CSPs based on polymers (Type 5) use both natural and synthetic polymers.

This grouping also contains **Type 6 CSPs using bound proteins**³⁵ which in the broadest sense are natural polymers.

This group of CSPs includes the phases which will be discussed throughout this thesis. It is therefore desirable to explore this group and the mechanisms of chiral recognition involved in detail.

1.4.2 Synthetic polymers as chiral stationary phases

Such synthetic polymers are produced using two methods,

- polymerisation in a chiral environment, using a chiral catalyst³⁶
- polymerisation of chiral monomers³⁷

Okamoto *et al.* were the first to exploit the use of a chiral catalyst. The polymerisation of triphenylmethyl methacrylate with a chiral sparteine-*n*-butyl lithium catalyst produces an isotactic polymer which is chiral owing to its helical secondary structure (Figs 1.4.3 and 1.4.4).³⁶ A triphenylmethyl methacrylate

polymer chain with a degree of polymerisation over about 30 is conformationally stable at room temperature, while a degree of polymerisation over approximately 80 units produces a polymer which is insoluble in common organic solvents.

This phase has been particularly useful in low temperature chromatography for the separation of isomers which racemize easily. The separation of tris(9-triptycyl)geranium chloride was described at $-30\text{ }^{\circ}\text{C}$ using methanol as a mobile phase.

Figure 1.4.3 Poly(triphenylmethyl methacrylate)

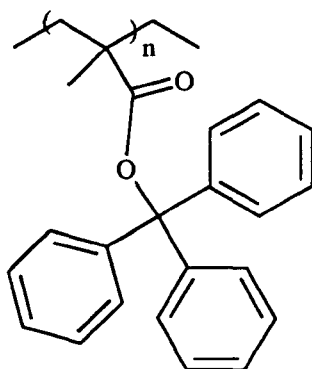
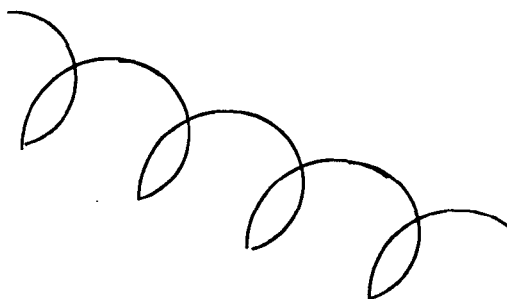


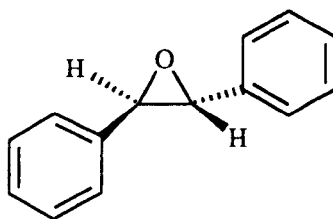
Figure 1.4.4 Helical structure forced by the presence of the triphenyl group



The polymer was coated on to silica and was found to be effective in the separation of some racemic alcohols, esters, amines and hydrocarbons. It is

generally accepted that separable analytes possess a rigid non-planar structure, for example *trans*-Stilbene oxide (Fig. 1.4.5)

Figure 1.4.5 *trans*-Stilbene oxide



The use of chiral monomer units is typified by polyacrylamide-based CSP³⁷. With these phases chirality is due to the chiral centre within the monomer and not to any macrostructural feature such as a helix. Huffer *et al.*³⁸ demonstrated the separation of chiral (5)-alkylated γ (δ)-lactones on a polyacrylamide based phase.

1.4.3 Bound protein phases

This type of phase is suited to the analysis of pharmaceutical or other biologically active molecules as the bound protein is likely to be very selective towards such analytes. The use of proteins in such a way is often termed ‘affinity’ chromatography. The development phases in this area used mainly bovine serum albumin³⁹ or acid glycoprotein. However these phases suffered from poor reproducibility and column deterioration.

A second generation of α_1 -acid glycoprotein bound phases proved to be successful for the separation of a range of analytes including cationic drugs such as cocaine and methadone.⁴⁰ α_1 -Acid glycoprotein is a human serum transport globular protein of about 41,000 Da molecular weight. This protein consists of

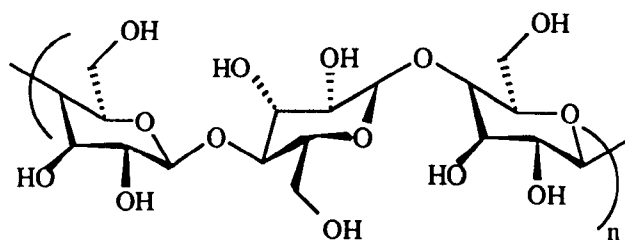
nearly 200 amino acid residues and five carbohydrate units. Due to the highly complex structure of the protein the mechanism of stereoselectivity is not fully understood.

Such bound protein phases are highly selective. However, they have a very low capacity so are not ideally suited to preparative separations. This brief review of chiral stationary phases has covered only a fraction of the overall number of phases which are currently commercially available to the analyst. One particular type of chiral stationary phase has however tended to dominate; these phases employ polysaccharides as the chiral selector.

1.5 POLYSACCHARIDES AND THEIR USE IN CSP

Polysaccharides are natural polymers of sugars, the most abundant being cellulose. Cellulose is a linear polymer of D-(+)-glucose coupled by β -1,4 linkages. The glucose units are in the chair confirmation and have 3 hydroxy residues in the equatorial orientation at the 2,3 and 6-positions (Fig. 1.5.0.)

Figure 1.5.0 Cellulose



Cellulose is optically active, at the anomeric carbon, and is highly ordered in structure. This high degree of order is caused by the intra-molecular hydrogen bonding between chains, which gives cellulose its crystallinity. This high degree of crystallinity and highly ordered structure promotes the formation of a helical

secondary structure.⁴¹ As discussed previously (Section 1.4) Dagliesh used paper as the stationary phase for chromatography, which was made up of cellulose chains, to resolve optically active amino acids. The use of cellulose as a CSP is particularly limited by the strong polar interaction which is possible between the analyte and the hydroxyl groups.

Hesse and Hagel⁴² were the first to use a derivatised form of cellulose to effect chiral separations. They produced the first completely acetylated microcrystalline cellulose using a heterogeneous reaction in benzene. They called this phase microcrystalline cellulose triacetate (MCCT) or CTA-I and found that it gave good enantioselectivity for several racemic compounds such as Troger's base. Hesse and Hagel described the reversal of elution order and the loss of resolution occurring when MCTA was dissolved then reprecipitated.⁴³ This phenomenon was attributed to the formation, through reprecipitation, of the less crystalline form of MCTA termed CTA-II. This cellulose derivative is also insoluble, owing to the presence of the hydroxyl groups.

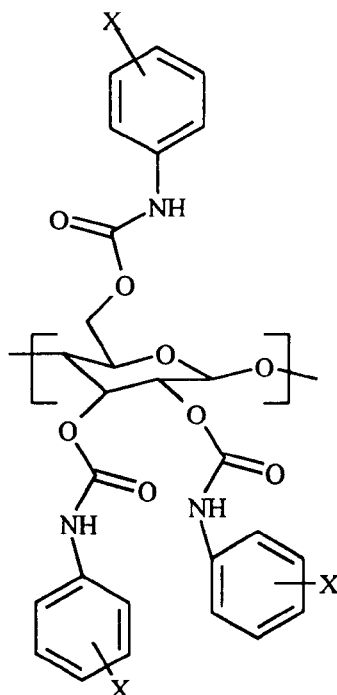
Okamoto⁴⁴ suggested that the chiral recognition ability of MCTA depends on the crystalline structure of native cellulose, and therefore, when dissolved in a solvent, different characteristics are displayed. When MCTA was deposited on to the surface of silica gel from a solution the phase produced was very different to unsupported MCTA. Okamoto⁴⁴ produced a phase of cellulose triacetate coated on to macroporous aminopropylated silica. He then expanded the study through the introduction of phenyl groups by using cellulose tribenzoate (CTB).⁴⁵ CTB and its derivatives show good chiral recognition when coated on to macroporous silica gel.⁴⁶ Wainer *et al.*⁴⁷⁻⁴⁸ have extensively investigated the chiral recognition mechanism of CTB. They suggested that adsorption to the

carbonyl group occurs through dipole-dipole and hydrogen-bonding interactions leading to insertion of the analyte into a chiral ravine or cavity. As well as coating CTB phases on to silica gels Francotte *et al.*⁴⁹ demonstrated the use of methylbenzoyl cellulose beads. These beads are mechanically stable and efficient. They also offer one the opportunity to carry out preparative separations. The use of phenyl groups in CTB phases provided an opportunity for structural variation.⁵⁰⁻⁵¹ It was found that substitution by electron-donating groups such as methyl improved the chiral recognition ability of the phase. The use of electron-withdrawing substituents such as halogen groups however, decreased this ability. These substituents may change the polarity of the carbonyl groups of the benzoate residues and are the most important site of enantiorecognition. Indeed, cellulose tris(methylbenzoate) phases are used with and without silica gel support. Cellulose can also be derivatised by reaction of phenyl isocyanates to produce carbamate derivatives.

1.5.1 Polysaccharide phenylcarbamates

The use of various electron-withdrawing or donating substituents on the phenyl ring had previously been studied with respect to cellulose benzoate phases. As with the benzoate phases the chiral recognition ability of the carbamate phase depends on the nature and position of the substituents on the phenyl ring (Fig. 1.5.1).⁵²

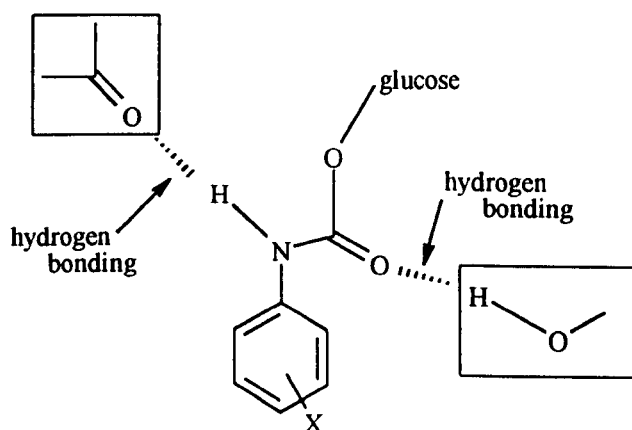
Figure 1.5.1 Cellulose tris(phenylcarbamate) derivatives



x can include methoxy, alkyl, halogen, nitro on one or more positions

The substitution of the phenyl ring determines the polarity of the carbamate linkage which is the ruling interaction site for chiral recognition (Fig. 1.5.2).

Figure 1.5.2 Interaction of analyte with the urethane linkage in carbamate group



These parameters can be investigated using ^1H -NMR which will measure any changes in the nature of the -NH- part of the urethane residue. When the phenyl

group was derivatised with methoxy or nitro groups, i.e. strongly electron donating and withdrawing respectively, the phase showed low chiral recognition. It was suggested that this was due to the interaction of these very polar groups with the analytes thereby preventing them from interacting with the site of chiral recognition, the urethane linkage. The position of these substitutions is also critical to the chiral separation ability of the phase and methyl or chloro groups in the 3,5 positions are particularly effective.

Yashima *et al.*⁵³ pursued the mechanism of enantioselectivity of cellulose triphenylcarbamate (CTPC) through computational studies. Previously Zogt and Zugenmaier⁵⁴ studied CTPC using X-ray analysis to determine secondary structure. They determined that a fibre of CTPC has a left-handed threefold (3/2) helical structure. Yashima based his studies on an octamer of CTPC, which is described as displaying hydrogen-bonding between the NH protons of the carbamate groups at the 6-position and the carbonyl oxygens at the 2-positions. This bonding pattern is believed to produce a chiral cavity which allows discrimination to occur between the 2 enantiomers present.

Daicel responded to the increase in derivatised polysaccharides discussed in the literature, to produce a range of commercially available chiral stationary phases (Fig. 1.5.3)

Figure 1.5.3 Commercially available chiral stationary phases produces by Daicel

Derivative	Commercial name
Microcrystalline cellulose triacetate	Chiralcel CA-1
Cellulose triacetate*	Chiralcel OA
Cellulose tribenzoate*	Chiralcel OB
Cellulose tris(phenylcarbamate)*	Chiralcel OC
Cellulose tris(3,5-dimethyl phenylcarbamate)*	Chiralcel OD (OD-H or OD-R)
Cellulose tris(4-chlorophenylcarbamate)*	Chiralcel OF
Cellulose tris(4-methylphenylcarbamate)*	Chiralcel OG
Cellulose tris(4-methylbenzoate)*	Chiralcel OJ
Cellulose tricinnamate*	Chiralcel OK
Amylose tris(3,5-dimethyl phenylcarbamate)*	Chiralpak AD
Amylose tris[(S)-1-phenylethylcarbamate]*	Chiralpak AS

* these phases are coated on to bonded silica

As discussed in both Chapters 1 and 2 chiral separations have been carried out very successfully with derivatised polysaccharides coated on to both silica gel and PGC.⁵⁰ Carbamate polysaccharides have several characteristics which underpin this ability. These can be summarised as:

- a highly ordered crystalline structure
- interaction of analyte with urethane group in a chiral environment

The implication of the helical secondary structure is the creation of a chiral 'cavity' or 'ravine' which produces an enantiodiscriminatory environment. Recently Booth *et al.*⁵⁶ have examined the mode of enantiorecognition for a range of amylose-based phases. Amylose is a natural polymer analogous to cellulose. Whereas cellulose is constructed of glucose units joined by β -1,4 linkages, amylose contains glucose units joined by α -type linkages. They found that for the analytes examined, the order of elution is a function of the chirality of the amylose backbone, that is the nature of the chiral ravine. The magnitude of the enantioselective separation was found to depend on the chirality of the carbamate side chain. As discussed in section 1.4.1, the number of interaction sites in a derivatised polysaccharide phase is still vigorously debated. It is therefore, not possible to say unequivocally that all enantioselectivity of every analyte is always due to a 'three-point' interaction process.⁵⁷

1.5.2 Use of porous graphitic carbon in liquid chromatography

Many different types of analytes both chiral and achiral have been separated on PGC. PGC is particularly suited to the separation of geometric isomers which are very similar in structure.⁵⁸ An example is the separation of the *meta*-isomer from the *para* and *ortho*-isomers of a disubstituted benzene under isocratic elution conditions. It is possible to separate all three isomers by imposing a simple organic gradient. The order of elution of these compounds is reversed compared to bonded phases such as C₁₈ silica. Knox *et al.*⁵⁹ described the same reversal of elution order for geometric xylene isomers. The ability of PGC to distinguish between geometric isomers is believed to be due to the fact that the substituent on

the ring dictates sterically how the solute can approach and interact with the surface of PGC. The main retention mechanism with PGC is through specific donor-acceptor interactions with the delocalised band of electrons at the surface.

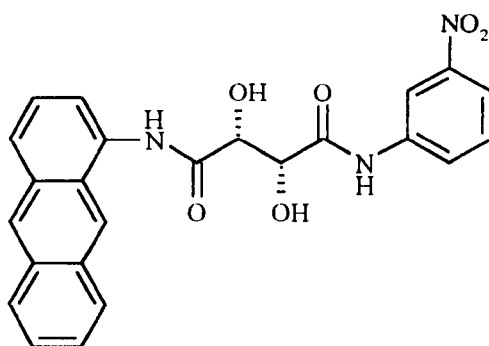
⁶⁰ This will be discussed further in Chapter 2.

PGC has also been used to separate diastereoisomers using either surface modification or chiral phase additives. Knox and Wan ⁶¹ coated PGC with a near-monolayer of an adsorbed enantiomeric modifier, the L or D enantiomer of *N*-(2-naphthalene-sulphonyl)-phenylalanine, which acts as an adsorbed stationary phase. Through the complexation of cupric ions they were able to demonstrate the baseline resolution of α -amino and α -hydroxy acids. Both Josefsson *et al.* ⁶² and Karlsson *et al.* ⁶³ have shown that PGC is a suitable phase for chiral ion-pair chromatography.

The use of chiral additives has been demonstrated by Karlsson *et al.* ⁶⁴ who used *N*-benzoxycarbonylglycyl-L-proline to separate enantiomeric polyaromatic amines.

PGC has also been used in supercritical fluid chromatography. Wilkins *et al.* ⁶⁵ found that PGC was an ideal support for physically anchored chiral selectors. The anchor was based on polycyclic compounds. Anthracene was found to offer the best results. The chiral selector was derived from tartaric acid (Fig. 1.5.4).

Figure 1.5.4 Chiral selector and anchor group



It was suggested that anthracene is completely adsorbed to the surface of the PGC. Indeed the phase was found to be extremely rugged and robust. This phase was found to be applicable to the separation of compounds such as benzoin and ibuprofen.

As previously discussed in this section, PGC has often been used as the support in chiral mobile phase additive chromatography. Most recently Karlsson *et al.*⁶⁴ describe the use of PGC in the separation of aminoalcohols using *N*-derivatised dipeptides as the chiral counter-ions in the mobile phase. The use of PGC as a support for a derivatised polysaccharide type phases was first published by Grieb *et al.*⁵⁵. They describe the production and proposed optimisation of PGC coated with cellulose tris(3,5-dimethylphenyl carbamate). A review and the continuation of this work is discussed in Chapter 2 of this thesis. This work showed that PGC is a very suitable support for the use of chiral polymers to produce a chiral stationary phase for HPLC.

1.5.3 Solvent considerations

The majority of separations on derivatised polysaccharide coated phases have been carried out under non-polar conditions. Usually hexane/2-propanol is cited

as the solvent mixture of choice for neutral analytes. The addition of a silanol suppressor, such as diethylamine, with basic analytes⁶⁵ reduces peak tailing as does the use of an ionisation suppresser, such as trifluoroacetic acid, for acidic analytes.⁶⁶ Organic modifiers are also often used in the mobile phase to improve the observed resolution, these include ethanol and other straight or branched chain alcohols.⁶⁷

The use of derivatised polysaccharide coated phases under reversed-phase conditions was demonstrated by Ichida *et al.*⁶⁸ They used perchlorate buffered acetonitrile mobile phases for the separation of analytes including verapamil. Ishikawa and Shibata used a mixture of water and acetonitrile for the separation of neutral analytes, they added an anionic ion-pair reagents such as perchlorate and for acidic analytes the use of a strong acid such as perchloric acid improved the chromatography.⁶⁹

1.6 SUMMARY

The use of chiral stationary phases to obtain single pure isomers is very important and on both the analytical scale and the preparative scale is set to continue. The phases developed by Okamoto *et al.*⁴⁴ have proved to be widely applicable, and have found a huge market in the pharmaceutical and related industries.

PGC has been shown to be a good phase for chiral separations as it can be modified both by adsorbing the chiral selector to the surface to produce a pseudo-bonded phase or by coating the surface with a monolayer of chiral selector. The use of PGC as a support for polymeric phases has not been investigated to the best of our knowledge, except within this group. It is the use of PGC as a

support for optically active polymers and their application to chiral chromatography which is the basis of this thesis.

CHAPTER 2

APPLICATION OF POROUS GRAPHITIC CARBON(PGC) AS A SUPPORT FOR CELLULOSE TRIS (3,5- DIMETHYL PHENYL CARBAMATE)

Much work has been done on the use of various silicas and indeed PGC as a support for cellulose carbamates and in particular cellulose tris-(3,5-dimethylphenyl carbamate).⁶⁵ Initial work by Matlin and Grieb into the suitability of PGC as a support examined several aspects of the complete phase. This chapter reviews that work and discusses supplementary work so as to draw conclusions as to the nature of the optimum PGC-based cellulose tris-(3,5-dimethylphenyl) carbamate phase.

2.0.1 Optimum cellulose type

The optimum cellulose to use to synthesise CDMPC has been previously investigated.⁶⁵ It was concluded that, for bonded silica, Avicel gave better results. Carbamate derivatives of Avicel and Sigmacel Type100 celluloses were examined using size exclusion chromatography to establish their respective polydispersities (PDi) and molecular weight (M_n) (Fig. 2.0) relative to a polymethylmethacrylate standard. Polydispersity described the range of molecular weights observed, the

higher the polydispersity the broader the range. M_n is the number average molecular mass.

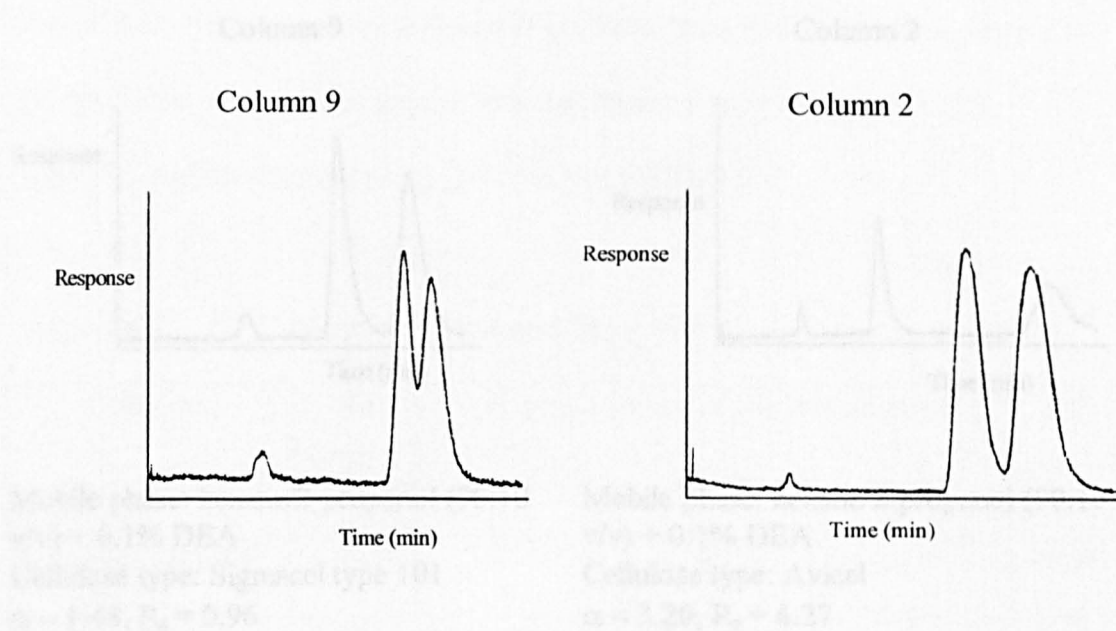
This is often used instead of weight average molecular mass (M_w), polydispersity is defined as M_w/M_n . All SEC analysis was carried out in THF as the solvent with 0.1% toluene as a flow marker.

Table 2.0 SEC data for Avicel and Sigmacel derivatives⁶⁵

Cellulose	M_n	Average number of glucose units per chain (DPn)	PDi
Avicel	51000	83	5.46
Sigmacel Type 100	100000	164	4.18

It was reasoned that because Avicel has the shorter chain length it is better able to fit into the porous structure of the particle and therefore produce a more homogenous coating, indeed it was discovered that the optimum loading for Avicel on APS-silica was 20% w/w as compared to 15% for Sigmacel. Upon later investigation in to the optimum cellulose to use with PGC however, Sigmacel had discontinued Type 100 and replaced it with Type 101 which the manufacturers claimed to be identical. Two columns were produced using the two available types of cellulose. Column 9 contained Sigmacel type 101 and Column 2 contained Avicel cellulose. The columns were compared for 3 analytes, 1 neutral (benzoin methyl ether), 1 basic (alprenolol) and 1 acidic (2-phenoxypropionic acid)

Figure 2.0.2 Comparison of separation of benzoin methyl ether

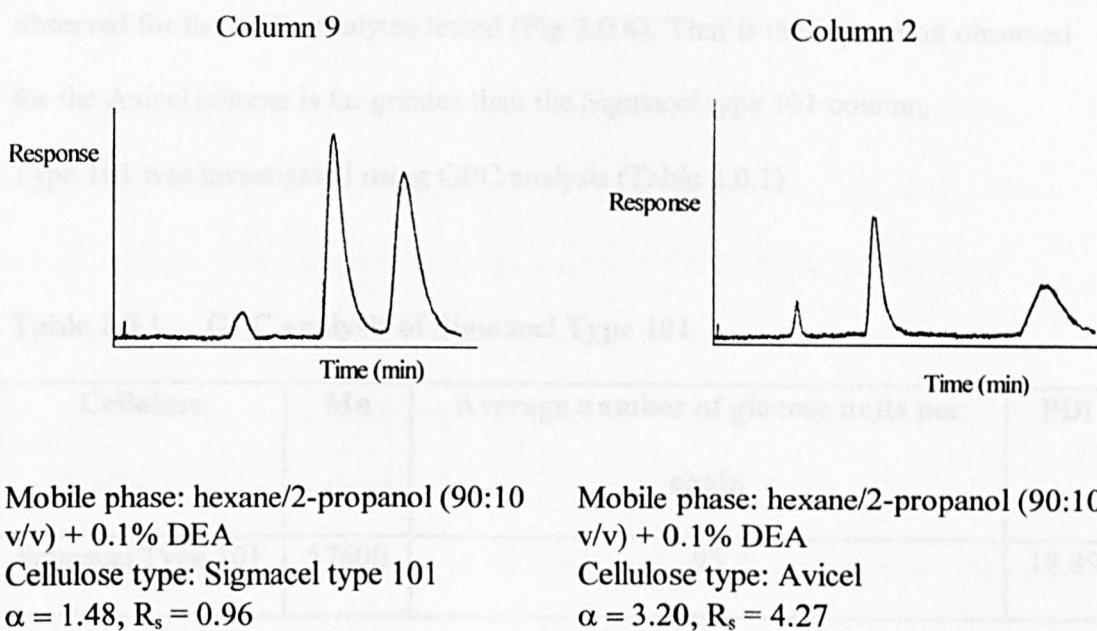


Mobile phase: hexane/2-propanol
(90:10 v/v)
Cellulose type: Sigmacel type 101
 $\alpha = 1.21$, $R_s = 0.74$

Mobile phase: hexane/2-propanol
(90:10 v/v)
Cellulose type: Avicel
 $\alpha = 1.37$, $R_s = 1.19$

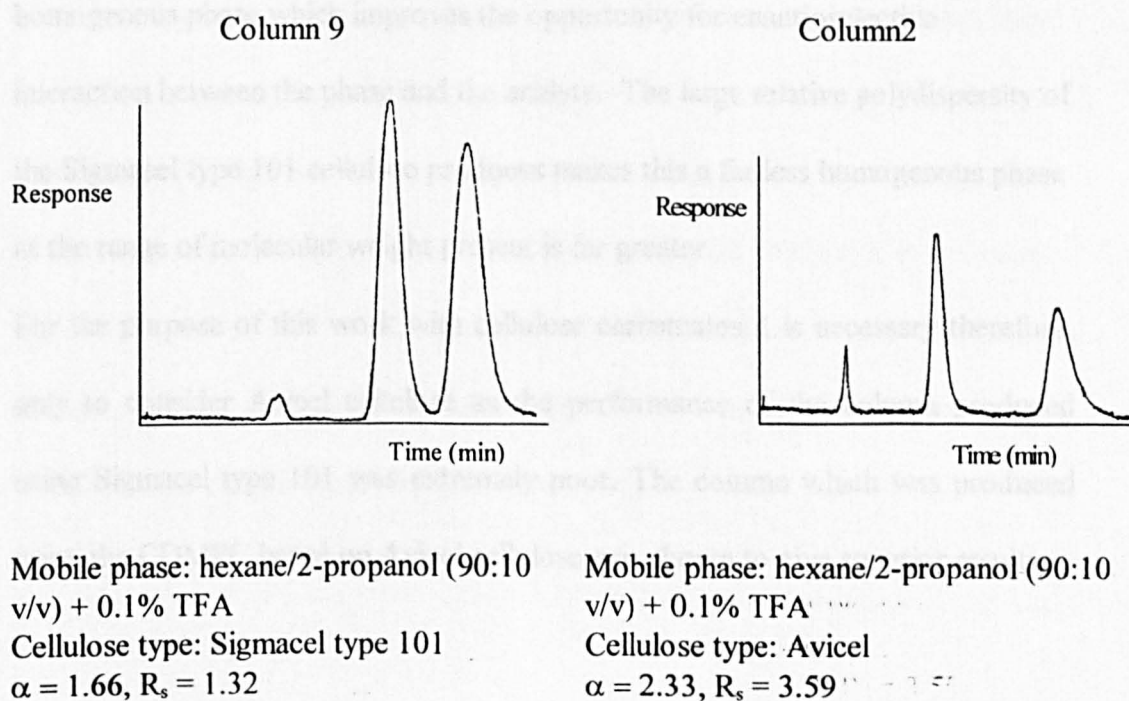
It can be seen that there is marked difference in the chromatography produced by the 2 columns. Benzoin methyl ether is slightly less retained on column 9 than column 2. However, the peak shape displayed by column 9 is broader than column 2. This is especially visible in the flow marker which gives a very wide peak on column 9. R_s and α are also greatly reduced for column 9, with baseline resolution no longer observed (Fig. 2.0.2).

Figure 2.0.3 Comparison of separations of alprenolol



Again for alprenolol (Fig 2.0.3), the broader peak shape and loss of retention on column 9 is observed. Although resolution is still baseline on column 9, it is much reduced.

Figure 2.0.4 Comparison of separations of 2-phenoxy propionic acid



The same characteristics of column 9 seen for neutral and basic analytes are also observed for the acidic analytes tested (Fig 2.0.4). That is the separation observed for the Avicel column is far greater than the Sigmacel type 101 column.

Type 101 was investigated using GPC analysis (Table 2.0.1)

Table 2.0.1 GPC analysis of Sigmacel Type 101

Cellulose	Mn	Average number of glucose units per chain	PDi
Sigmacel Type 101	57600	95	18.89

The reason for the very large polydispersity of Sigmacel type 101 is its bimodal distribution of molecular mass. It is obvious therefore that Sigmacel Type 100 and Type 101 are not identical and Type 101 can not be compared to Type 100 in a study of this nature. It can be suggested that Avicel produces a more homogenous phase which improves the opportunity for enantioselective interaction between the phase and the analyte. The large relative polydispersity of the Sigmacel type 101 cellulose produces makes this a far less homogenous phase as the range of molecular weight present is far greater.

For the purpose of this work with cellulose carbamates it is necessary therefore, only to consider Avicel cellulose as the performance of the column produced using Sigmacel type 101 was extremely poor. The column which was produced using the CDMPC based on Avicel cellulose was shown to give superior results.

2.1 OPTIMUM LOADING OF CDMPC ON PGC

It had been suggested that the optimum loading of CDMPC on PGC was 25% w/w⁶⁵ This was higher than observed for the same particle size APS-silica. This is due to the relatively large mean pore diameter of PGC (250Å) compared to APS-silica. This larger pore allows a higher density of coating to be applied to the surface before the particles begin to adhere to one another because the surface and porous structure are overloaded.

The protocol for the application of the phase had also been examined. It was suggested that a multiple step application of the CDMPC to the PGC surface would be advantageous. It was believed that this would produce a phase of greater homogeneity than if the application was carried out in one step.

2.1.1 Optimum coating method

Two columns were prepared using the same materials and conditions. Both were made using a coating ratio of 25% w/w CDMPC to PGC. However, one column was prepared using a one-step coating method and the other using a multiple step or batch method. The batch method involves coating the PGC with, in this case, 5 equal portions of CDMPC. This column will be referred to as Column 1. The column produced using the one-step method will be referred to as Column 2.

Both of these columns were tested with six racemic analytes, two neutral, two acidic and two basic (Fig. 2.0).

Figure 2.1 Comparison of batch and single step coating methods

Analyte	Column	k_1	k_2	α	R_s
BME	2	2.66	3.68	1.39	1.83
2-PA	2	1.10	1.63	1.49	1.38
MA	2	3.88	4.71	1.21	1.05
2-PPA	2	2.80	6.90	2.46	3.91
AL	2	0.61	1.49	2.44	2.67
ORP	2	0.61	1.05	1.72	1.64
BME	1	2.51	3.49	1.39	2.12
2-PA	1	1.05	1.68	1.60	2.86
MA	1	3.63	4.41	1.21	1.42
2-PPA	1	2.85	7.73	2.71	4.92
AL	1	0.71	1.68	2.38	2.98
ORP	1	0.71	1.24	1.76	2.30

Mobile phases : BME(benzoin methyl ether), hexane/2-propanol (95:5 v/v); 2-PA(2-phenethyl alcohol), hexane/n-butanol (95:5 v/v); 2-PPA(2-phenoxy propionic acid), hexane/2-propanol/TFA (95:5:0.1 v/v); MA(mandelic acid), hexane/ethanol/TFA (95:5:0.1 v/v); AL(alprenolol), hexane/2-propanol/DEA (80:20:0.1 v/v); ORP(orphenadrine), hexane/2-propanol/DEA (90:10:0.1 v/v).
Flow rate: 0.5 ml/min

Neutral analytes

In one case the observed α value was higher for Column 1 than Column 2 and in the other case no difference was observed. An increase in the α value suggests an increase in the number or availability of sites of enantioselectivity. In both cases, however, the R_s value has increased. This reflects both the increase in selectivity and better peak shape observed on Column 1.

Acidic Analytes

The result described for neutral analytes was repeated for the acidic analytes.

Overall better results were gained from Column 1. It was necessary to use an acidic mobile phase additive when running acidic analytes in order to reduce peak tailing and retention. This technique was also described for cellulose carbamate phases based on silica. The implications of this for the PGC based phase will be discussed later.

Basic Analytes

For the basic analytes tested in both cases a higher R_s value was observed for Column 1 compared to Column 2. The situation with respect to α values however, is less clear as one result is higher for Column 1 and one is lower.

2.1.2 Interpretation of Results from Table 2.1.1

The results suggest that Column 1(batch method) is superior to Column 2 (single-step method). This means that the batch method produces a higher quality phase than the single step coating method. This is further illustrated by the respective plate height calculations for the 2 columns (Table 2.1.1);

Table 2.1.1 Plate Height results for Columns 1 and 2

Column	Plate Height /mm
1	0.19
2	0.22

Plate height was calculated for the first eluting enantiomer of 2-PA in both cases.

A lower plate height for column 1 was observed for all 6 enantiomers tested. This means that the height equivalent to one resolving plate is less with the batch method than with the single-step method. These results suggest that the batch method produces a phase with significantly differing characteristics than a phase produced by a single step coating procedure.

These characteristics are:

- **increased phase homogeneity**
- **increased availability of sites for chiral discrimination**

The differences between the phases are clearly seen in the chromatographic results. It is desirable however to try to establish the physical nature of such differences. The coated particles were examined using two techniques,

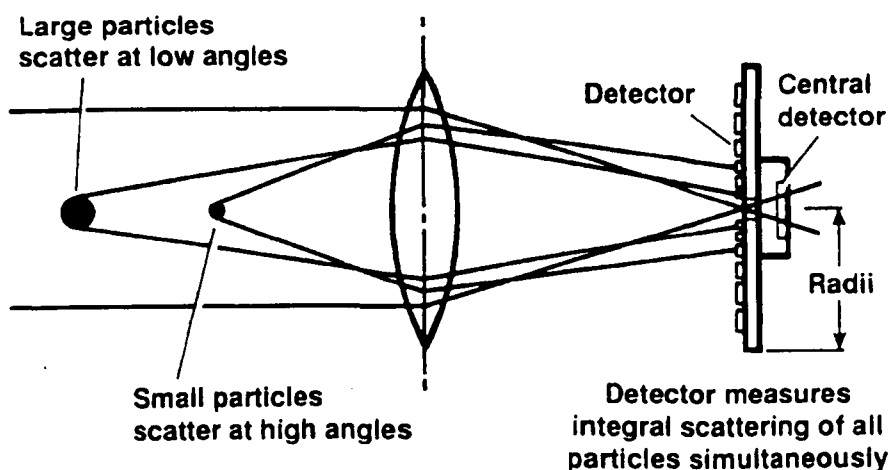
- **Laser light scattering**

- **Scanning electron microscopy**

2.1.3 Investigation of the surface character of Column 1 and Column 2 phases by laser light scattering

Laser light scattering measures the average particle size in any given sample by the laser light scattering pattern obtained from that sample in suspension (Fig. 2.1.3).

Figure 2.1.3 A schematic of laser light scattering particle size instrument



This technique was found to be inaccurate for actual particle size determination compared to the results obtained from the SEM. This was however due to the fact that the refractive index of PGC was not corrected for. The sample was also suspended in methanol, and since methanol will swell the CDMPC coating and therefore may give a false representation of particle size. Both of these factors mean that the absolute value obtained from the laser light scattering is not

representative of the sample. However the results are of value in a comparative study such as this (Table 2.1.4). The sample was analysed using a Malvern Instrument Mastersizer X. The sample was suspended in methanol with sodium dodecylsulphate added as a dispersant.

Table 2.1.4 Comparison of single-step and batch methods of coating by laser light scattering

Sample	Observed particle size, μm	Distribution
PGC (124.11), $7\mu\text{m}$	11.55	single
Column 1	20.70	bimodal
Column 2	13.35	bimodal

The particle size observed for Column 1, made using the batch coating process was larger than for Column 2, made by the single-step process. It can be suggested that this is due to the increased tendency of the CDMPC to swell in the first sample. The particles have a greater surface area as they are still very porous compared to the particles coated using the single-step method.

2.1.4 Investigation of surface character of Column 1 and Column 2 phases by scanning electron microscopy (SEM)

Scanning electron microscopy uses a beam of electrons which is moved over the surface of the sample to produce a real-time image of the topography of the sample surface. This technique is inherently more sensitive and accurate than light scattering and can be used to gain absolute particle size. The electron beam

is generated by a tungsten filament, the fine beam of electrons being scanned across the sample by the scan coils. As this proceeds, any low energy electrons or other radiation produced by each point on the sample are recorded. The sample is simultaneously scanned by a point from a cathode ray tube which is modulated by the signal from the radiation/electron detector. The combination of these two signals produces the images of the sample surface which are required.

The work described here was carried out on a Cambridge Instruments Stereoscan S250 Mk3. The sample was presented on an aluminium sample stub and was sputter coated with gold to improve detection.

Comparison of single-step and batch coating methods

The PGC particles which have been coated using the batch method appear to have several differences from those coated using the single-step method. The porosity of the batch coated particles appears to be more evident than for the single-step particles (Fig.s 2.1.5 and 2.1.6).

Figure 2.1.5 SEM of Batch coated particles

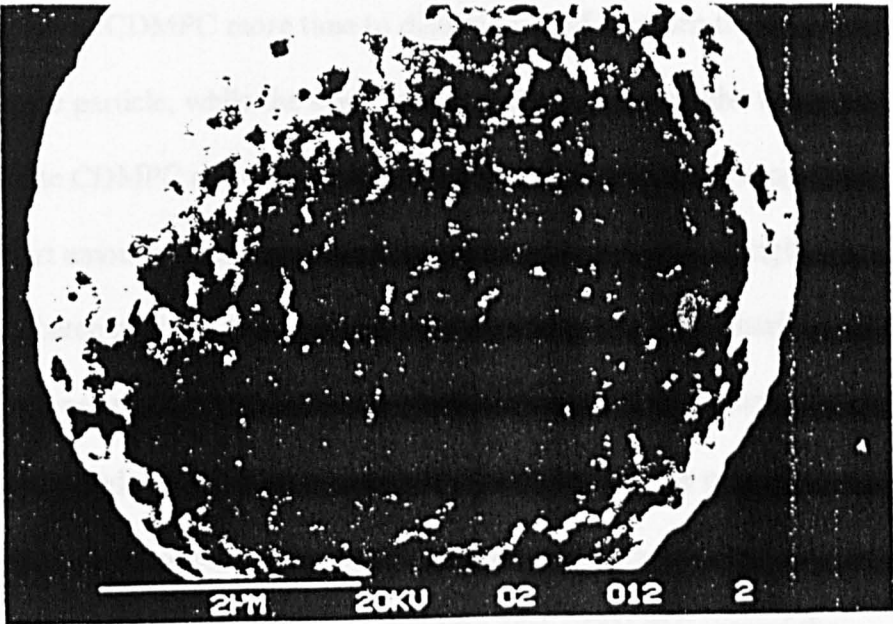
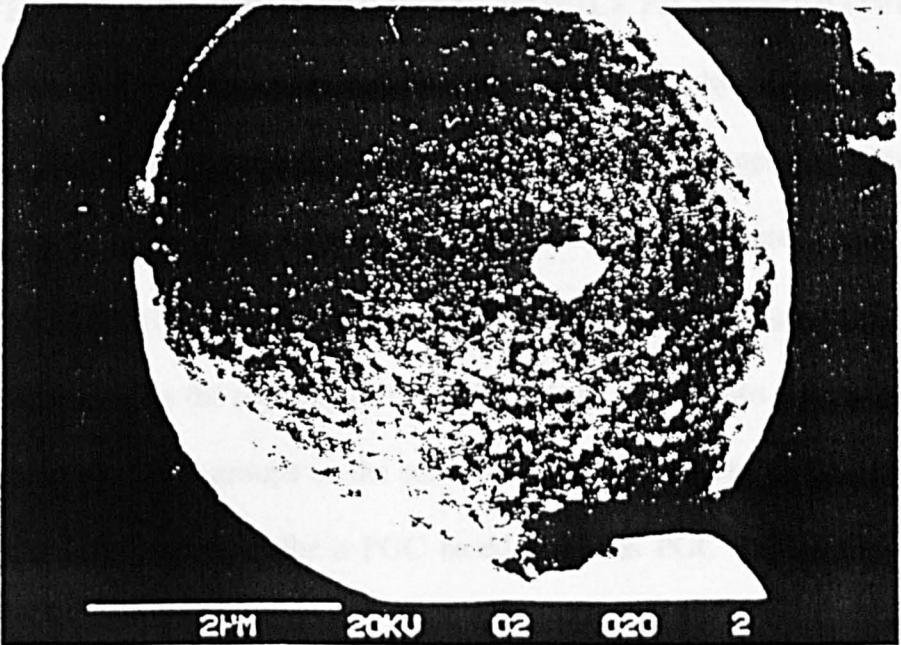


Figure 2.1.6 SEM of single-step coated particles



This supports the proposal that the improvement of the chromatography of Column 1 compared to Column 2 was due to the increase in surface homogeneity. The SEM study provides evidence for the suggestion that the batch coating method allows the CDMPC more time to distribute itself between the surface and the pores of the particle, while the single step method tends to inhibit the transport of the CDMPC on to the pores. It can be supposed that owing to the relatively short amount of time over which the coating is applied in single-step compared to batch addition that the coating does not have time to distribute itself evenly into the pores and on to the surface before all the solvent is removed and the process is halted. It also may be owing to the increase in the concentration of the coating sample in solution in the single-step process. The increased concentration may inhibit effective mass transfer of the CDMPC around the particle.

2.2 THE USE OF ACIDIC AND BASIC MOBILE PHASE ADDITIVE

The use of organic mobile phase additives in chromatography on silica based phases is common. For basic analytes the addition of a silanol suppresser, usually diethylamine (0.1% v/v)⁶⁷ or for acidic analytes an ionisation suppresser such as trifluoroacetic acid (0.5% v/v)⁶⁸ recommended to reduce peak tailing. The use of these modifiers masks the majority of the non-selective interactions of the analyte with any residual silanol groups on the surface of the silica. It was hoped that this would be less of a problem for a PGC based phase as PGC has relatively no surface functionality in comparison to silica. However, the use of both acidic and basic additives improved chromatography on the PGC based phase.

2.2.1 Acidic mobile phase additives

It was found that in contrast with the APS silica based phase acidic analytes could be successfully resolved on the PGC based phase without the addition of a mobile phase additive. It was the case however, that the addition of an acidic co-solvent improved the separation of the racemic mixture and reduced peak tailing.⁶⁵ The initial study conducted by Grieb showed increases in both R_s and α however, no pattern was established for the retention characteristics of the column.

2.2.2 Effect of TFA on peak widths, retention and resolution

A series of four acidic analytes were resolved on an optimised CDMPC on a PGC column (Column1) both with and without TFA (Table 2.2).

Table 2.2 The Effect of TFA on the chromatographic behaviour of acidic analytes

Analyte	TFA concentration %	t_0	t_1	t_2	w_1	w_2	k_1	k_2	α	R_s
MAA	0	1.95	10.55	13.5	1.4	1.8	4.41	5.92	1.34	1.84
MAA	0.1	1.95	9.6	12.65	1.18	1.65	3.92	5.49	1.40	2.16
2-PBA	0	1.95	5.75	10.7	0.85	1.7	1.95	4.49	2.30	3.88
2-PBA	0.1	1.95	5.55	10.9	0.82	1.95	1.85	4.59	2.49	3.86
MA	0	1.95	16.65	22	3.25	3.4	7.54	10.28	1.36	1.61
MA	0.1	1.95	14.6	18.55	2.15	2.8	6.49	8.51	1.31	1.60
2-PPA	0	1.95	6.1	13.35	1.05	2.3	2.13	5.85	2.75	4.33
2-PPA	0.1	1.95	5.9	13.1	1	2.2	2.03	5.72	2.82	4.50

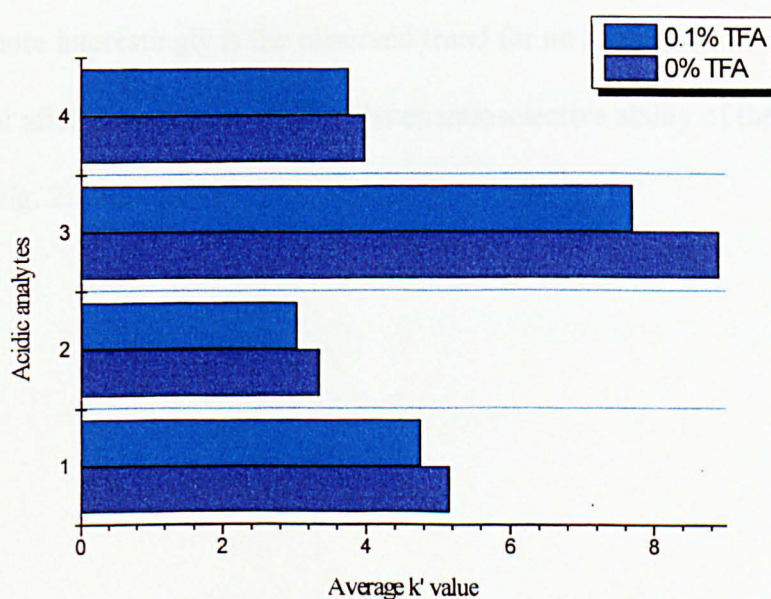
Mobile phases : MAA, 2-PBA, MA and 2-PPA, hexane/2-propanol (90:10 v/v).

Flow rate : 0.5 ml/min

It can be seen that the addition of TFA to the mobile phase decreases the capacity factors of most acidic analytes. The exception to the overall improvement in separation is mandelic acid which shows a slight decrease in α value and no change in resolution. This situation will be discussed in more detail later.

The column is being examined under normal phase conditions, therefore, no water is present. This eliminates any effect due to a decrease in pH from the addition of an acid. It can be suggested therefore that the observed decrease in retention is due to the competitive binding of TFA to sites of non-stereospecific interaction on the surface of the stationary phase. As PGC is essentially void of surface functionality it can be assumed that the TFA is interacting mainly with the CDMPC portion of the phase. This is further displayed by Figures 2.2.2 and 2.2.3.

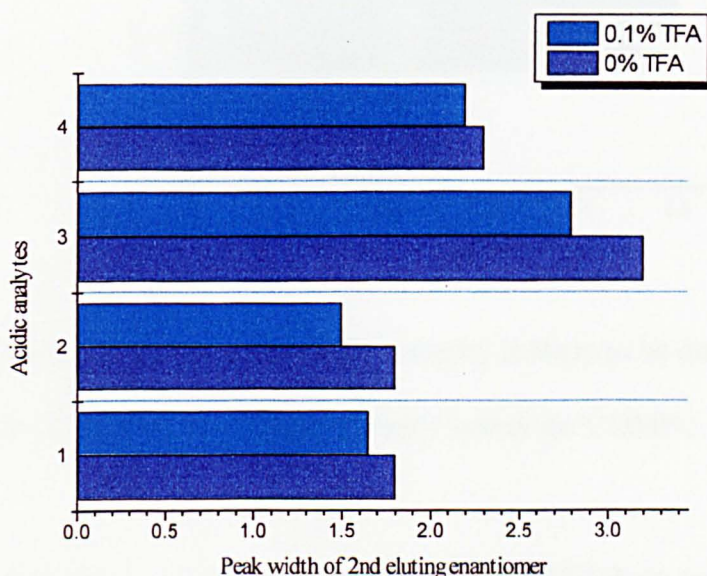
Figure 2.2.2 The Effect of TFA on capacity factors



Acidic analytes : 1, MAA; 2, 2-PBA; 3, MA; 4, 2-PAA.

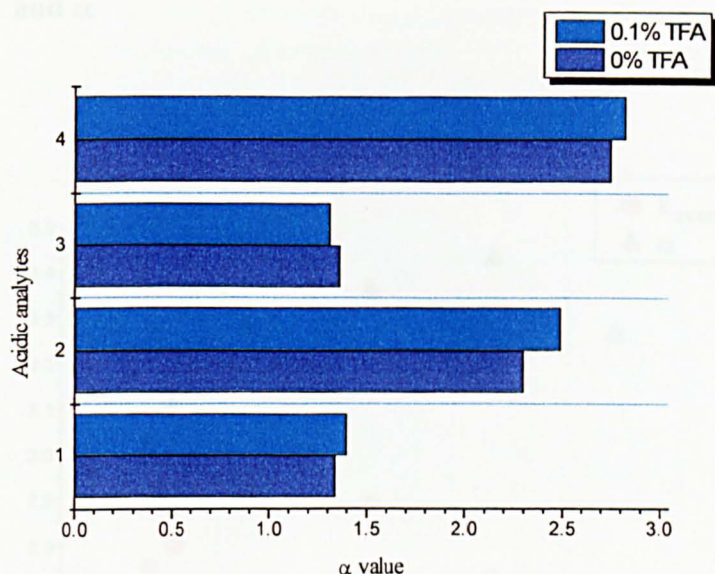
The addition of TFA to the mobile phase decreases the retention of the analyte. As the analyte is spending less time on the column there is less opportunity for non-specific interactions to occur. This acts to reduce peak tailing (Fig. 2.2.3).

Figure 2.2.3 The Effect of TFA on peak width



However, more interestingly is the observed trend for an increase in α value. This suggests that after the addition of TFA the enantioselective ability of the column increases (Fig. 2.2.4).

Figure 2.2.4 The Effect of TFA on α value

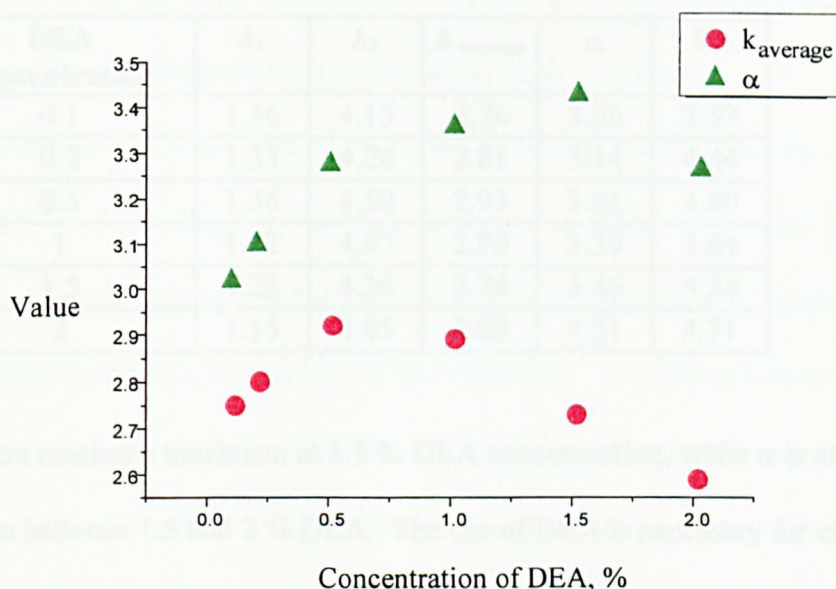


This perceived increase in enantioselectivity is likely to be due to TFA masking a non-stereoselective interaction probably within the CDMPC.

2.2.3 The effect of changing concentration of DEA on column performance

In contrast to chiral acids it has been observed that in the absence of DEA as a mobile phase additive, chiral bases are not eluted from naked or CDMPC coated PGC phases. However, the addition of 0.1% DEA to the mobile phase facilitates elution and produces resolution of the enantiomers. However, the effect of changing the concentration of DEA was unknown. The effect of changing the concentration of DEA between 0 to 2% (Fig 2.3.0).

Figure 2.3.0 The effect of changing the concentration of DEA on k_{average} and α



It can be seen that a maximum for both α and k_{average} is achieved between 1-1.5% DEA. This suggests that the sites of non stereospecific interaction are all masked at this concentration and any increase in DEA at this point will not improve chromatography. The maximum results from two opposing effects:

- an increase in stereoselectivity with the increasing DEA which predominates at lower concentration values
- a decrease in retention times due to increasing polarity of the mobile phase which is observed at higher concentration values

Table 2.3.1 The effect of DEA concentration on retention and resolution characteristics

DEA concentration	k_1	k_2	k_{average}	α	R_s
0.1	1.36	4.15	2.76	3.06	3.57
0.2	1.35	4.26	2.81	3.14	4.44
0.5	1.36	4.50	2.93	3.31	4.80
1	1.32	4.47	2.90	3.39	4.64
1.5	1.23	4.26	2.74	3.46	5.24
2	1.15	4.05	2.60	3.51	4.71

Resolution reaches a maximum at 1.5 % DEA concentration, while α is at a maximum between 1.5 and 2 % DEA. The use of DEA is necessary for elution, indicating that the interactions which DEA masks are very strong and retentive. The retention mechanism of PGC has been studied by several groups, but usually under reversed- phase conditions. Reversed-phase conditions permit ionisation owing to the presence of water. However ionisation is not dominant under normal phase conditions. The main interactions which exist under normal phase conditions will therefore be the electronic interaction with the π -cloud of delocalised electrons present at the surface of PGC. Bassler *et al* ⁶⁰ investigated the chromatography of substituted aromatic compounds under non-polar conditions and concluded that as well as dispersive interactions, electronic interaction with the delocalised band of electrons at the surface of PGC was possible. Lim *et al* ⁶⁹ concluded that the retention on PGC of inorganic and organic cations and anions was due to a mixture of reversed-phase and electronic interactions. They termed this mechanism 'Electronic Interaction

Chromatography'. As our system is used in normal-phase, it can be suggested that electronic interactions will dominate.

Karlsson *et al*⁶³ suggested that strong adsorption sites with limited capacities are responsible for the retention of aminoalcohols on PGC under normal phase conditions with low concentration of a chiral ion pair reagent.

More recently Elfakir and Dreux⁷⁰ used PGC for the qualitative analysis of glucosinlates and desulfoglucosinolates. They used a variety of organic mobile additives and examined their effect on the retention of 5 analytes. They found that the additives $\text{HClO}_4 > \text{NaClO}_4 > \text{TFA} > \text{KH}_2\text{PO}_4$. In each case there was only a small change in retention when the concentration of the organic modifier was increased. The number of theoretical plates was also determined and was found to increase significantly with the increase in concentration of the organic modifier. Consequently, the characteristics of the system were found to be dependent on the nature and the concentration of the organic modifier. Although this study was carried out under reversed-phase conditions it is analogous to those obtained with the use of DEA under normal phase conditions.

In conclusion, it can be suggested that the addition of acidic and basic analytes improve the chromatography of the test analytes under normal phase as well as reversed-phase conditions. This phenomenon is more pronounced with basic organic modifiers such as diethylamine. It has been suggested by Josefsson that the interaction the lone pair of electrons on the amine on the analyte interact with delocalised band of electrons at the surface of PGC and it is this which results in longer retention times. DEA provides another source of amine which can compete with the non-selective interaction of the analyte with the delocalised system of electrons.

The work carried out with basic analytes agrees with that of Josefsson.⁶²

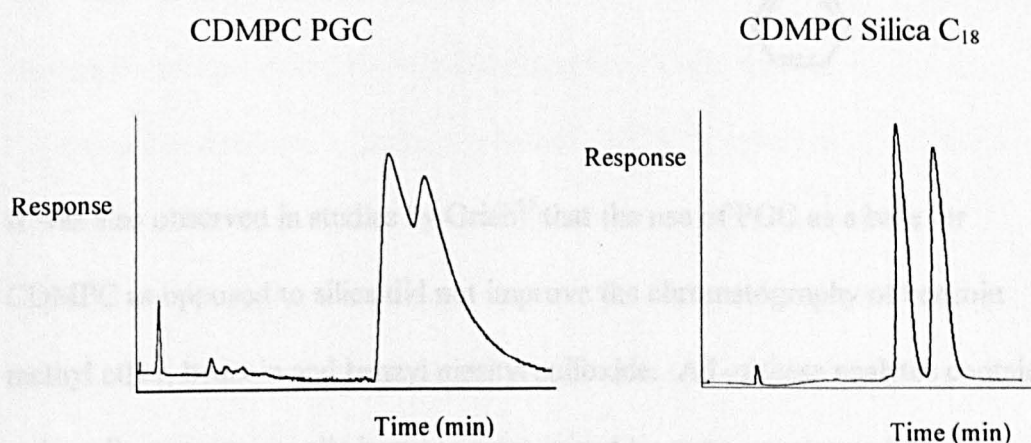
Accordingly, it can be suggested that the main mechanism of retention under normal phase conditions is interaction with the delocalised band of electrons at the surface of PGC.

The work with acidic analytes also shows a small decrease in retention and an moderate increase in resolution on the addition of TFA. This also suggests the presence of non-selective interaction. This is to a lesser extent than observed with basic analytes.

2.3 PROBLEM COMPOUNDS ON PGC

It has been previously observed⁶⁵ that some compounds do not give acceptable chromatographic separations on PGC based phases regardless of mobile phase additives or other conditions. This is demonstrated in Figure 2.3.1.

Figure 2.3.1 Separation of Flavanone enantiomers on PGC and silica based phases



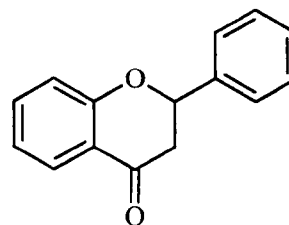
Mobile phase: hexane/2-propanol (90:10)
Flow rate: 1ml/min

Mobile phase: hexane/2-propanol (90:10)
Flow rate: 0.5ml/min

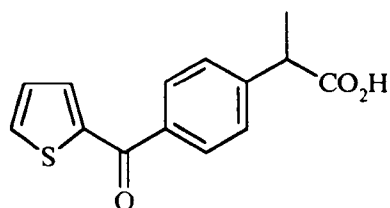
Other compounds which display poor chromatography on the PGC based phases include, those shown in Fig 2.3.2.

Fig 2.3.2 Problem compounds on PGC

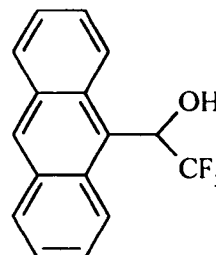
Flavanone



Suprofen



1-(9-Anthryl)-2,2,2-trifluoroethanol



It was also observed in studies by Grieb⁶⁵ that the use of PGC as a base for CDMPC as opposed to silica did not improve the chromatography of benzoin methyl ether, benzoin and benzyl mesityl sulfoxide. All of these analytes contain 2 polycyclic systems, usually benzene rings joined by some unsaturated group, usually a carbonyl group.

The analytes in Fig. 2.3.2 also contain multiple aromatic systems. All of the analytes can be considered to have a high degree of rigidity. The ability of a molecule to fit on to the surface of PGC has been suggested as the dominant

factor in retention. It has been shown that anthracene is very strongly adsorbed as it can easily accommodate itself freely on to the flat surface of PGC.

This feature of PGC makes possible the separation of geometric isomers.

The problem compounds possess large planar aromatic systems which were predicted to be strongly adsorbed to the surface of PGC.

2.4 CONCLUSIONS

In support of the work of Grieb, 25 %w/w coating of CDMPC on PGC by the batch method is the optimum phase. This phase has been used to separate a range of neutral, acidic and basic analytes. The effect of both acidic and basic mobile phase additives has been studied and the mechanism of retention has been further investigated.

TFA was found to increase the capacity factor and reduce peak width for acidic analytes. It is assumed that this occurs owing to the binding of non-selective sites on the phase by the TFA in preference to the acidic analyte.

DEA was found to have a dramatic influence on the chromatography of bases.

On the addition of 0.1% DEA elution was obtained with resolution of the enantiomers. Changing the concentration of the DEA revealed two opposing effects, the most interesting of which was the increase in stereoselectivity which was observed at low concentrations of DEA.

It can be suggested that this is owing to the masking of sites of non-specific interaction. This is analogous to the situation observed with acidic analytes but is far more pronounced for bases.

The chromatography of problem compounds, such as flavanone, on PGC based phases has not been improved. However, it can be suggested that these

compounds are poorly resolved because of their highly planar aromatic structures which interact strongly with the delocalised π -system of electrons which is present at the surface of the PGC.

The use of porous graphitic carbon as a support for cellulose tris (3,5-dimethylphenyl) carbamate produced a durable phase which can be easily switched between polar and non-polar conditions⁶⁵. This offers an advantage over silica based phases which are sold commercially as polar or non-polar dedicated columns. The use of PGC as a support however, can not be commercialised at the present time due to the patent held by Daicel covering derivatised polysaccharide phases. For research purposes however, several areas of further work can be considered. The poor chromatography of compounds such as Suprofen on the PGC based phase compared to a silica based phase requires further work. The set of compounds described in this thesis did not provide a large enough group to allow any firm assessment of the structural characteristics which hinder the separation. The use of large polycyclic groups such as anthracene to block any interaction with the PGC may have improved the chromatography. The use of such a blocking agent or developing methods of improving the monolayer coverage to exclude unwanted interactions would be desirable. Methods of coverage other than evaporation such as precipitation may be more effective at delivering a homogeneous coating to the PGC surface. Derivatised polysaccharide phases can be considered to be possibly the most widely used phases for chiral separations within industry and academia. The use therefore, of PGC as a support expands the knowledge of these phases and the conditions under which they can be used.

CHAPTER 3

THE SYNTHESIS OF POLY-L-LEUCINE AND ITS ANALYSIS BY MALDI-TOF AND ESI MASS SPECTROMETRY

Chiral stationary phases in liquid chromatography have made a very large contribution to both the analysis and production of single pure enantiomers. The method is fast, accurate, flexible and effective. However, as a technique, it does have some characteristics which may make it unsuitable for a particular application. The analysis or resolution of a mixture of enantiomers, by definition, results in more than one component product. This therefore, means that the technique yields both enantiomers when only one may be required. This becomes a burden when the production moves to preparative scale, and may be prohibitive if the racemate is expensive, and of the two component product half is unwanted. The development of enantioselective organic synthesis has addressed this problem and offers many techniques for the synthesis of single enantiomers.

Enantioselective organic synthesis can be defined as the *de novo* synthesis of a chiral substance from an achiral starting material such that one enantiomer predominates over the other.

Methods for enantioselective organic synthesis included;

- use of enzymes in biotransformations - ‘natural’ chiral catalysts
- use of organic and inorganic chiral catalysts

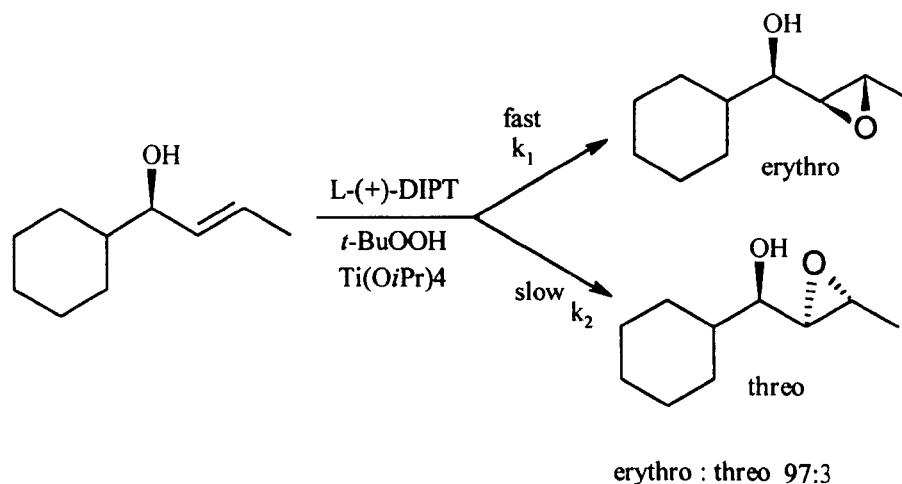
These techniques have also been applied to chiral separations in liquid chromatography. Examples of this were discussed in Chapter 1 when it was shown that biomacromolecules, in particular bovine serum albumin and α_1 -acid glycoproteins, have been used as chiral selectors in liquid chromatography. The use of metal-ligand complexes in chiral LC has also been mirrored by the use of similar complexes in enantioselective organic synthesis. Chiral ligand-exchange chromatography is performed by adding a selector ligand paired with a transition metal in the mobile phase. Many combinations of chiral selector, stationary phase, metal ion and selectand have been used. Lindner *et al.*⁷¹ used the following combinations for the resolution of dansylated amino acids (Fig. 3.0.1);

Figure 3.0.1 Chiral ligand exchange combinations

Chiral selector	Stationary phase	Metal ion	Selectand
L-2-isopropyl-4- <i>N</i> -octyl-diethylene-triamine	Silica C ₈ Reversed-phase	Zn ²⁺	DNS-D,L-amino acids
[(C ₃ - C ₈) - diene] <i>N</i> -octyl-L-Pro-amide	Silica C ₈ Reversed-phase	Zn ²⁺ , Cd ²⁺ Ni ²⁺ , Cu ²⁺ Hg ²⁺	DNS-D,L-amino acids and dipeptides

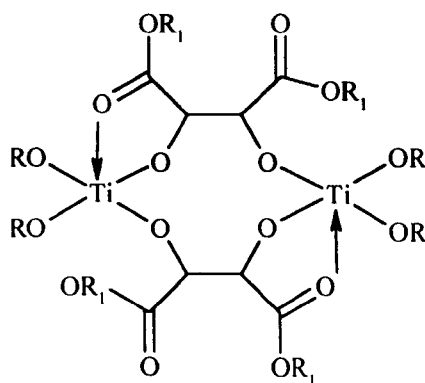
This approach was also used in enantioselective organic synthesis, and was possibly best demonstrated by the work of Sharpless *et al.*⁷² (Fig. 3.0.2). This work showed the highly efficient stereocontrolled epoxidation of allylic alcohols in conjunction with the kinetic resolution of the unreacted starting material. Sharpless demonstrated an enantiomeric excess of >96%.

Figure 3.0.2 Enantioselective synthesis followed by kinetic resolution



The use of the chiral ligand-transition metal approach was again highlighted by Sharpless working in conjunction with Katsuki,⁷³ who demonstrated the use of complexes such as the one shown in Figure 3.0.3 to effect enantioselective epoxidation.

Figure 3.0.3 Titanium complex implicated in Katsuki-Sharpless epoxidation



Techniques which are applied to enantioselective organic synthesis can also be used to effect a separation of isomers in chiral liquid chromatography. This is an obvious statement as a limited range of methods exist for the recognition of enantiomers, separation or selective synthesis occurs when the mechanism of recognition is stronger for one enantiomer than the other.

A precedent therefore exists for the transfer of ideas from enantioselective organic synthesis to chiral liquid chromatography.

This became a source of interest to us as more research was carried out into poly-amino acids and in particular poly-L-leucine and its application in enantiomeric organic synthesis. Following the work of Okamoto who used optically active polymers as chiral selectors in chiral liquid chromatography, it was decided to explore the opportunity of using a polypeptide as a chiral selector coated on to PGC in chiral HPLC. The use of homopolypeptides coated onto the surface of a support material has to our knowledge not been previously reported. L-amino acids offer a cheap and enantiomerically pure range of compounds with various derivatisable functionality. The use of poly-L-leucine provided an opportunity to explore the relationship between a homopolypeptide and PGC. Initially the use of poly-L-leucine provided a peptide which had been shown to have some degree of enantioselectivity under particular conditions⁸⁰. It was hoped that this would not be lost due to interaction with the PGC. Poly-L-leucine coated on to PGC therefore, provides a novel system to study with the opportunity to exploit other amino acids in the future.

groups. Polypeptides tethered to a cross-linked polystyrene were also studied. The work led to the conclusion that the nature of the terminal group did not influence the optical and chemical yield. However, tethering the poly-L-alanine to the insoluble polymer did mean that the catalyst was easier to recycle from the reaction mixture.

Figure 3.2.0 Structural variation in polypeptide catalyst

Catalyst	Degree of polymerisation (DP)	Chemical yield (%)	Enantiomeric excess (%)
Poly-L-alanine	19	76	80
Poly-L-alanine	>50	92	96
Poly-L-leucine	10	80	97

The weight of the polypeptide is therefore considered to be important. However, the secondary structure i.e. α -helical conformation, is also considered to be necessary to the activity of the catalyst. This was shown when Julia and Colonna produced a range of random copolymers of different amino acids, each amino acid with a different tendency to form an α -helix (Fig. 3.2.1).

Both alanine and leucine have a high tendency to form alpha helices when polymerised whereas valine has a low tendency. The nature and determining factors of the α -helical conformation are discussed in detail in Chapter 4.

Figure 3.2.1 Random copolymer polypeptide catalysts

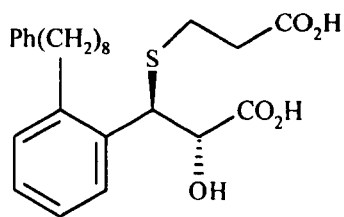
Catalyst	Tendency to form α -helix	Chemical yield (%)	$[\alpha]^{20}_{578}$ (CH ₂ Cl ₂)	Enantiomeric excess (%)
[(L-Leu) ₁ -(L-Ala) ₁]	High	67	-204	95
[(L-Val) ₁ -(L-Ala) ₁]	Low	39	-190.2	88
[(L-Val) ₇ -(L-Ala) ₃]	Lower	14	-83.9	39
[(L-Val) ₉ -(L-Ala) ₁]	Lowest	9	-25.8	17

The results from Figure 3.2.1 by Julia and Colonna show that the formation of the α -helix is crucial to the activity of the polypeptide catalyst.

3.3 APPLICATION OF THE WORK OF JULIA AND COLONNA TO INDUSTRIAL PROCESSES

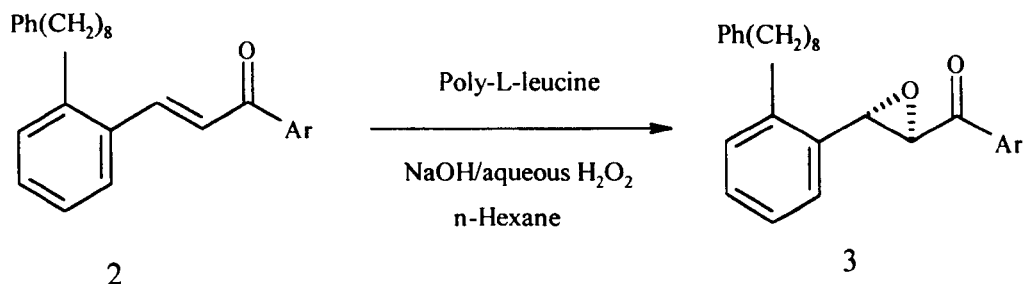
Asthma is a very serious disease in the Western world today which claims many lives and blights millions of others. The research into treatments led to the observation that leukotrienes are agents in the pathophysiology in asthma and related disease states. Lantos *et al.*⁸⁰ at SmithKline Beecham Pharmaceuticals developed a potent and selective leukotriene antagonist, SK & F 104353 (Figure 3.3.1)

Figure 3.3.1 Leukotriene antagonist, SK & F 104353



This molecule contains both a chiral alcohol and chiral thiol in the (2S,3R) stereoconfiguration. These groups are easily obtainable from a chiral epoxide. Lantos *et al.*⁸⁰ chose to use poly-L-leucine as the catalyst to produce a chiral epoxide because the reaction conditions are mild, the reaction is relatively simple to carry out and the enantioselectivities can be exceedingly high (Fig. 3.3.2).

Figure 3.3.2 Step 2 in synthesis of SK & F 104353



The compound 3 was produced in 82 % chemical yield and 95 % enantiomeric excess, after re-crystallisations the enantiomeric excess was increased to >99.8 %.

Poly-L-leucine was used in a large scale of >200g.

Poly-amino acids were also used in the synthesis of the antibiotics methymycin and erythromycin.

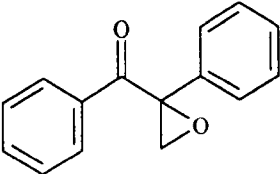
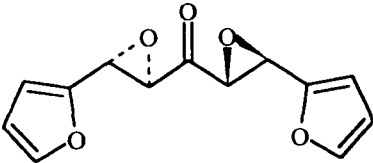
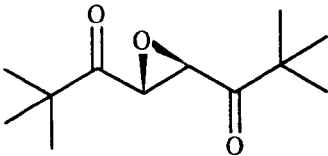
Poly-L-leucine was used in this case in preference to poly-L-alanine. One reason for this was that as poly-L-leucine is more sterically hindered and therefore less

susceptible to hydrolysis in the basic reaction medium. This means that the polymer is still active after it has been recovered from the reaction medium and can therefore be recycled.

The work of Julia and Colonna was developed by Roberts *et al.*⁸¹ who aimed to expand the range of analytes to which poly-L-leucine is applicable.

More recently Roberts⁸² has described the use of poly-L-leucine in the unexpected synthesis of a variety of epoxides derived from enones, an enynone, enediones and an unsaturated ketoester (Fig. 3.3.3).

Figure 3.3.3 Unexpected synthesis

Epoxide	Chemical yield (%)	Enantiomeric excess (%)
	78	59
	60	90
	>95	>95

Roberts *et al.*⁸³ examined the method of synthesis of the poly-L-leucine catalyst.

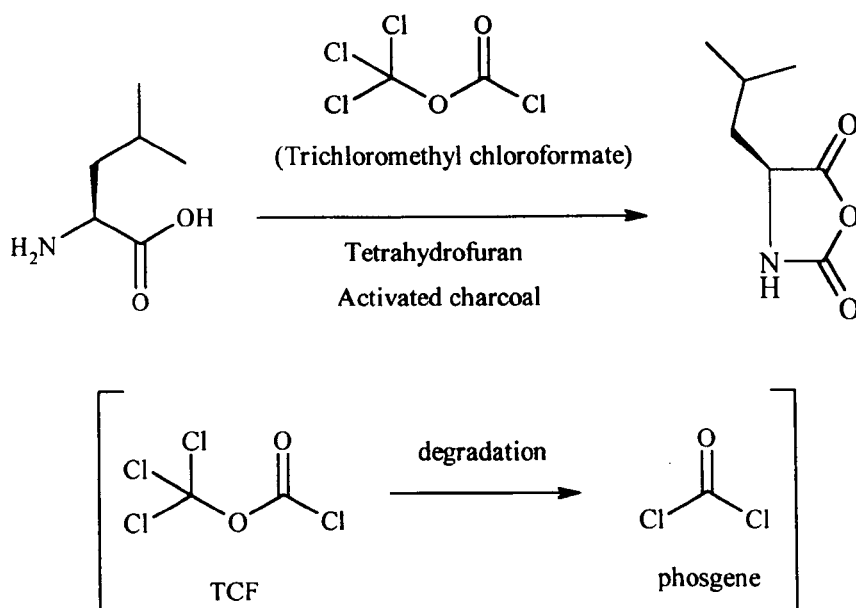
They discussed two different initiation methods and a method for immobilising the poly-L-leucine on polystyrene. Poly-L-leucine is available commercially, but, it is very expensive. Both Julia and Colonna, and Roberts used polypeptides which

they synthesised in-house to carry out the enantioselective catalysis. In the next section (3.4) is a discussion of the synthetic methods that we used to produce poly-L-leucine.

3.4 SYNTHESIS OF POLY-L-LEUCINE

The usual method of synthesis of homopolypeptides depends on the synthesis of an active monomer, such as the *N*-carboxy anhydride of the amino acid (Fig. 3.4.0),

Figure 3.4.0 Synthesis of L-leucine-*N*-carboxy anhydride



This method developed by Kataki *et al.*⁸⁴ uses activated charcoal and a temperature (55°C) high enough to bring about the decomposition of trichloromethyl chloroformate to phosgene which is the active component in the synthesis of L-leucine NCA. Trichloromethyl chloroformate is used at a 40% excess. This is sufficient for complete conversion of amino acid to amino acid NCA. The polymerisation procedures depend on L-leucine NCA being very pure.

This is often the case without need for any further purification, however recrystallization from diethyl-ether is recommended.

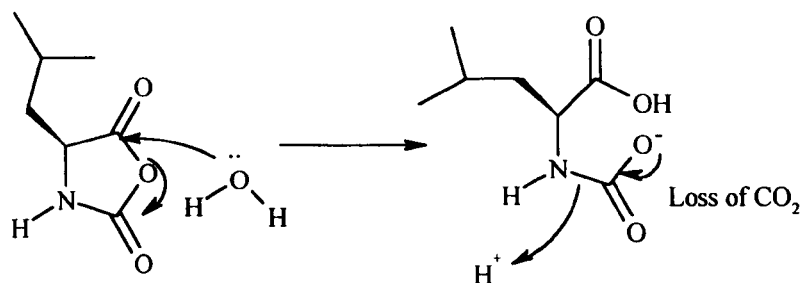
3.4.1 Initiation by water

This monomer is polymerised through initiation by a nucleophile, in particular water or an amine. L-leucine-NCA was polymerised in a humidity cabinet to produce a homopolypeptide with terminal carboxy and amine functionality (Fig. 3.4.1).

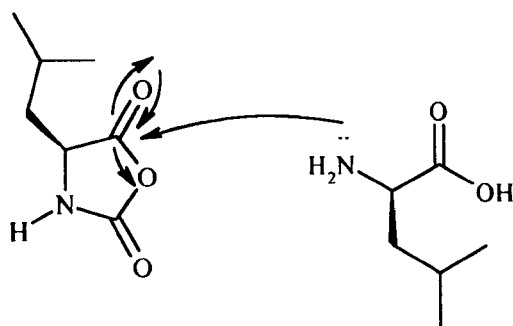
L-Leucine NCA, which is a white crystalline powder, is placed on a tray in the humidity cabinet and polymerisation takes place over 3 days approximately.

Figure 3.4.1 Homopolymerisation of L-leucine-NCA in a humidity cabinet

Initiation



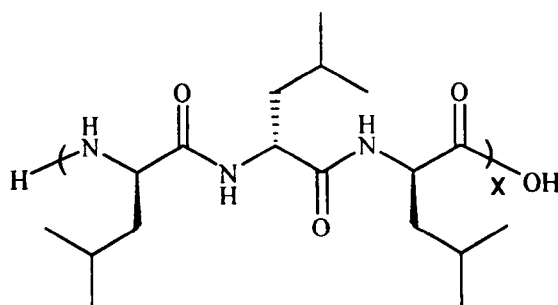
Propagation



This method depends on the fact that the L-leucine NCA must be extremely pure. Nucleophilic attack by water opens the anhydride with the loss of carbon dioxide. This provides an amine functionality to propagate the further ring opening of L-leucine NCA. A proposed mechanism of termination is attack by the nucleophilic amine group on the carbonyl group adjacent to the amine in L-leucine NCA. This results in the formation of a urea derivative terminated by two free carboxyl residues. This mechanism will be discussed in the sections relating to mass spectrometry later in this chapter.

It is suggested however, that the majority of termination occurs when the monomer is completely depleted. This produces a homopolypeptide which has both free amine and carboxy terminal functionalities (Fig. 3.4.2).

Figure 3.4.2 Free peptide synthesised by water initiation

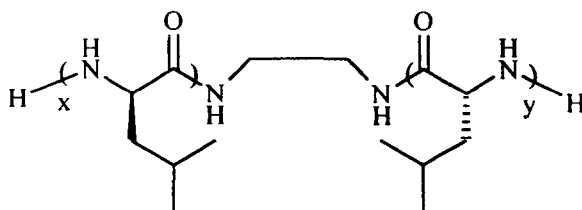


3.4.2 Initiation by amine

The initiation of L-leucine is also carried out in solution by a diamine, the reaction requiring a NCA/initiator ratio of 30:1. Ethylenediamine was used, which acts as a nucleophile and the mechanism of initiation is the same as with water. The reaction is carried out under stringent anhydrous conditions in dichloromethane.

The initiation by a diamine produces a polypeptide which is terminated by amine groups only (Fig. 3.4.3).

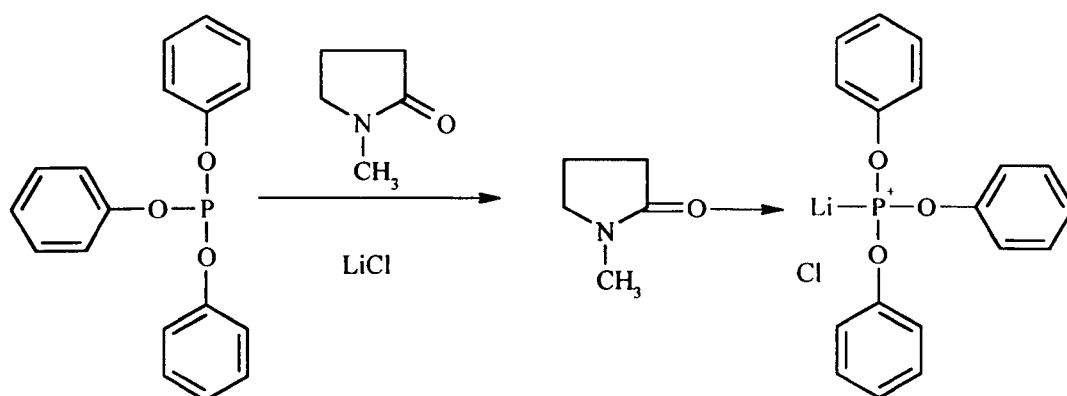
Figure 3.4.3 Ethylenediamine initiated polymerisation of L-leucine NCA



3.4.3 Synthesis of poly-L-leucine from L-leucine

This method has the advantage of using L-leucine as the monomer. The synthesis of L-leucine NCA produces phosgene as the active species. However, this makes the synthesis operationally demanding. Hagashi *et al.*⁸³ described the use of polyvinyl pyrrolidone of various molecular weight ranges as a matrix to support the polymerisation of L-leucine. The synthesis uses *N*-methyl pyrrolidine, LiCl and triphenylphosphite which combine to form an active species which initiates the polymerisation (Fig. 3.4.4)

Figure 3.4.4 Proposed active species in polymerisation of L-leucine

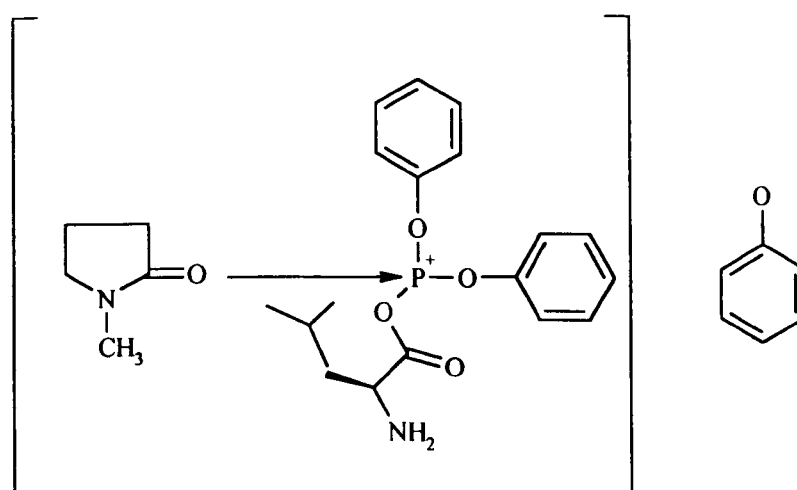


A

This complex has Cl⁻ as a counter ion and labile phosphine ligands which can be substituted by L-leucine molecules through reaction with the carboxylic acid residue (Fig. 3.4.5).

Figure 3.4.5 Proposed mechanism of initiation by complex in Figure 3.4.4,

A + L-leucine



Activation of the L-leucine allows the reaction of the activated carboxyl group with the free amine of another L-leucine molecule. This produces a homopolypeptide with free carboxyl and amine terminal functionality. *N*-methyl pyrrolidine is used as the solvent with a 1:1 ratio of L-leucine to triphenyl phosphite. The reaction mixture is refluxed for 16 hours. This is essentially a method of condensation polymerisation, the formation of cyclic polymers often occurs with such methods as the concentration of monomer falls. This was examined through the use of MALDI-TOF mass spectrometry.

All of these methods of polymerisation were applied on a 1 g scale to produce poly-L-leucine. This made it possible to examine the characteristics of this range of products using a range of techniques, ultimately as a chiral stationary phase in HPLC.

3.4.4 Problems with the analysis of poly-L-leucine

The main problem with the analysis of poly-L-leucine is its distinct lack of solubility. This is wholly due to the α -helical confirmation of the peptide chain which is stabilised by intrachain hydrogen bonding. The α -helix is necessary to the activity of poly-L-leucine as an asymmetric organic catalyst as seen in Section 3.2.

L-Leucine can be solubilized by disruption of the intrachain hydrogen bonds. This can be done by protonation by an acid, in particular trifluoroacetic acid (TFA).

The use of neat TFA as a solvent is not desirable in many techniques such as liquid chromatography and particularly in size exclusion chromatography and this prevents easy access to molecular weight and polydispersity information. Nuclear magnetic resonance (NMR) has been used for analysis as *d*-TFA is available. In

addition, the analysis of large molecules, such as poly-L-leucine, is inherently difficult owing to their size. This is most obvious in NMR when the slow tumbling motion of such molecules leads to considerable signal broadening. Several other techniques have been used to probe the structure of poly-L-leucine and they will be discussed in detail later. One technique that has been proved to be effective for the analysis of polymers including proteins and peptides, is mass spectrometry and in particular MALDI-TOF and ESI.

3.5 ANALYSIS OF POLY-L-LEUCINE BY MALDI-TOF AND ESI MASS SPECTROMETRY

Both MALDI-TOF and ESI are considered to be soft ionisation techniques. This makes them suitable for the analysis of homopolypeptides as the fragmentation of the polymer chains can be avoided. This makes it possible to observe the complete structure including end-groups, which offers a probe into the mechanism of the synthesis.

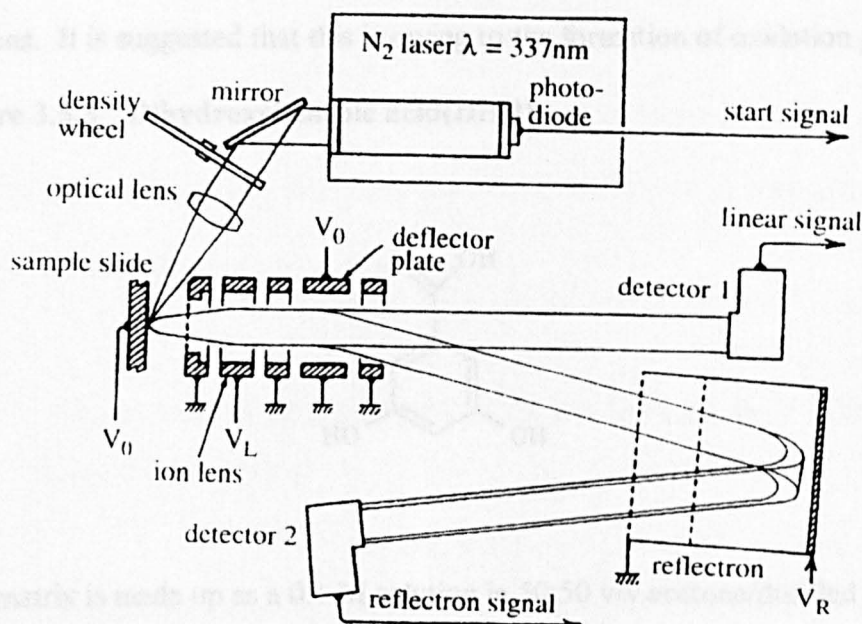
3.5.1 MALDI-TOF Mass Spectrometry

Matrix Assisted Laser Desorption/Ionisation Time-of-Flight mass spectrometry (MALDI-TOF), as the name suggests, uses another molecule which must be highly UV-absorbing, to act as a matrix to aid transfer of the sample to the gas phase. This technique was first described by Karas and Hillenkamp⁸⁴, and Tanaka *et al.*⁸⁵ in 1988. As described in Fig. 3.5.1 energy from the pulse of the laser, which is focused on to the solid sample, is transferred to the analyte molecules which are then ionised and vaporised. The production of intact, gaseous ions was most successfully described by Karas and Hillenkamp who were the first to use an organic molecule that adsorbed UV-light as a matrix. A solution of analyte and

matrix is placed on a stainless steel sample slide and allowed to dry. The solid sample contains homogeneously dispersed analyte molecules in a vast excess of matrix molecules. The energy of the pulse is transferred to the matrix and not directly to the analyte. A fraction of the matrix is vaporised carrying intact sample molecules into the gas phase. A charge is also transferred to the sample. This process of vaporisation and ionisation is not fully understood.

It can be seen in Fig. 3.5.1 that the Kratos III MALDI-TOF has the ability to be used in either reflectron or linear modes. In reflectron mode a longer flight tube is used to record the time-of-flight data. This decreases the sensitivity and increases the resolution of the detector. The opposite effect is observed when the machine is run in linear mode. This study used only reflectron mode. In linear mode the signal to noise ratio was too high to permit accurate interpretation of the data. Generally however, the data recorded in linear mode included higher masses than observed in reflectron mode. However, the resolution was too poor for individual signals to be distinguished.

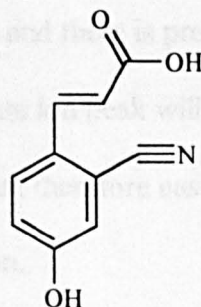
Figure 3.5.1 Schematic of Kratos III MALDI-TOF



3.5.2 Sample preparation

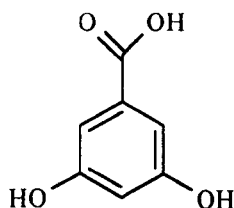
The matrix which is commonly used for proteins and peptides is α -cyano-4-hydroxy cinnamic acid (ACCA) (Fig. 3.5.2) or other cinnamic acid derivatives such as 3,5-dimethoxy-4-hydroxy-cinnamic acid.⁸⁶ For the study of poly-L-leucine ACCA was found to give more consistent results and will therefore be the only cinnamic acid derivative matrix to be considered.

Figure 3.5.2 α -cyano-4-hydroxy cinnamic acid (ACCA)



A popular matrix for use with synthetic polymers is dihydroxybenzoic acid (DHB) (Fig. 3.5.3), it was observed during this study that this matrix improves with ageing. Approximately 3 weeks after preparation the colour of the matrix darkens. It is suggested that this is owing to the formation of oxidation products.

Figure 3.5.3 Dihydroxybenzoic acid(DHB)



The matrix is made up as a 0.1 M solution in 50:50 v/v acetone/distilled water. It is usual to dope the matrix with a salt. In our studies, this was, sodium chloride. The glassware which is used to prepare both the matrix solution and the analyte solution contains both sodium and potassium ions. These ions are picked up by the analyte and the matrix. The presence of these ions means that when the analyte is vaporised both sodium and potassium ions are gained by the analytes. When such a MALDI-TOF spectrum is recorded, two series of peaks are observed. One series will have sodium ion attachment and therefore have 23+ the mass of the analyte peak, while the potassium series of peaks have 39+ the mass of the analyte peak. Accordingly the matrix is doped with sodium chloride so sodium ions are present in excess and there is preferential attachment. When this spectrum is recorded only a sodium ion peak will be observed. This technique produces simpler spectra which are therefore easier to interpret. The salt is added to the matrix as a 0.001M solution.

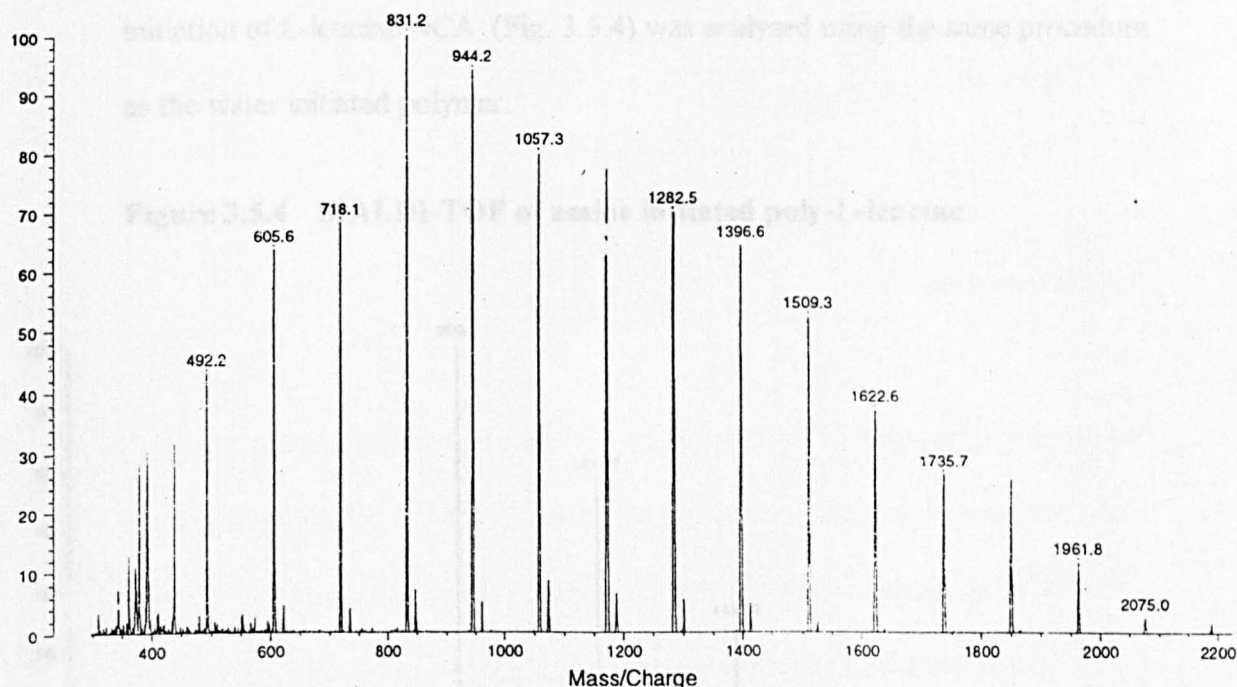
Poly-L-leucine is presented as a 1 mg/ml solution, although this may change depending on the nature of the analyte. The solutions are placed on to a stainless steel slide which has 20 small wells to hold the samples. The matrix (0.4 μ l) is spotted on to the slide using a syringe and allowed to dry. This is repeated once and the sample is placed on top of the matrix using the same procedure. The analyte and matrix may be premixed. However, in the case of poly-L-leucine, the matrix and analyte were added separately.

3.6 ANALYSIS OF POLY-L-LEUCINE BY MALDI-TOF MASS SPECTROMETRY

The lack of solubility of poly-L-leucine is a concern when producing a sample for analysis. It is important to include all molecular weight ranges in the analyte to ensure accurate analysis. Accordingly, poly-L-leucine is used as a solution of trifluoroacetic acid. The use of 100% trifluoroacetic acid(TFA) is not possible as when the sample is spotted on to the slide as the surface tension of the acid is too low to produce a droplet. It was therefore necessary to add water to the analyte to aid droplet formation. Poly-L-leucine is therefore used in 95/5 v/v TFA/water. All the spectra shown in this chapter were recorded on a Kratos III MALDI-TOF machine. Fig. 3.5.3 shows the spectrum of poly-L-leucine produced in the humidity cabinet (1 week) from L-leucine-NCA. The sample was washed with diethyl ether to remove any unreacted L-leucine NCA.

Figure 3.5.3 MALDI-TOF of Poly-L-leucine from L-leucine NCA

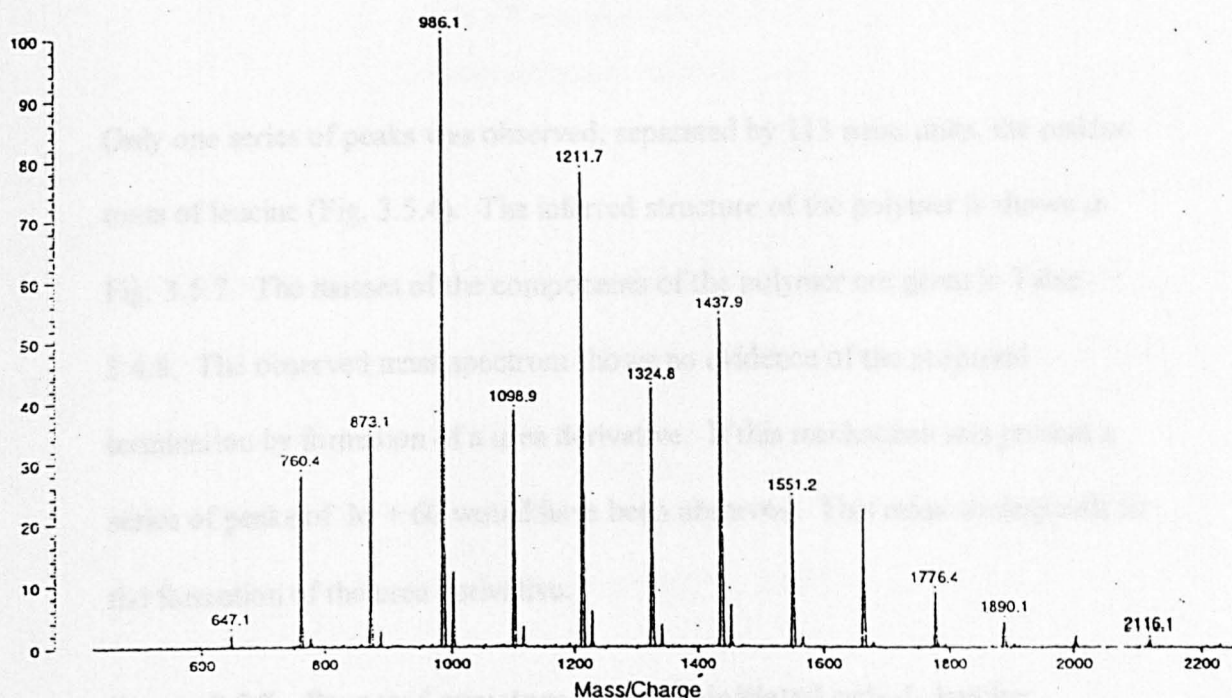
(Water initiation)



In Fig. 3.5.3 is shown the range of poly-L-leucine chains which are detected, the most probable peak (Mp) observed by MALDI-TOF is 1199.8 which corresponded to a poly-L-leucine chain of 10 units. The molecular weight range observed increases to approximately 3000 Da. MALDI-TOF is very mass sensitive, this means that although we observe a mass range from 400 - 3000 Da this may not be the whole mass range represented in the sample. Much higher masses may be present in the sample and these will not be observed in MALDI-TOF. It is not however, accurate to say that the intensities observed are representative for the whole analyte.

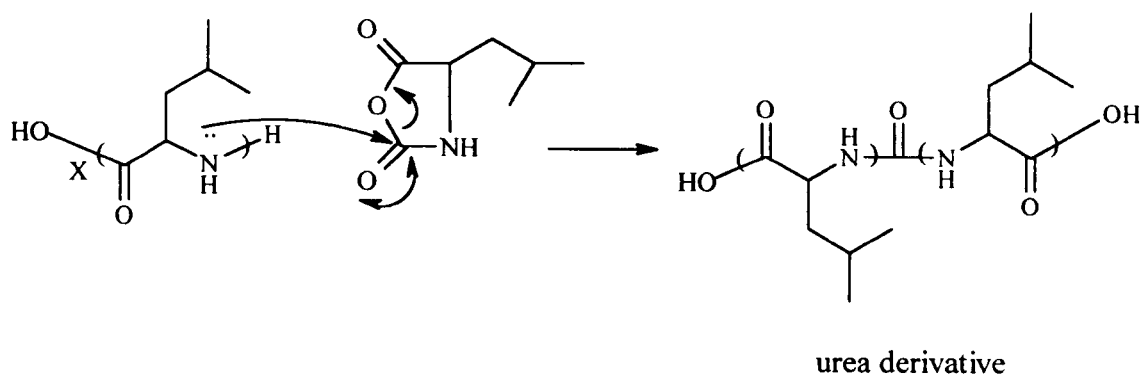
MALDI-TOF is accurate for the masses of poly-L-leucine chains which are observed. This makes possible the determination of end-group masses and the constitution of the chain. Accordingly, MALDI-TOF can distinguish between poly-L-leucine made by various methods. Poly-L-leucine made by the amine initiation of L-leucine NCA (Fig. 3.5.4) was analysed using the same procedure as the water initiated polymer.

Figure 3.5.4 MALDI-TOF of amine initiated poly-L-leucine



In Fig. 3.5.4 is shown a distinctly different spectra from that of Fig. 3.5.3. The amine used to initiate the polymerisation was ethylenediamine. The reaction was catalysed by triethylaluminium. The monomer:initiator ratio used was 120:1 and the catalyst was added in a 1:1 ratio with the initiator. The proposed mechanism of termination through attack by terminal amine on the α -carbonyl group to the amine of L-leucine NCA (Fig. 3.5.5) was not observed in MALDI-TOF.

Figure 3.5.5 Proposed termination mechanism of amine-initiated polymerisation of L-leucine NCA



Only one series of peaks was observed, separated by 113 mass units, the residue mass of leucine (Fig. 3.5.4). The inferred structure of the polymer is shown in Fig. 3.5.7. The masses of the components of the polymer are given in Table 3.4.8. The observed mass spectrum shows no evidence of the proposed termination by formation of a urea derivative. If this mechanism was present a series of peaks of $M + 60$ would have been observed. This mass corresponds to the formation of the urea derivative.

Figure 3.5.7 Proposed structure of amine-initiated poly-L-leucine

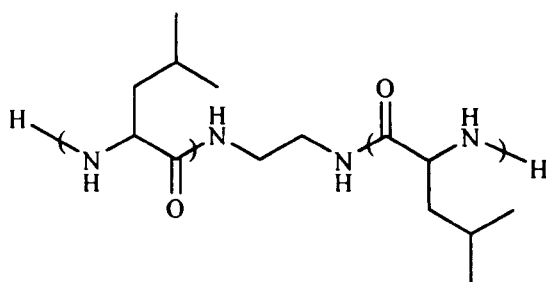
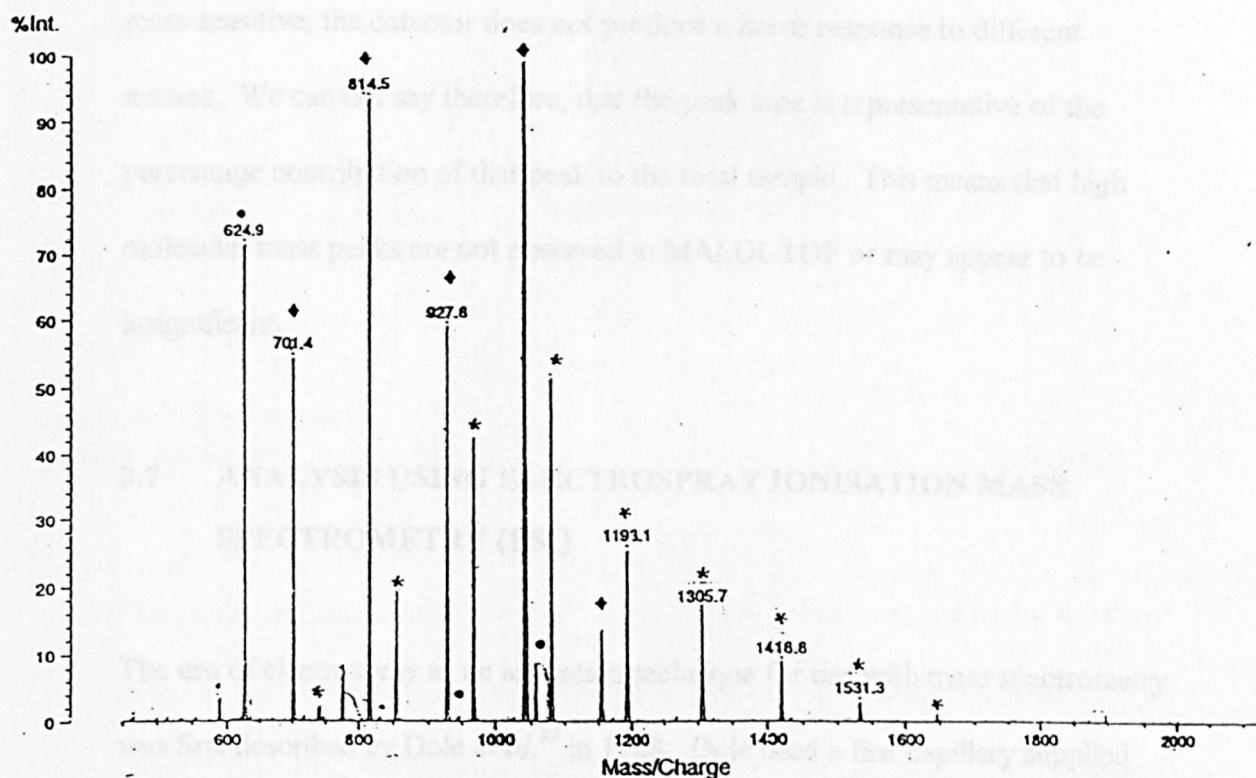


Table 3.5.8 MALDI-TOF characteristics of amine initiated poly-L-leucine

Characteristic	Mass
Na ⁺ ion attachment	23
Leucine residue	113
Terminal hydrogen	2
Inclusion of amine initiator	58

The alternative method for the synthesis of poly-L-leucine was to use L-leucine as the monomer(Section 3.4.3) through the use of triphenyl phosphite and N-methyl pyrrolidine. This is a very different mechanism of polymerisation than when NCA-leucine is used as the monomer, this results in a very different MALDI-TOF mass spectrum with multiple series of peaks (Fig. 3.5.8).

Figure 3.5.8 MALDI-TOF of poly-L-leucine synthesised from L-leucine using triphenyl phosphite and N-methyl pyrrolidine



This MALDI-TOF spectrum has three clear series of peaks (Table 3.5.9),

Table 3.5.9 Multiple series observed in Figure 3.5.8

Marker	Structure	Typical mass(M + 23)
♦	Cyclic(Leu) _x	1040.5
*	H.(Leu) _x .O ⁻ Na ⁺	1079.9
•	H.(Leu) _x .OH	1058.9

Although MALDI-TOF shows us that polymerisation has occurred and what the resulting polymer consists of, it does not give us any information about the molecular weight characteristics of the polymer. Since, MALDI-TOF is very mass sensitive, the detector does not produce a linear response to different masses. We can not say therefore, that the peak area is representative of the percentage contribution of that peak to the total sample. This means that high molecular mass peaks are not observed in MALDI-TOF or may appear to be insignificant.

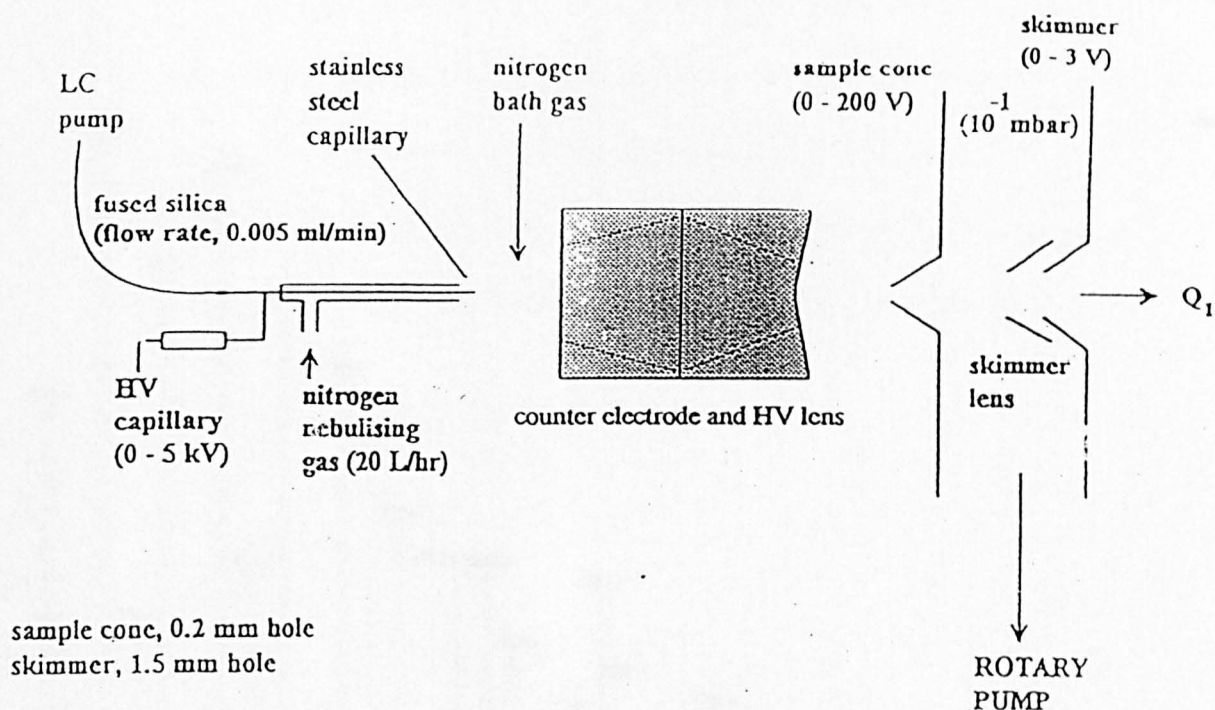
3.7 ANALYSIS USING ELECTROSPRAY IONISATION MASS SPECTROMETRY (ESI)

The use of electrospray as an ionisation technique for use with mass spectrometry was first described by Dole *et al.*⁸⁷ in 1968. Dole used a fine capillary supplied with an nebulising gas and applied voltage to produce a fine spray which could be analysed.

ESI can therefore, be described as the electrostatic nebulisation of a charged analyte solution, followed by the evaporation of the resultant droplets, to produce both singly and multiply charged gas phase molecular ions. ESI is a relatively soft ionisation technique and is performed at atmospheric pressure.

ESI discussed in this thesis was carried out on a VG “Quattro II” tandem quadrupole instrument equipped with an electrospray ionisation source (Fig. 3.7.0).

Figure 3.7.0 Schematic of the “Quattro II” electrospray source

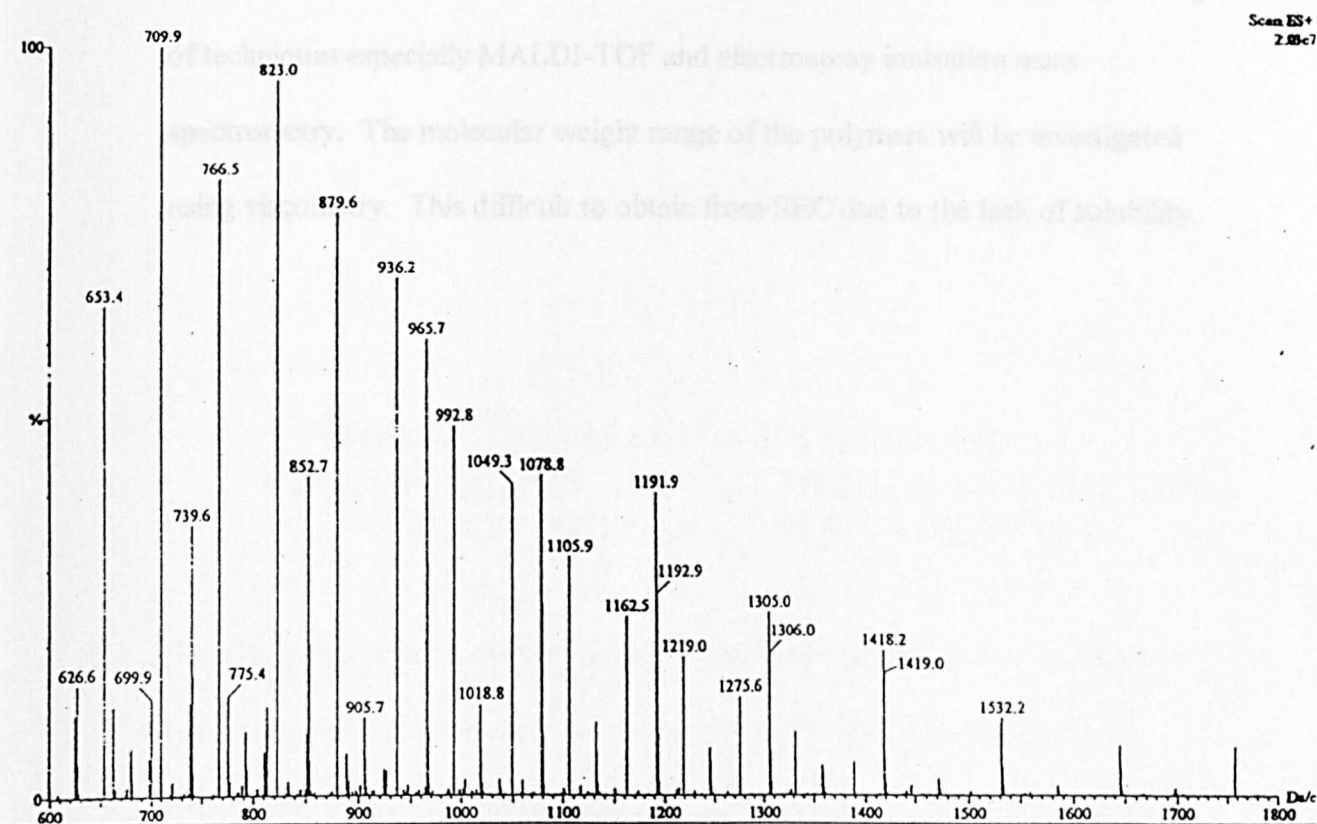


The production of multiply charged ions is advantageous as the effective mass range of the mass analyser is increased considerably. Very large compounds (greater than 100,000 Da) can therefore be detected by a mass analyser of modest mass/charge(m/z) range. This means that a quadrupole mass analyser is commonly used with ESI.

The solvent system chosen for the analysis of poly-L-leucine was crucial as it had to allow the sample to be presented as a solution of trifluoroacetic acid, which is the only solvent which would allow total dissolution of the polymer. The solvent chosen for this was chloroform:methanol:water (20:1:1) which is an unusual solvent in ESI.

The analysis of amine initiated poly-L-leucine shows several series of peaks which result from multiply charged ions (Fig. 3.7.1)

Figure 3.7.1 ESI mass spectrum of amine initiated poly-L-leucine



ESI, like MALDI-TOF, does not give an accurate representation of the molecular weight profile of the whole sample. It does however, let us probe the primary structure of poly-L-leucine. As molecular weight is an important factor in the determination of secondary structure and has been shown in both cellulose derivatives and poly-L-leucine to be important in the level of enantiorecognition which is expressed. In the next chapter therefore, methods for the control and determination of molecular weight of poly-L-leucine will be discussed.

3.8 CONCLUSIONS

The use of several methods to synthesise poly-L-leucine produces a range of structural characteristics. These structural differences can be examined by a range of techniques especially MALDI-TOF and electrospray ionisation mass spectrometry. The molecular weight range of the polymers will be investigated using viscometry. This difficult to obtain from SEC due to the lack of solubility.

CHAPTER 4

CHARACTERISATION OF STRUCTURAL CONFORMATION AND CONTROL OF MOLECULAR WEIGHT PROFILE OF POLY-L-LEUCINE

This chapter is intended to examine the characteristic of poly-L-leucine which may make it suitable for use in a chiral stationary phase. The α -helical secondary structure of poly-L-leucine has been discussed previously (Section 3.2) and the need for a regular structure in a chiral stationary phase based on polysaccharides was discussed in Section 1.5. It is desirable however, to probe the conformation of poly-L-leucine and how differences in synthesis effect this and the application to chromatography.

The manipulation of the molecular weight profile of poly-L-leucine can offer several different types of peptide to use for chromatography. The molecular weight of poly-L-leucine was controlled using the technique of solid phase peptide synthesis to produce a peptide of predetermined mass. The molecular mass of poly-L-leucine produced using techniques discussed in Section 3.4 was also manipulated using continuous extraction. The products of both processes were examined by MALDI-TOF and ESI mass spectrometry.

4.1 SOLID PHASE PEPTIDE SYNTHESIS (SPPS)

In 1963 Merrifield ⁸⁹ first described the technique of solid phase peptide synthesis, it was for the development of this technique which he was awarded the Nobel Prize for Chemistry in 1984. This technique has proved valuable for the synthesis of an extensive library of peptides. ⁹¹

The essence of SPPS is to retain the proven solution phase chemistry but to add a covalent attachment step which links the peptide chain to an insoluble peptide support. The solid phase avoids the need for solvent extraction, filtration and recrystallisation which are all necessary in classical liquid phase method.

The peptide is extended through a series of coupling steps which must proceed with high yield and accuracy to ensure that the final product is homogenous. The coupling steps are driven by the presence of excess reagents, which are removed by filtration and washing. This technique lends itself very well to automation although the scale is smaller than when the technique is carried out manually.

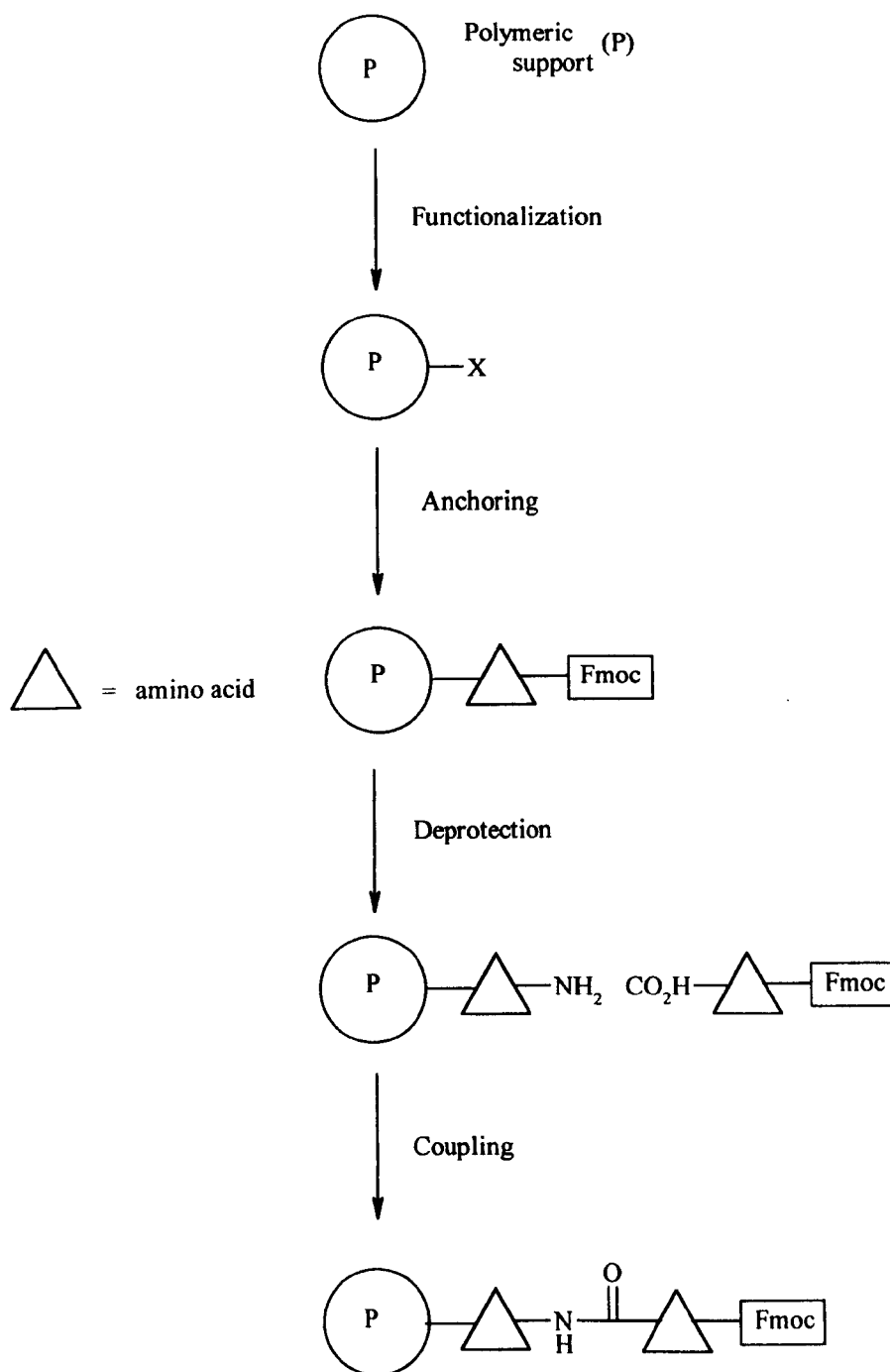
It was decided that poly-L-leucine should be produced as a 15-mer as it was believed that 15 amino acid residues would produce an α -helical secondary structure. It was hoped that the absolute control of molecular weight would allow us to probe the mechanism of enantiorecognition displayed by poly-L-leucine and the role of the α -helix.

All of the solid phase peptide synthesis discussed in this chapter was carried out in the laboratory of Dr Brian Ridge (Department of Chemistry, University of Exeter) under the supervision of Dr Ridge and Miss M. Palmer.

There are several variables in SPPS, these include;

- Protection scheme
- Polymeric support
- Coupling reagents
- Monitoring techniques
- Cleavage techniques

Figure 4.1.0 Schematic of stepwise solid-phase peptide synthesis of linear peptides

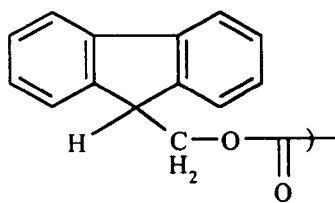


4.1.1 Protection chemistry

Protection of either the amine or carboxy terminal functionality allows control of the reaction between the end residue of the nascent peptide chain and the

incoming amino acid. This prevents reaction between the bulk amino acids in solution. One of the most popular forms of protection is the use of Fmoc (N^{α} -9-fluorenylmethoxycarbonyl) (Fig. 4.1.0) protection of the amino functionality. The use of this temporary base labile group was first described by Carpino *et al.*,⁹¹ Fmoc-amino acids are completely stable to acids and can be stored at 0°C with little decomposition. Fmoc-amino acids are usually prepared from fluorenylmethyl succinimidyl carbonate (Fmoc-OSu).

Figure 4.1.0 N^{α} -9-fluorenylmethoxycarbonyl (Fmoc) protecting group



It is this method of protection which was chosen to be used for the synthesis of poly-L-leu₁₅ because of the mild deprotection step and the commercial availability of Fmoc-L-leucine.

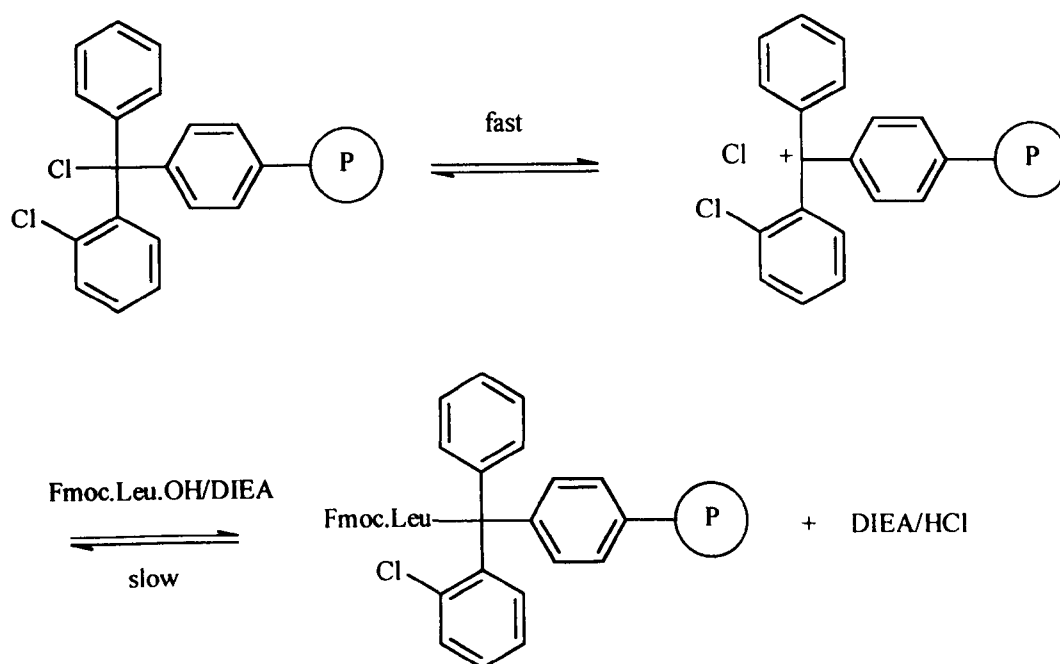
4.1.2 Polymeric Support

The support is often a polystyrene suspension polymer which had been cross-linked with 1% of 1,3-divinylbenzene; this produces 0.2mmol/g⁻¹ to 1.0mmol/g⁻¹ functionality at the surface of the bead. The dry beads are usually 50µm in diameter although when the beads are swollen for use this can increase to 300µm.

Almost all SPPS is carried out in the C→N direction and therefore the first reaction in the series is to anchor the initial amino acid to the bead either through a suitable handle or directly through the carboxy functionality.

Fmoc amino acids have been traditionally used with Wang resins⁹². These use 4-alkoxybenzyl alcohol resin/4-hydroxymethylphenoxy (HMP/PAB) linker. In the synthesis of poly-L-leucine however, the Barlos resin⁹³ was used. This resin (Fig. 4.1.1) uses 2-chlorotrityl chloride as the linker which allows a loading for the first amino acid of typically between 0.5-0.8 mmol/g.

Figure 4.1.1 Barlos resin



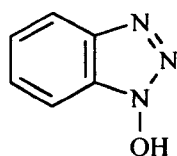
4.1.3 Coupling procedure

There are 4 major kinds of coupling techniques that are used in step-wise SPPS;

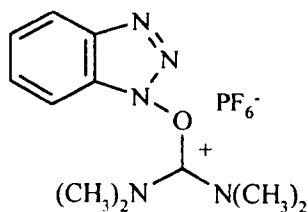
- *In-situ* reagents
- Active esters
- Pre-formed symmetrical anhydrides
- Acid halides

In-situ reagents are typified through the use of N,N'-dicyclohexylcarbodiimide (DCC)⁹⁴ which is also used in solution couplings. Such couplings are often carried out in the presence of 1-hydroxybenzotriazole (HOBt) which accelerates the reaction, suppresses racemisation and inhibits dehydration of the carboxamide side chain of the amino acid to the corresponding nitrile. HOBt (Fig. 4.1.2) is a coupling reagent in its own right as it acts as an active ester. It was active esters which were chosen to be used as the coupling technique in the synthesis of poly-L-leu₁₅. The hydroxybenzotriazole ion stabilises the transition state of the reactive intermediate through anchimeric assistance. This brings the free amine of the amino acid residue in line to react with the active ester of the carboxy group of the resin bound peptide chain. 2-(1H-Benzotriazole-1-yl)-1,1,3,3-tetramethyluronium hexafluorophosphate (HBTU) (Fig. 4.1.2) which acts in the same manner as HOBt was also used in the synthesis of poly-L-leu₁₅ as it provides the hydroxybenzotriazole ion and acts to prevent racemisation of the optically pure amino acids.

Figure 4.1.3 Active ester coupling reagents



HOBt



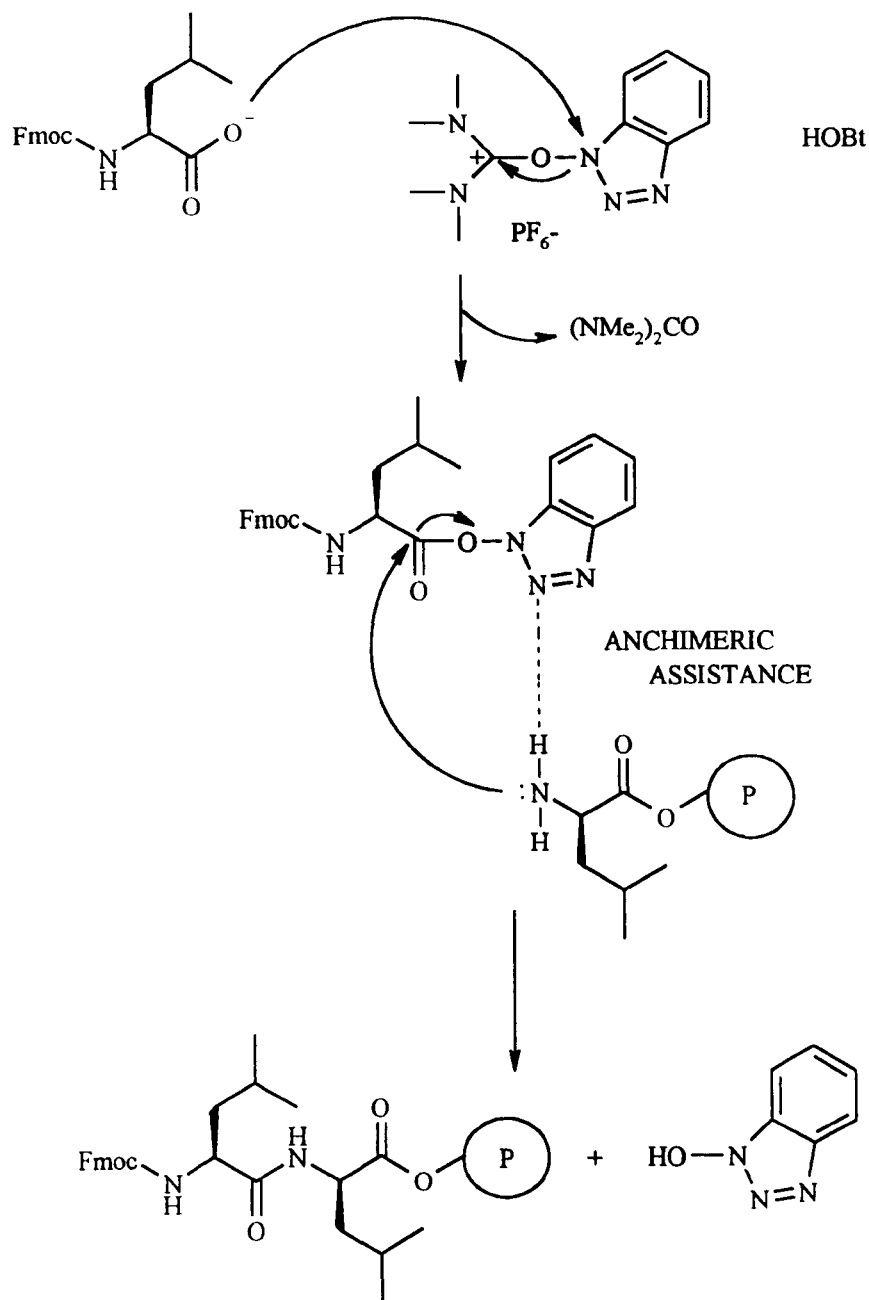
HBTU

1-Hydroxybenzotriazole

2-(1H-Benzotriazole-1-yl)-1,1,3,3-tetramethyluronium hexafluorophosphate

The proposed mechanism for coupling using HOBt/HBTU is shown in Figure 4.1.4. This mechanism begins with the activation of Fmoc.Leu.OH by diisopropylethylamine (DIEA) through the deprotonation of the carboxylic acid residue. The deprotonated acid then goes on to form an active ester (Fig. 4.1.4).

Figure 4.1.4 Formation of the active ester using HOBt

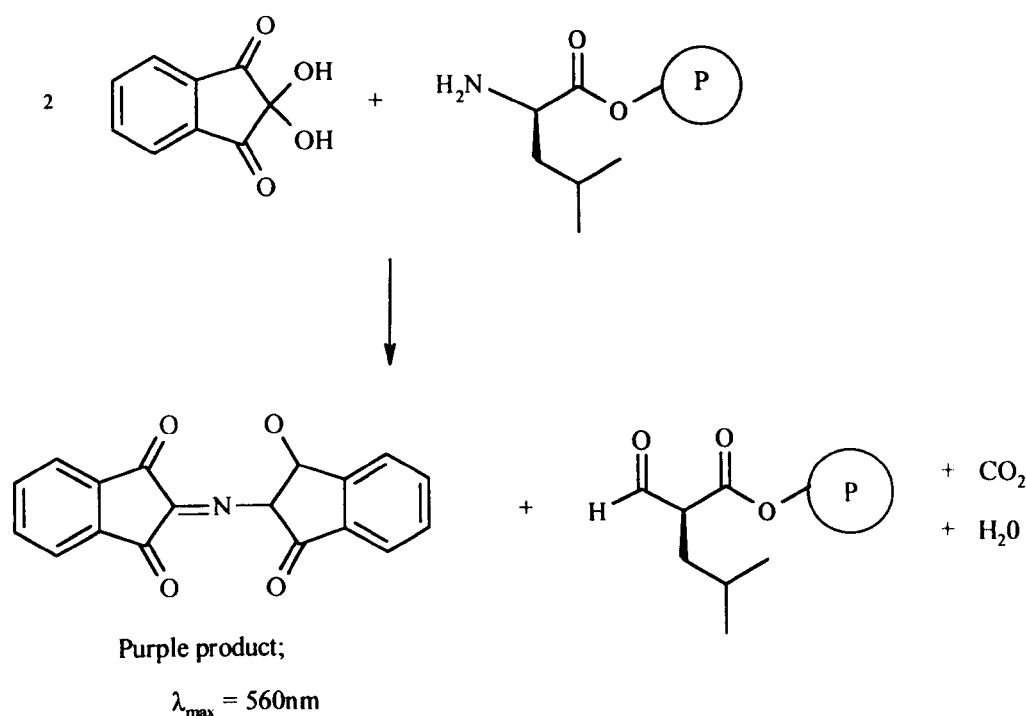


Both HOBt and HBTU provide the hydroxybenzotriazole ion which stabilises the transition state of the reactive intermediate by anchimeric assistance. This brings the free amine of the new leucine in to line to react with the active ester of the carboxy group of the resin bound peptide chain. HBTU has a dual purpose in this

synthesis; it provides excess hydroxybenzotriazole ion, and it is also an excellent agent to prevent racemisation of the optically pure amino acids.

At this point in the synthesis a test is required to ensure that the next residue has been successfully joined to the resin bound peptide chain, this test is called the Kaiser test.⁹⁵ The Kaiser test is based on the use of ninhydrin which produces a colour change in the presence of free amine residues (Fig. 4.1.5). Therefore the coupling of amino acid to the resin bound chain can be considered to be complete on the observation of a negative Kaiser test.

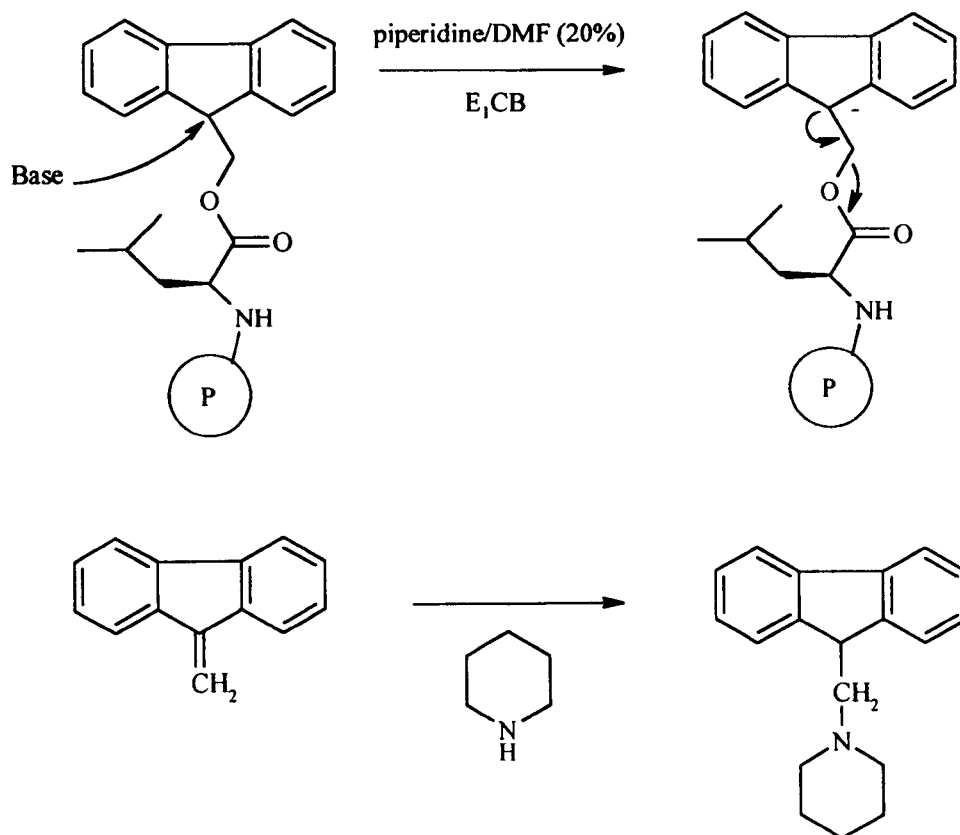
Figure 4.1.5 Kaiser test



As well as the Kaiser test it is important to have an understanding of how much of the original loading of peptide chain is still involved in coupling. It is inevitable that as the couplings proceed some peptide chains will not be available for reaction due to microheterogeneity; this is the main reason for aiming to have

100% reaction every time. The loading study is conducted as an assay of the presence of Fmoc residues (Fig. 4.1.6). Fmoc is cleaved with piperidine which leads to the formation of the piperidine-dibenzofulvene adduct; the production of this adduct is conveniently monitored at $\lambda = 290\text{nm}$.

Figure 4.1.6 UV assay of Fmoc protecting group



The absorbance of the solution at 290nm can be converted into a loading value through a formula developed by Ridge and Palmer⁹⁶ (Fig. 4.1.7),

Figure 4.1.7 Formula to determine loading in sequential SPPS

$$y = \frac{Ax}{1.650}$$

where;

A = absorbance at $\lambda=290\text{nm}$

y = loading, mmol/g

x = mass of sample in grams

4.2 THE SYNTHESIS OF POLY-L-LEU₁₅

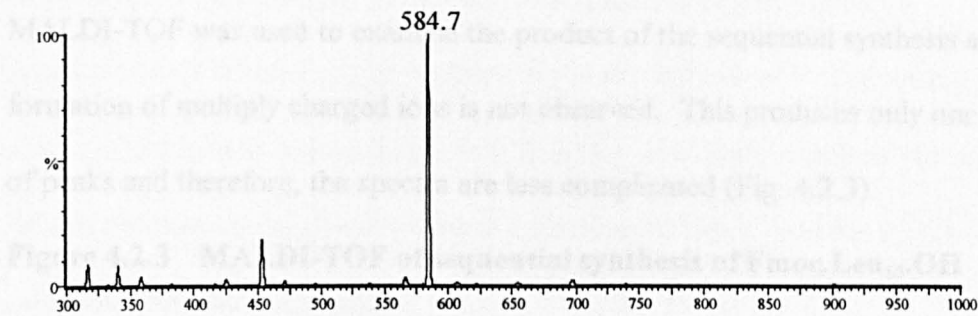
The technique of sequential solid phase peptide synthesis discussed in the previous Section allows absolute control over the number of amino acids in the chain. The initial approach to the synthesis of poly-L-leu₁₅ was to use a sequential approach, which proceeded without problem until the coupling of residue 7. Although the coupling had been carried out in the same way as all previous couplings when the Kaiser test was carried out it was positive. This positive test to the presence of free amine suggested that the reaction was either partially complete or had not occurred at all. This failure was unexpected. The coupling was repeated with a higher concentration of reagent and the reaction was heated to $37 \pm 2.0^\circ\text{C}$. The synthesis was completed, (the details can be found in Chapter 6).

The synthesis was also carried out using the coupling of penta-peptides to avoid these problem coupling steps. Both of these peptides were analysed using mass spectrometry.

4.2.1 Analysis of H.Leu₁₅.OH synthesised by coupling of penta-peptides

It was necessary to examine H.Leu₅.OH before the coupling of the penta-peptides was carried out (Fig. 4.2.1).

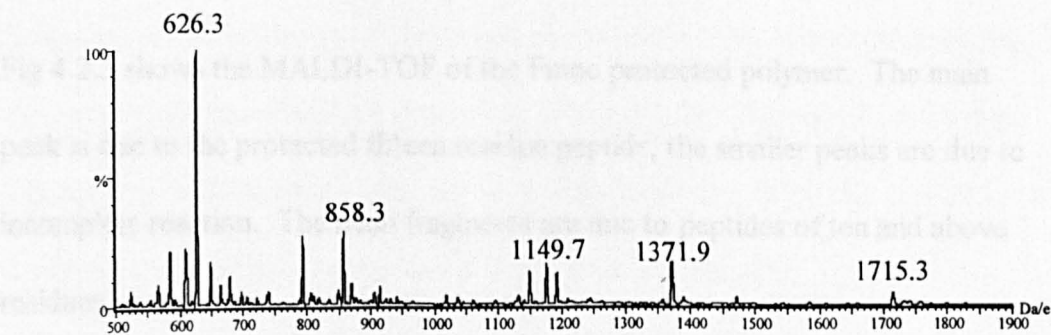
Figure 4.2.1 ESI mass spectrum of H.Leu₅.OH



Mass/Charge	Species
584.7	H.Leu ₅ .OH

The analysis of H.Leu₁₅.OH made by the coupling of penta-peptides showed that several species were present under the ionisation conditions used (Fig. 4.2.2).

Figure 4.2.2 ESI mass spectrum of H.Leu₁₅.OH synthesised by penta-peptide coupling



Mass/Charge	Species
1715.3	(H.Leu ₁₅ .OH) ⁺
1372.0	(Fmoc.Leu ₁₀ .OH) ⁺
1149.7	(H.Leu ₁₀ .OH) ⁺
858.1	(H.Leu ₁₅ .OH) ²⁺

4.2.2 Analysis of sequential synthesis by MALDI-TOF

MALDI-TOF was used to examine the product of the sequential synthesis as the formation of multiply charged ions is not observed. This produces only one series of peaks and therefore, the spectra are less complicated (Fig. 4.2.3).

Figure 4.2.3 MALDI-TOF of sequential synthesis of Fmoc.Leu₁₅.OH

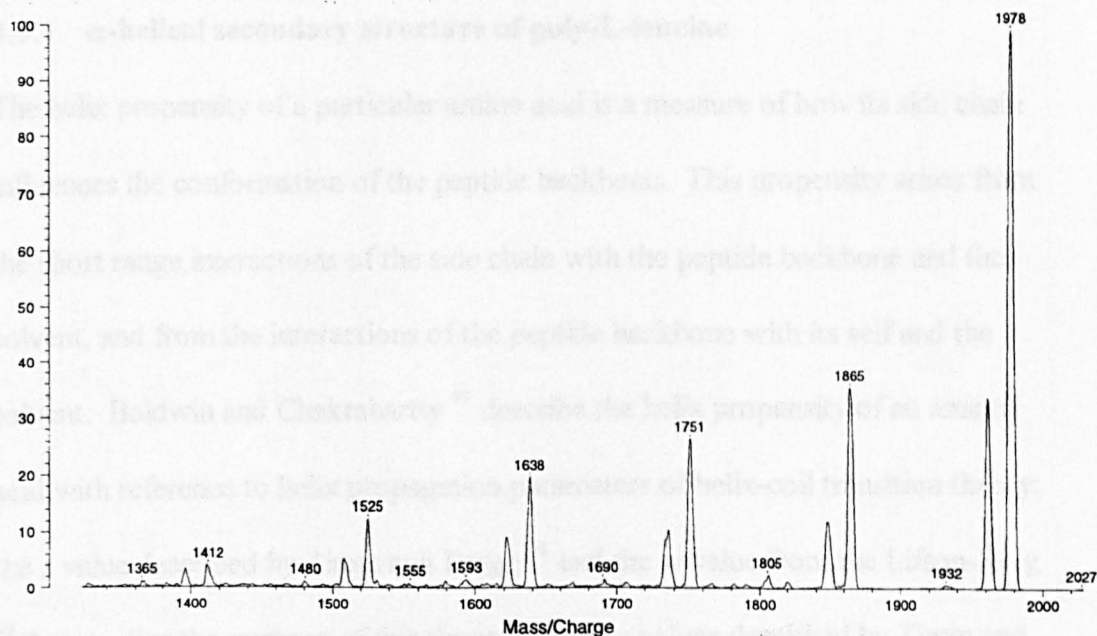


Fig 4.2.3 shows the MALDI-TOF of the Fmoc protected polymer. The main peak is due to the protected fifteen residue peptide, the smaller peaks are due to incomplete reaction. The main fragments are due to peptides of ten and above residues.

4.3 CHARACTERISATION OF THE STRUCTURAL CONFORMATION OF POLY-L-LEUCINE

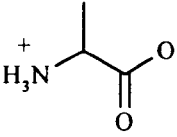
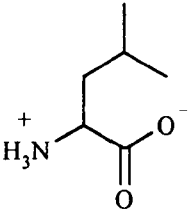
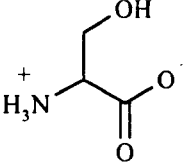
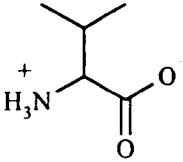
It was discussed in Chapter 2 that the α -helical secondary structure of cellulose derivatives used in the Chiralcel phases is necessary to the enantiorecognition of

the phase. The α -helical secondary structure of poly-L-leucine was also shown to be necessary to its ability to participate in asymmetric organic synthesis successfully. It is necessary to understand the mechanism of formation and the nature of the α -helix in poly-L-leucine. It is also necessary to ensure that an α -helix is produced through the synthesis of both poly-L-leu₁₅ and the synthetic methods discussed in Chapter 3.

4.3.1 α -helical secondary structure of poly-L-leucine

The helix propensity of a particular amino acid is a measure of how its side chain influences the conformation of the peptide backbone. This propensity arises from the short range interactions of the side chain with the peptide backbone and the solvent, and from the interactions of the peptide backbone with its self and the solvent. Baldwin and Chakrabarty⁹⁷ describe the helix propensity of an amino acid with reference to helix propagation parameters of helix-coil transition theory; the s value described by Zimm and Bragg⁹⁸ and the w value from the Lifson-Roig⁹⁹ theory. For the purpose of this thesis only the s values described by Zimm and Bragg are discussed, however the trends observed for these values are mirrored by the w values described by Lifson-Roig (Table 4.3.1). The use of such values can determine the tendency of an amino acid to produce a helix; this may be used to predict the location of a particular amino acid in a protein.

Table 4.3.1 Helix propensity (*s* values) values for several amino acids

Residue	Structure	AK/AQ	EAK	E ₄ K ₄
Alanine		1.54	1.81	2.19
Leucine		0.92	1.03	1.55
Serine		0.36	0.28	0.86
Valine		0.22	0.18	0.93

These *s* values are based on reference to different monomeric peptides of known structure and configuration, the helix propensity of an amino acid was measured by substituting the guest amino acid at one or more positions in the reference peptide. The change in the conformation of the peptide was measured by circular-dichroism then analysed using one of the helix-coil transition theories discussed previously.

Leucine has a high tendency to form an α -helix, while alanine was observed to have the highest tendency. Serine appears to be indifferent to forming α -helices,

while valine is resistant to the formation of an α -helix. Although the s values do not agree numerically they are however, highly correlated, and the differences between the sets are systematic. The disagreement can be explained by the activity of non-helix propensity factors including; helix capping and ion-pair interactions that are not corrected for in the analysis.

4.3.2 The structure of leucine and its implication for the helix propensity

Leucine has a high propensity to form an α -helix for the following reasons;

- little loss of side-chain entropy on helix formation
- the small non-polar side chain can participate in hydrophobic interactions with the peptide backbone
- side chain can not participate in hydrogen-bonding which can destabilise the helix backbone

The hydrophobic side chain has a strong tendency to avoid exposure to the aqueous environment. This is largely due to a entropic effect reflecting the unfavourable free energy of forming a water-hydrocarbon interface. This therefore, favours the formation of a low-energy secondary structure which in the case of poly-L-leucine is an α -helix.

4.3.3 Implication of the polymeric structure

The characteristics of a polymer are determined by its secondary structure which in turn is determined by the primary structure, that is the monomers from which it is constructed. The macrostructure (secondary structure) of the polymer determines its physicochemical characteristics such as solubility, melting temperature and crystallinity. Poly-L-leucine is highly insoluble due to its α -helical secondary structure. It is possible to form a solution of poly-L-leucine

using trifluoroacetic acid as a solvent. It can be suggested that this strong acid disrupts the hydrogen-bonding which forms the helix. When the helix is broken the structure becomes less rigid and is dissolved.

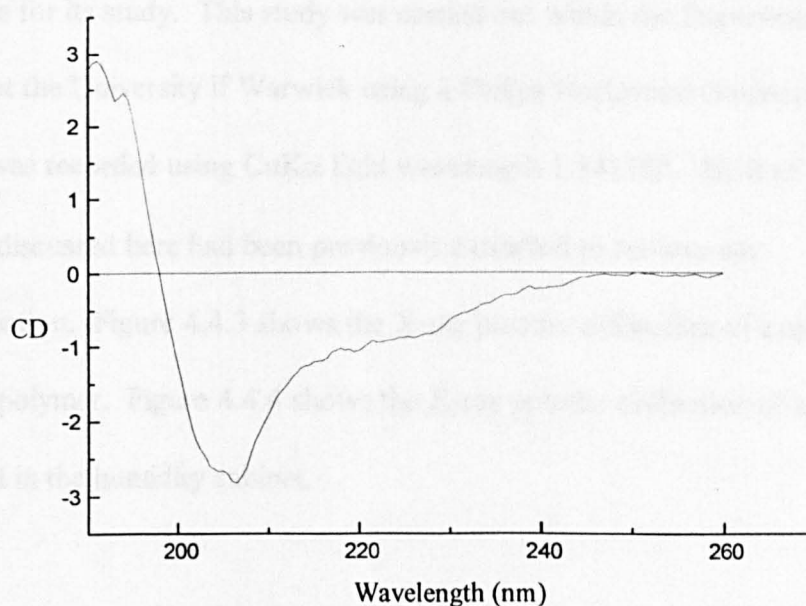
4.4 ANALYSING THE SECONDARY STRUCTURE OF POLY-L-LEUCINE

As poly-L-leucine is insoluble without destroying the helix it is not possible to examine the secondary structure within a liquid state. H.Leu₁₅.OH is sufficiently soluble in acetonitrile to carry out analysis using circular dichroism.

4.4.1 Circular dichroism of H.Leu₁₅.OH

The CD spectrum for H.Leu₁₅.OH is shown in Figure 4.4.1.

Figure 4.4.1 CD of H.Leu₁₅.OH



A right-handed α -helix has several distinct characteristics in CD. Essentially, these are large maxima at 190nm and two smaller maxima at 208 and 220nm.

The CD spectra of H.Leu₁₅.OH does display a maxima at 190nm, the maxima at 208 and 220nm are however, less obvious. It can be suggested that this is due to 'end effects'. The four amino acid residues at the two ends of the peptide do not contribute largely to the helical structure. For H.Leu₁₅.OH this means that half of the peptide is not involved in the rigid structure. These end residues are influenced by the effects of the bulk solvent. As 3.8 residues are required to complete one turn of the helix, a maximum of two turns is possible in H.Leu₁₅.OH. The α -helical structural motif of H.Leu₁₅.OH is therefore limited. In Chapter 5 we examine the effect of this on the enantio-recognition ability of this peptide.

4.4.2 X-ray powder diffraction of poly-L-leucine

The lack of solubility of poly-L-leucine makes X-ray powder diffraction an ideal technique for its study. This study was carried out within the Department of Physics at the University of Warwick using a Philips Horizontal Goniometer. The spectra was recorded using CuK α light wavelength 1.54178Å. Both of the samples discussed here had been previously extracted to remove any contamination. Figure 4.4.3 shows the X-ray powder diffraction of a amine initiated polymer. Figure 4.4.4 shows the X-ray powder diffraction of a sample produced in the humidity cabinet.

Figure 4.4.3 Amine initiated poly-L-leucine

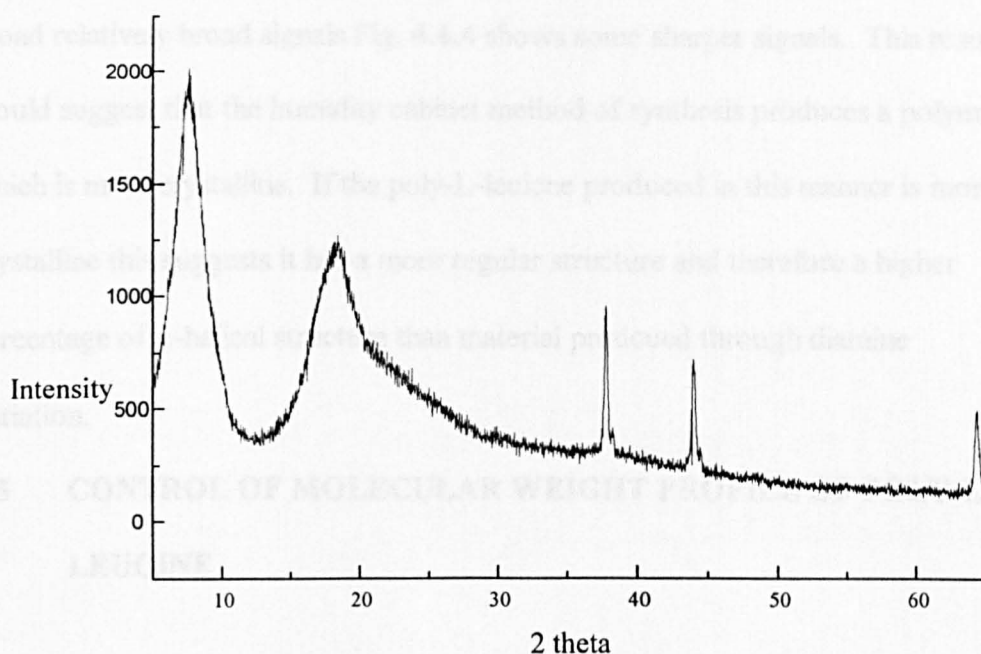
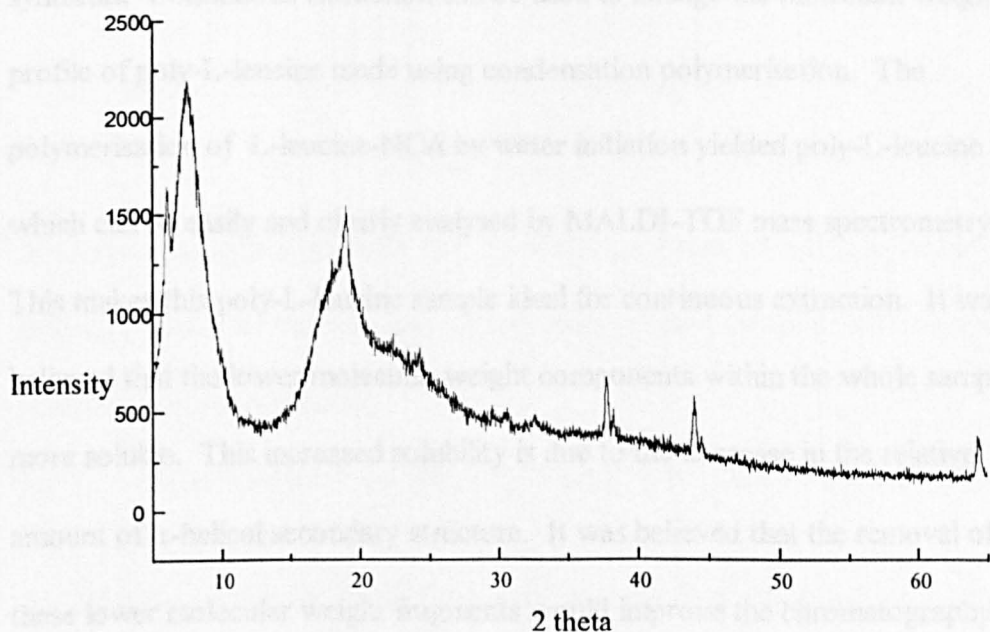


Figure 4.4.4 Poly-L-leucine from humidity cabinet



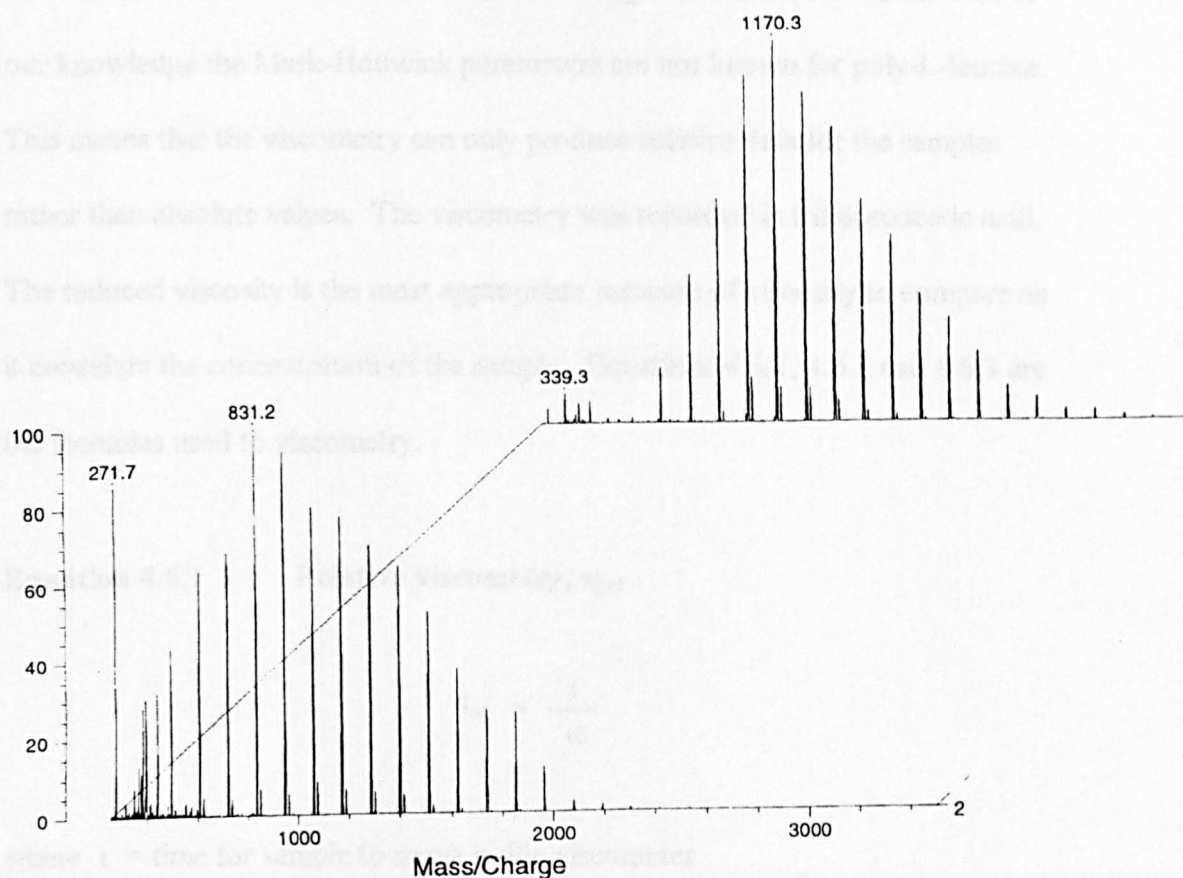
The very sharp signals which appear after 30 2θ are due to the aluminium slide on which the sample was mounted. Sharp signals are due to any material which has a high level of crystalline structure while amorphous regions generate broad signals.

Comparing the two samples it can be suggested that although both samples give broad relatively broad signals Fig. 4.4.4 shows some sharper signals. This result would suggest that the humidity cabinet method of synthesis produces a polymer which is more crystalline. If the poly-L-leucine produced in this manner is more crystalline this suggests it has a more regular structure and therefore a higher percentage of α -helical structure than material produced through diamine initiation.

4.5 CONTROL OF MOLECULAR WEIGHT PROFILE OF POLY-L-LEUCINE

It has been shown in previous sections that the molecular weight of poly-L-leucine can be absolutely controlled using the technique of solid phase peptide synthesis. Continuous extraction can be used to change the molecular weight profile of poly-L-leucine made using condensation polymerisation. The polymerisation of L-leucine-NCA by water initiation yielded poly-L-leucine which can be easily and clearly analysed by MALDI-TOF mass spectrometry. This makes this poly-L-leucine sample ideal for continuous extraction. It was believed that the lower molecular weight components within the whole sample are more soluble. This increased solubility is due to the decrease in the relative amount of α -helical secondary structure. It was believed that the removal of these lower molecular weight fragments would improve the chromatography of the complete phase. This is due to the observed increase in the molecular weight and the resulting increase in overall α -helical content. Figure 4.5 shows the results of the continuous extraction.

Figure 4.5 MALDI-TOF showing poly-L-leucine before and after continuous extraction



It can be seen from Figure 4.5 that the foreground spectra which is the sample before continuous extraction has a lower mass centred distribution that the sample after continuous extraction.

4.6 MEASUREMENT OF MOLECULAR WEIGHT PROFILE OF POLY-L-LEUCINE

As discussed previously poly-L-leucine is insoluble in anything but very strong acids. This precluded the use of GPC to determine the relative molecular weights and polydispersity of different samples. Poly-L-leucine was examined using viscometry and NMR which both provide an insight into the molecular weight characteristics of poly-L-leucine.

4.6.1 Viscometry

Poly-L-leucine samples which were synthesised using both L-leucine NCA initiated by amine and water were examined using this technique. To the best of our knowledge the Mark-Houwink parameters are not known for poly-L-leucine. This means that the viscometry can only produce relative data for the samples rather than absolute values. The viscometry was recorded in trifluoroacetic acid. The reduced viscosity is the most appropriate measure of viscosity to compare as it considers the concentration of the sample. Equations 4.6.1, 4.6.2 and 4.6.3 are the formulas used to viscometry.

Equation 4.6.1 Relative viscometry, η_{rel}

$$\eta_{rel} = \frac{t}{t_0}$$

where t = time for sample to move inside viscometer
 t_0 = time for solvent to move inside viscometer

Equation 4.6.2 Specific viscometry, η_{sp}

$$\eta_{sp} = \left[\frac{t}{t_0} \right] - 1$$

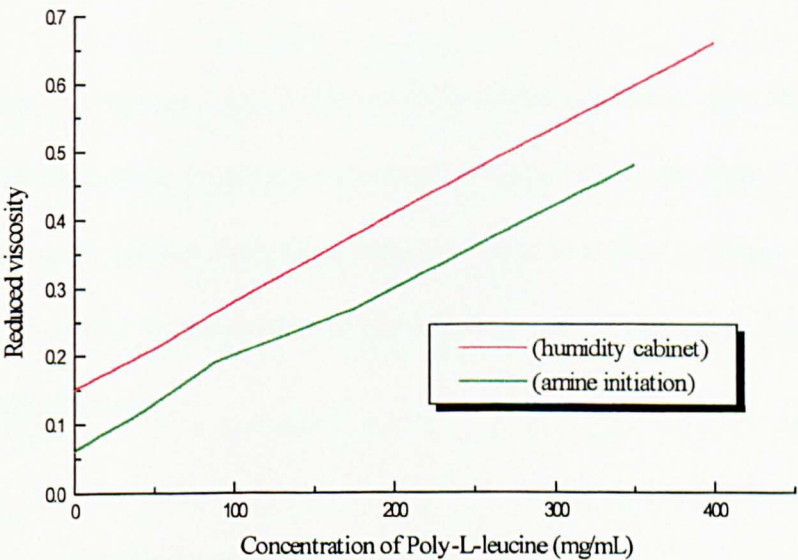
where t = time for sample to move inside viscometer
 t_0 = time for solvent to move inside viscometer

Equation 4.6.3 Reduced viscometry, η_{red} .

$$\eta_{red} = \frac{\eta_{sp}}{C}$$

where C = concentration

Graph 4.6 Reduced viscosity of Poly-L-leucine samples



When concentration is equal to zero we measure the viscosity of the sample. This value is directly related to the molecular weight of the sample via the Mark-Houwink constants. To the best of our knowledge the Mark-Houwink constants for these samples are not known, it can be assumed however, due to the closeness of general structure between the samples these constants may be similar. The molecular weight of poly-L-leucine synthesised using L-leucine polymerised in a humidity cabinet is higher than the L-leucine NCA polymerised using a diamine.

4.7 CONCLUSIONS

A high degree of control over molecular weight of poly-L-leucine was observed through the use of solid phase peptide synthesis. This method did not however, produce the homogenous product which was originally expected due to unforeseen experimental difficulties. Analysis of the 15-mer peptide using circular dichroism showed that although the peptide tended to form an α -helix the terminal residues of the peptide were not strongly involved in the formation of this secondary structure. The analysis of poly-L-leucine has been limited by its lack of solubility in all but high strength acid.

CHAPTER 5

THE APPLICATION OF POLY-L-LEUCINE TO CHIRAL HPLC

It was shown in Chapters 1 and 2 that optically active polymers, especially those based on cellulose, have been very successful as chiral stationary phases for HPLC. The synthesis and analysis of poly-L-leucine described in Chapters 3 and 4 show many similar characteristics to the cellulose-based materials. These characteristics include;

- **α -helical secondary structure**
- **optically active monomer unit**

The combination of PGC with CDMPC was successful for the separation of a wide range of analytes. It was hoped that coating PGC with poly-L-leucine would be equally successful and produce a durable and versatile phase.

5.0 APPLICATION OF CHROMATOGRAPHY TO CHIRAL LIQUID CHROMATOGRAPHY OF DIPEPTIDES

The use of end capped poly-leucine and poly L-phenyl alanine as enantioselective agents in liquid chromatography has been described by Hirayama *et al.*¹⁰⁰ They

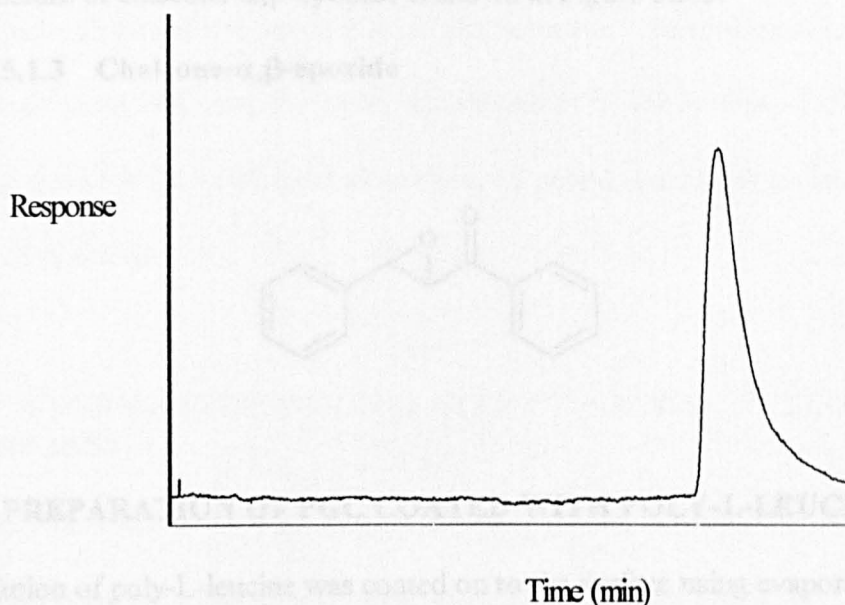
discussed the separation of D-D and L-L dipeptides containing leucine and one other amino acid. NCA L-leucine was co-polymerised with γ -benzyl-L-glutamate by amine initiation as well as being used to produce poly-L-leucine. They prepared polymer bonded and non-bonded phases for use under normal phase conditions. The non-bonded spheres were produced by evaporation of a suspension of the polymer while the bonded phase was produced using cross linked polymer spheres with amine functionality on the surface. They evaluated the influence of the N-terminal protecting group on the enantioselectivity of the phase. They found that the larger, more bulky the group the lower the enantioselectivity of the phase. They concluded that this was due to the increase in steric hindrance of the peptide toward the analyte.

Hirayama *et al.*¹⁰⁰ considered the secondary structure of the polymer to be very important in the level of enantioselectivity it displayed. They determined by FT-IR that the polymers they had produced contained a high percentage of α -helix. They suggested that the successful use of leucine in a chiral stationary phase was due to the presence of the high α -helical content and the stereospecificity of the leucine residues within the helix.

5.1 CHOICE OF ANALYTES

Julia and Colonna described chalcone- α,β -epoxide as the first analyte to which poly-L-leucine successfully showed some enantioselectivity. This analyte was used to test column B with reference to blank PGC (Fig. 6.2.2 and Fig. 6.2.1).

Figure 5.1.1 Chalcone- α,β -epoxide on blank PGC

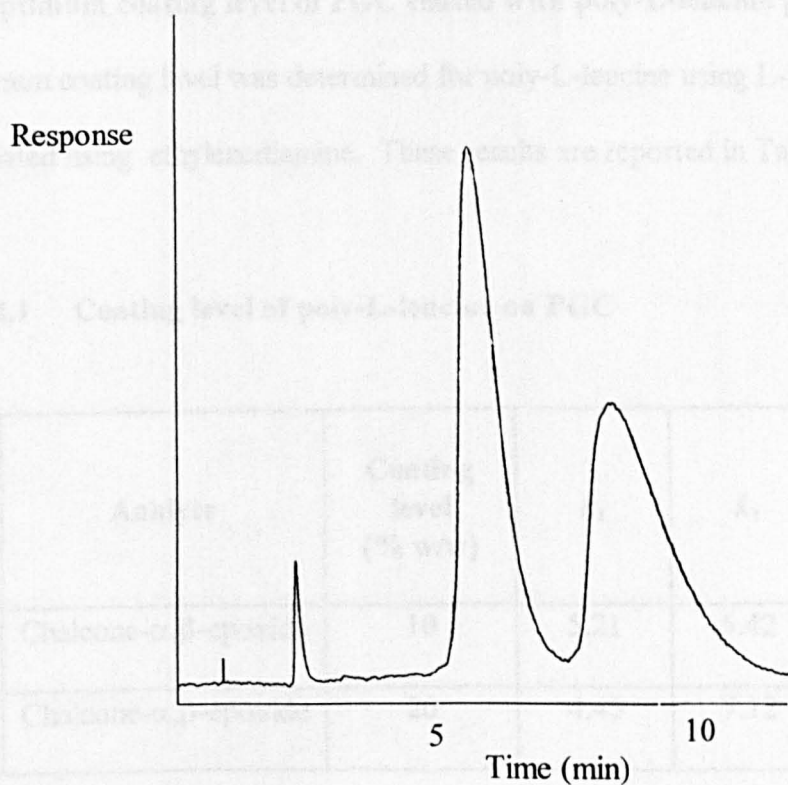


Mobile phase: acetonitrile/water (90:10 v/v)

Flow rate: 1.0 mL/min

Retention time: 16.2 min

Figure 5.1.2 Chalcone- α,β -epoxide on poly-L-leucine coated PGC

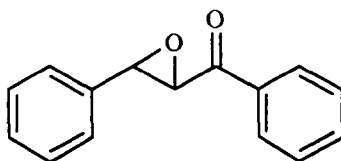


Mobile phase: acetonitrile/water (90:10 v/v)

Flow rate: 1.0 mL/min

The structure of chalcone- α,β -epoxide is shown in Figure 5.2.3.

Figure 5.1.3 Chalcone- α,β -epoxide



5.2 PREPARATION OF PGC COATED WITH POLY-L-LEUCINE

The solution of poly-L-leucine was coated on to the surface using evaporation, the phase was then sieved and dried overnight. The phase was slurry packed using polar solvents. Typically the phase was packed in to a 100 mm column, unless otherwise stated.

5.2.1 Optimum coating level of PGC coated with poly-L-leucine phases

The optimum coating level was determined for poly-L-leucine using L-leucine NCA initiated using ethylenediamine. These results are reported in Table 6.1.1

Table 5.2.1 Coating level of poly-L-leucine on PGC

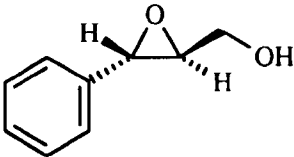
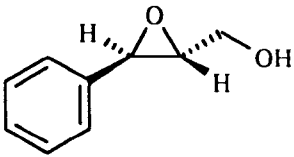
Column	Analyte	Coating level (% w/w)	k_1	k_2	α
A	Chalcone- α,β -epoxide	10	5.21	5.42	1.04
B	Chalcone- α,β -epoxide	20	4.45	7.12	1.61

A loading level of 30 % w/w was attempted. The PGC particles were very overloaded with poly-L-leucine and could not be sieved. The optimum loading of poly-L-leucine on PGC was therefore, determined to be 20 % w/w. This loading level was used for the coating of all samples of poly-L-leucine regardless of its method of synthesis.

5.3 ORDER OF ELUTION DISPLAYED BY POLY-L-LEUCINE PHASES

Julia and Colonna found that the main enantiomer produced with poly-L-leucine was levorotatory and in the case of chalcone- α,β -epoxide the absolute configuration is (2*R*, 3*S*). Two pure single optical isomers were used to test the order of elution of poly-L-leucine phases. The results of this study are shown in Table 5.3.1.

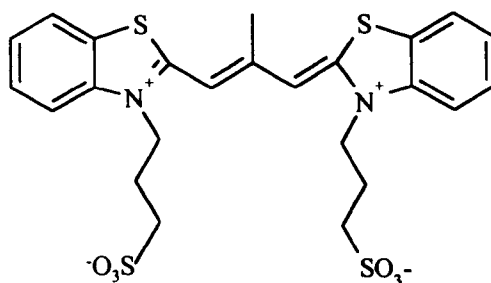
Table 5.3.1 Isomers used to test order of elution

Name	Structure	Elution time (min)	Rotation direction
(2 <i>S</i> ,3 <i>S</i>)-(-)-3-phenyl glycidol		7.05	levorotatory
(2 <i>R</i> ,3 <i>R</i>)-(+)-3-phenyl glycidol		7.55	dextrorotatory

In the case of this particular compound (Fig. 5.3.1) the (*S*)-(-)-enantiomer elutes first. This result suggests that the transient interaction complex between poly-L-leucine and the (*R*)-(+)-enantiomer is more stable than that between poly-L-leucine and the (*S*)-(-)-enantiomer. In asymmetric organic synthesis⁷⁷ the use of poly-L-alanine and poly-L-leucine generates the levorotatory enantiomer as the major product.

The preference of a homopoly-L-peptide for (*R*)-(+)-enantiomers has been shown by Hirayama *et al.*¹⁰⁰ They describe the interaction of poly-L-lysine with a cyanine dye NK-2012 (Fig. 5.3.2).

Figure 5.3.2 Cyanine dye NK-2012



In the presence of poly-L-lysine the achiral dye molecules dimerize to form chiral aggregates with (*R*)-(+)-chirality. Poly-L-lysine is a right-handed α -helix, the same structural motif observed with poly-L-leucine. This supports the work described in Table 5.3.1. The implication of this study will be discussed with respect to a proposed mechanism of enantiorecognition for poly-L-leucine later in this chapter.

5.4 COMPARISON OF POLY-L-LEUCINE TYPES

As previously discussed poly-L-leucine was synthesised using four different methods;

- L-leucine NCA initiated by water (Column C)
- L-leucine NCA initiated by diamine (Column B)
- L-leucine polymerised by triphenyl phosphite in *N*-methyl pyrrolidine
- solid phase synthesis of H.Leu₁₅.OH (Column D)

Three of these methods produced poly-L-leucine that was believed to be suitable for application to HPLC. The polymerisation of L-leucine NCA using water or a diamine to initiate the reaction produced linear polymers which can be considered to have an α -helical secondary structure. The peptide H.Leu₁₅.OH, although this was found to contain some contamination by lower mass fragments, is essentially monodispersed relative to the other poly-L-leucine samples.

The use of triphenyl phosphite in *N*-methyl pyrrolidine has been shown by MALDI-TOF to contain cyclic peptides. As it is not possible from MALDI-TOF to assess what percentage of the sample is cyclic peptide, this sample was not used for chromatography. This thesis is particularly interested in the relationship between enantioselectivity and the α -helical secondary structure. The presence of cyclic peptides is therefore, not desirable. The results of these columns with chalcone- α,β -epoxide is shown in Table 5.3.0

Table 5.4.0 Comparison of different poly-L-leucine samples

Column	k_1	k_2	α	R_s
B	4.45	7.13	1.61	1.30
C	4.33	8.57	1.98	1.49
D	4.82	-	-	-

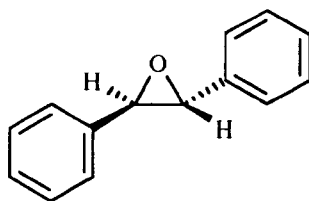
Mobile phase: Acetonitrile/water (90:10 v/v), column B contains diamine initiated poly-L-leucine, column C contains water initiated poly-L-leucine, column D contains H.Leu₁₅.OH. Flow rate: 0.5ml/min

Column B displays baseline separation of chalcone- α,β -epoxide with good peak shape. Column C displays both higher selectivity and resolution than column B. It displays baseline separation with good peak shape. Column D showed no separation for chalcone- α,β -epoxide and displays a very tailed peak. For the separation of chalcone- α,β -epoxide therefore, the use of poly-L-leucine synthesised using water initiation is most successful.

5.4.1 Unexpected separation of *trans*-Stilbene oxide

Chalcone- α,β -epoxide was the first analyte to be used successfully with poly-L-leucine as an asymmetric organic catalyst.⁷⁷ It forms the structural basis for many of the analytes which have been successfully used with poly-L-leucine. The need for the presence of an α,β -unsaturated ketone functionality was considered to be necessary for the action of poly-L-leucine. It was unexpected therefore, when *trans*-stilbene oxide (Fig. 5.4.1) was successfully resolved on a poly-L-leucine column.

Figure 5.4.1 *trans*-Stilbene oxide



trans-stilbene oxide was therefore used to compare columns B and C (Fig. 5.4.2)

Figure 5.4.2 Comparison of different poly-L-leucine samples using *trans*-stilbene oxide

Column	k_1	k_2	α	R_s
B	5.20	5.69	1.09	0.49
C	4.35	4.92	1.13	0.71
D	4.65	-	-	-

Mobile phase: Acetonitrile/water (90:10 v/v), column B contains diamine initiated poly-L-leucine, column C contains water initiated poly-L-leucine, column D contains H.Leu₁₅.OH. Flow rate: 0.5ml/min

The results shown for chalcone- α,β -epoxide are repeated for *trans*-stilbene oxide.

The use of poly-L-leucine made from L-leucine-NCA by water initiation produces the most successful phase. Column C displays the largest capacity factor, α , which suggests that this form of poly-L-leucine has a higher level of enantiorecognition than poly-L-leucine made by amine initiation.

5.4.2 Explanation of differences between Columns B and C

It was shown in Chapter 4 that the molecular weight of amine initiation poly-L-leucine was lower than the water initiated sample. It can be suggested therefore, that the water initiated polymer has a higher level of α -helical structure. It can also be suggested that the inclusion within the polymer of the diamine initiator may disrupt the secondary structure. This however, has not been investigated.

Roberts *et al.*⁸¹ have investigated the use of various poly-L-leucine samples including polymers made by both water and amine initiation. Using this procedure described by Itsuno¹⁰⁰, Roberts *et al.*¹⁰² also produced an immobilised poly-L-leucine sample (Section 3.4.4). The immobilised poly-L-leucine gave superior enantiomeric purity and chemical yield compared with non-immobilised samples. Roberts *et al.*^{101,102} found that material produced using the humidity cabinet gave both higher optical and chemical yield than the amine-initiated polymer. This supports the results obtained from columns B and C. It can be suggested that the method of synthesis of poly-L-leucine effects the secondary structure and therefore, the enantioselective ability of the polymer.

5.5 THE EFFECT OF MOLECULAR WEIGHT ON THE

ENANTIOSELECTIVITY OF POLY-L-LEUCINE PHASES

Molecular weight has been controlled using solid phase peptide synthesis and continuous extraction. Both of these peptides were applied to chromatography.

5.5.1 The application of H.Leu₁₅.OH to chromatography

It was shown in Sections 5.3.0 and 5.4.2 that column D does not resolve either of the analytes tested. This column was produced using poly-L-leucine using solid phase peptide synthesis. Although from examination by MALDI-TOF

H.Leu₁₅.OH contains peptides with 10,11,12,13 and 14 residues. These peptides are due to the incomplete synthesis of each stage in the solid phase synthesis. Comparing this peptide to a polymer made by condensation polymerisation it can be considered to be essentially monodisperised. Analysis of H.Leu₁₅.OH by circular dichroism, discussed in Section 4.3, discusses the percentage of α -helical secondary structure contained within the 15-residue peptide. The rather low percentage can be considered to be due to the end-effects of the peptide. The terminal four amino acid residues of the peptide will be interacting with the bulk solvent, this prevents them from being wholly included in the intra-chain hydrogen bonding which holds the α -helical structure together. In a peptide of 15 residues therefore, half the peptide is not wholly involved in forming the helical structure. This low helical content could explain the lack of enantioselectivity observed for this peptide.

5.5.2 The application of a continuously extracted poly-L-leucine to chromatography

The result of the continuous extraction of poly-L-leucine made by water initiation of L-leucine NCA is discussed in Chapters 4 and 6. A column (column E) was produced using this polymer in the usual manner. Some results of this column are shown in Table 5.5.2

Table 5.5.2 Continuous extraction polymer column - column E

Analyte	k_1	k_2	α	Rs
Chalcone- α,β -epoxide	4.39	9.02	2.05	1.52
<i>trans</i> -stilbene oxide	4.38	5.19	1.18	0.95

These results are better than was observed for columns B and C. It can be suggested therefore, that continuous extraction does provide a polymer with increased enantioselectivity due to the increase in molecular weight distribution due to the removal of lower mass fragments.

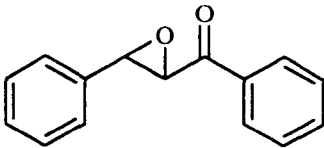
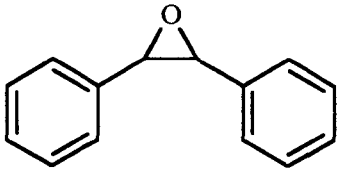
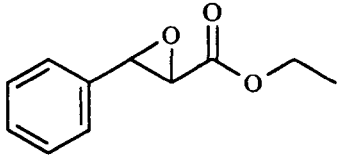
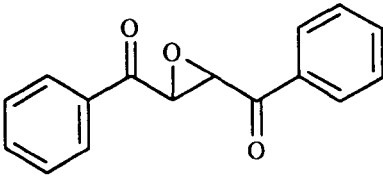
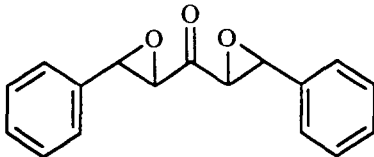
5.6 PRODUCTION OF OPTIMUM COLUMN

To explore the use of several different analytes we produced an optimum column. Poly-L-leucine which had undergone continuous extraction was chosen as the enantioselective section of the phase. The phase was produced as a 20% w/w loading, this was packed into a 250mm x 4.6 i.d. column. This column was used to successfully resolve several racemic epoxides discussed in Table 5.6.1.

These epoxides have several structural characteristics, and in essence they are all electron-deficient epoxides. To the best of our knowledge *trans*-stilbene oxide has not been discussed in the literature previously with reference to poly-L-leucine.

This compound differs as it does not contain an α -ketone group. This compound is resolved completely on a poly-L-leucine based column. This suggests that although an α -ketone group may improve the interaction between poly-L-leucine and the analyte it does not appear to be a necessity. Ethyl-(\pm)-3-phenyl glycidate is the only compound discussed which does not contain two phenyl groups. This compound does show the lowest resolution and capacity factors. This suggests that the enantioselective interaction between this compound and poly-L-leucine is relatively weak. From these results it can be seen that the presence of an α -ketone group to the epoxide which has an aromatic system either side, provides the highest level of enantioselective interaction.

Table 5.6.1 Successful chromatography on 250mm column

Name	Structure	k_1	k_2	α
Chalcone- α,β -epoxide		4.35	10.68	2.56
<i>trans</i> -stilbene oxide		4.33	5.82	1.34
ethyl-(\pm)-3-phenyl glycidate		2.05	2.42	1.18
<i>trans</i> -4-phenylbut-2-ene-1,4-dione		5.58	12.45	2.13
<i>bis</i> -(3-phenyl-oxiranyl methanone)		6.47	12.30	1.90

5.6.2 Separation of *bis*-phenyl-oxiranyl methanone

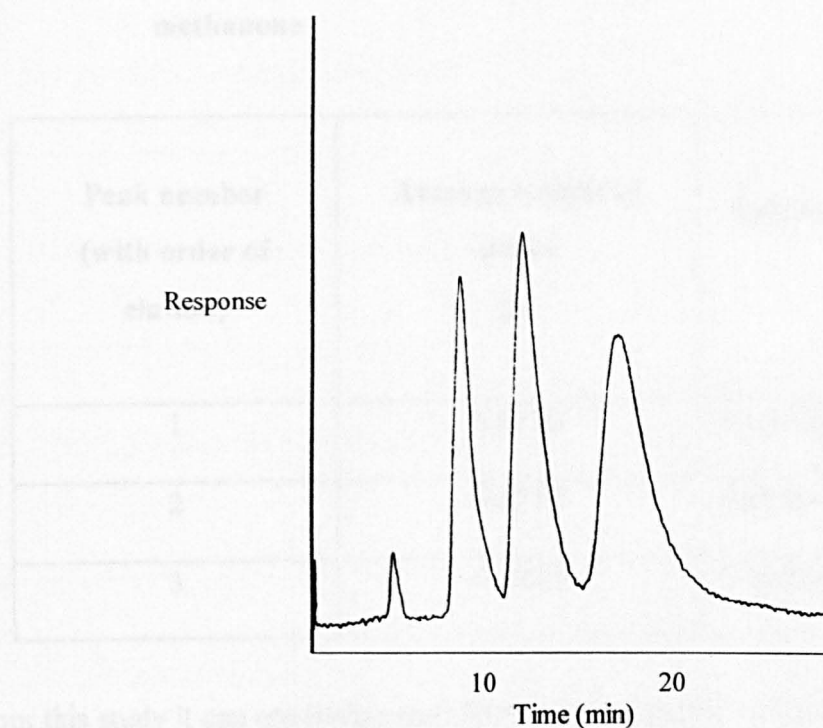
This compound exists as a mixture of two pairs of enantiomers (Fig. 5.6.2).

Figure 5.6.2 Mixture of enantiomers

Left hand side epoxide	Right hand side epoxide	Characteristic
<i>R,S</i>	<i>R,S</i>	half of enantiomer pair
<i>R,S</i>	<i>S,R</i>	meso mixture
<i>S,R</i>	<i>R,S</i>	meso mixture
<i>S,R</i>	<i>S,R</i>	half of enantiomer pair

When this mixture of isomers is resolved on a column the meso mixture would not be resolved. This would lead to three peaks being observed. The separation of *bis*-phenyl-oxiranyl methanone is shown in Fig. 5.6.3.

Figure 5.6.3 Resolution of *bis*-phenyl-oxiranyl methanone on column E



Mobile phase: acetonitrile/water (90:10 v/v)
Flow rate: 0.5 mL/min

Fig. 5.6.3 shows the expected three peaks. The small peak at the front of the chromatogram is flow marker. It is possible to assign these peaks by weight. The peaks which correspond to the pair of enantiomers should be equivalent in weight. The meso mixture will be of less weight as the formation of this mixture is not favoured. Fig. 5.6.4 shows the assignment of these peaks.

Figure 5.6.4 Assignment of peaks in the resolution of *bis*-phenyl-oxiranyl methanone

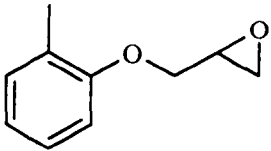
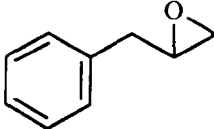
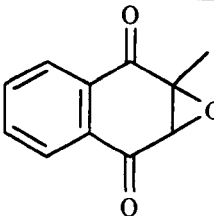
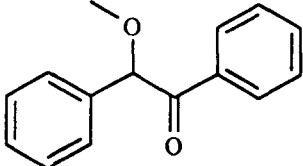
Peak number (with order of elution)	Average weight of peaks (g)	Assignment
1	0.0156	meso mixutre
2	0.0234	enantiomer 1
3	0.0243	enantiomer 2

From this study it can concluded that 24.6% of the sample of *bis*-phenyl-oxiranyl methanone is produced as a meso mixture of enantiomers, (*R,S*), (*S,R*) and (*S,R*), (*R,S*). Having characterised the peaks within the spectra it is possible to determine selectivity and resolution values for the enantiomers. The α -value for the two enantiomers was found to be 0.53, while the resolution value was found to be 1.23, which corresponds to baseline resolution.

5.7 UNSUCCESSFUL CHROMATOGRAPHY

In the same way that as an asymmetric organic catalyst poly-L-leucine was inactive with certain compounds, the use of poly-L-leucine in a CSP has also been shown to be unsuccessful for particular compounds. These compounds are shown in Table 5.7.1.

Table 5.7.1 Unsuccessful analytes for poly-L-leucine column E

(±)-glycidyl-2-methylphenyl ether	
(±)-1,2-epoxy-3-phenoxy propane	
(±)-2,3-epoxycyclohexanone	
benzoin methyl ether	

The unsuccessful compounds in two cases contain terminal epoxides, poly-L-leucine does not offer any selectivity between these enantiomers. Benzoin methyl ether does not contain an epoxide. On cellulose based phases this compound is very well resolved. Poly-L-leucine does not separate these enantiomers. (±)-2,3-epoxycyclohexanone was used by Julia *et al.*⁷⁹ and its synthesis was found not to be effected by the presence of poly-L-leucine. This compound was not resolved on the poly-L-leucine column.

5.8 PROPOSED MECHANISM OF ENANTIORECOGNITION OF POLY-L-LEUCINE

Julia *et al.*⁷⁹ suggest that hydrogen bonding between the carbonyl functionality of the chalcone and the peptide group of poly-L-leucine is responsible for the asymmetric synthesis of the epoxide. The resolution of *trans*-stilbene oxide on a

poly-L-leucine column shows that although this hydrogen bonding between the polymer and the carbonyl group may be a contributory factor to the enantioselectivity of the phase it can not be the whole reason. Interaction between the epoxide and poly-L-leucine appears to be far more important. The order of elution study shows that levorotatory enantiomer eluted first and this enantiomer is the major product from asymmetric synthesis. This suggests that the levorotatory epoxide enantiomer interacts less strongly with poly-L-leucine than the dextrorotatory epoxide enantiomer. It could be suggested that the transition state of the levorotatory enantiomer with poly-L-leucine is of lower energy and therefore, dominates. This leads to the synthesis of levorotatory product in preference to dextrorotatory product. In our work the only compound present was the epoxide, no α,β -unsaturated ketone was present. We can not say therefore, that the interaction which cause poly-L-leucine to discriminate between epoxides are necessarily the interactions which cause the production of single enantiomers from an α,β -unsaturated ketone.

It can be suggested that hydrogen bonding between the electron-deficient epoxide and the peptide group determines the enantioselectivity. The non-uniformity of the separations observed tell us that this interaction is different in the different samples of poly-L-leucine produced. To establish whether the primary structure of diamine initiated poly-L-leucine or its lower molecular weight profile relative to poly-L-leucine produced in the humidity cabinet is responsible for the differences observed in enantioselectivity will require more work. Computer modelling of the polymers could be used draw conclusions as to the nature and energy of the binding of an epoxide. Establishing the role of molecular weight depends on the ability to control the synthesis and develop adequate techniques for analysis.

5.9 CONCLUSIONS

It has been shown that porous graphitic carbon coated with poly-L-leucine is an effective chiral stationary phase for high performance liquid chromatography.

Although the range of analytes resolved on these columns is limited to epoxides, this is consistent with the work of Julia and Colonna, and Roberts with the exception of the resolution of *trans*-stilbene oxide. It has been demonstrated that poly-L-leucine produced from the homopolymerisation of L-leucine-NCA in a humidity cabinet and its subsequent continuous extraction produced the optimum phase of this study. MALDI-TOF allowed us to probe the primary structure of poly-L-leucine produced using several methods. Using comparative MALDI-TOF spectra we can suggest that the extracted poly-L-leucine had a higher molecular weight distribution and this appears to contribute to the increase in enantio recognition. The secondary structure of poly-L-leucine has been probed by FT-IR and circular dichroism and has been shown to be dominated by the α -helical structural motif. This helical secondary structure appears also to be very important in the enantio recognition ability of the poly-L-leucine samples tested. Although the exact nature of the enantio recognition of poly-L-leucine has not been absolutely determined it has been shown that poly-L-leucine can discriminate between enantiomers while it is coated on to a surface.

The range of compounds tested both in this study and in the literature in general suggests that poly-L-leucine has a highly specific structural requirement from the analyte in order to display any enantioselectivity. This feature however, limits the applicability of this phase. The commercial possibilities for this phase are extremely limited due to the highly specific nature of the enantiomers which it will separate. The production of this phase does however, introduce useful

technology and methods which may be exploited in the future to produce CSP which can rival derivatised polysaccharides. The use of amino acids in CSP offers an interesting opportunity to exploit the wide range of functionality available. Many amino acids have pendant functionality such as aspartic acid and tyrosine which contain carboxyl and phenolic residues respectively. This functionality offers the opportunity for derivatisation in an analogous manner to the carbamate and benzoate derivatisation of polysaccharide phases. The production of a helical secondary structure which appears to be necessary for enantioselectivity could be encouraged through the production of co-polymers with amino acids which possess a high tendency to form helices such as leucine and alanine. The use of such polymers can be envisaged not only in CSP but also as immobilised catalysts for asymmetric organic synthesis.

CHAPTER 6

EXPERIMENTAL

6.0 SOLVENTS, CHEMICALS AND INSTRUMENTATION

All infra-red spectrometry was carried out using a Perkin-Elmer 1720X series FT-IR instrument. The ultra-violet spectrometry data was recorded using a Unicam 8700 series spectrometer. All melting point data was recorded using a Gallenkamp digital melting point apparatus and are uncorrected. Analysis of the percentage content carbon, hydrogen and nitrogen was taken at the University of Warwick using a Leeman Labs. Inc. CE440 elemental analysis apparatus. In all case duplicate analysis was carried out. Nuclear magnetic resonance (NMR) data were recorded using a Bruker ACF 250, proton NMR was recorded at 250 MHz and the carbon NMR was recorded at 62.9 MHz. The multiplicity of the data is reported as; s = singlet, d = doublet, t = triplet, q = quartet, quin = quintet, m = multiplet and br = broad. Coupling constants, J, are reported in Hz.

Thin layer chromatography (TLC) was carried out using silica-gel 60 plates with fluorescent indicator (Merck).

Chromatography was carried out using silica gel (Keislegel 60), compressed air was applied to produce flash chromatography.

All Hypercarb PGC and silica were gifts from Hypersil. Sigmacel cellulose was purchased from Sigma (UK) and Avicel cellulose was purchased from Merck (Germany). 3,5-dimethylphenyl isocyanate was purchased from Lancaster (UK). *N,N*-dimethylacetamide and trifluoroacetic acid were purchased from Aldrich (UK).

Pyridine was obtained from Fluka. All other solvents (HPLC grade) were obtained from Rathburn (UK).

In the synthesis of poly-L-leucine using solid phase peptide techniques all reagents were purchased from Novabiochem and were used without further purification, with the exception of hydroxybenzotriazole (HOBt). HOBt was purchased from Lancaster and was recrystallised from methanol to constant melting point. DMF was purchased from Rathburn (AR grade) and was distilled before use.

6.1 SYNTHESIS OF CDMPC

This reaction was carried out in a fume hood as 3,5-dimethylphenyl isocyanate is lachrymatory and toxic.

Cellulose was dried over P_2O_5 for 24 hours, then refluxed in dry pyridine (50 mL/g of cellulose) for 24 hours to ensure complete wetting of the cellulose. The reaction was then allowed to cool to ambient temperature, 3,5-dimethylphenyl isocyanate (3.5 equivalents) was added. The reaction was refluxed

filtered and washed with ice cold methanol (5 x 20 mL) or until the odour of pyridine is no longer detected. The cellulose carbamate was dried at 50 °C to constant weight. Yields are shown in Table 6.1.

Table 6.1 Yields of the synthesis of CDMPC

Sample	Cellulose type	Amount of cellulose(g)	Amount of isocyanate (mL)	Yield (g)	Yield (%)
CDMPC-1	Avicel	1.60	5.0	4.40	73.9
CDMPC-2	Avicel	1.60	5.0	5.80	97.35
CDMPC-3	Sigmacel	1.60	5.0	5.70	94.0

6.2 ELEMENTAL ANALYSIS

The results are shown in table 6.2.

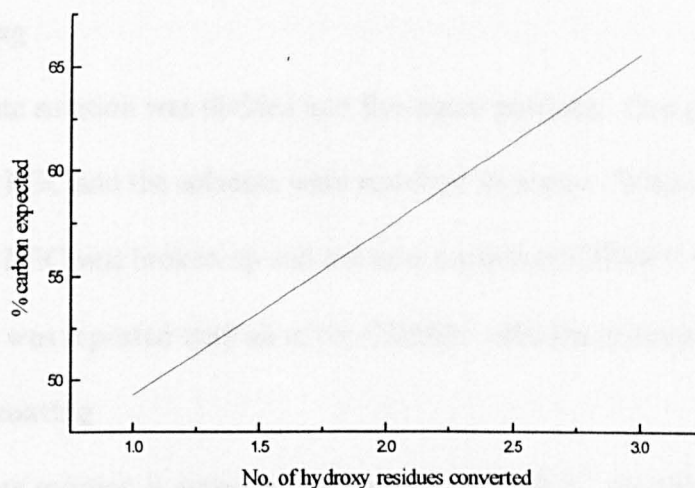
Table 6.2 C,H and N results for CDMPC

Sample	% carbon	% hydrogen	% nitrogen	% conversion of OH groups*
Theoretical values	65.67	6.14	6.97	100
CDMPC-1	63.89	6.12	6.54	93.4
CDMPC-2	64.02	6.13	6.65	96.8
CDMPC-3	63.85	6.10	6.61	92.6

* calculated by using the line of best fit through carbon values for mono, di and tri-substituted derivatives and then substituting the percentage carbon value to

obtain the number of groups which have been successfully derivatised (Graph 6.2.1).

Graph 6.2.1 Conversion of cellulose by 3,5-dimethylphenyl isocyanate



6.3 PREPARATION OF CDMPC-COATED PHASES

6.3.1 Preparation of CDMPC-coated APS phase

Hypersil APS (Batch 3156, 3.0 g, 5 μ m) was refluxed for 30 minutes in THF (60 mL). CDMPC-2 (0.75 g) was dissolved in THF(20 mL) and *N,N*-dimethylacetamide (2.22 mL). The carbamate solution was added to the PGC and placed on a rotary evaporator in a baffled flask to aid mixing of the two solutions. A light vacuum is applied to the baffled flask for 1 hour. The temperature is raised to 35-40 $^{\circ}$ C, the solvents are therefore removed to yield a white powder. To removed all traces on *N,N*-dimethylacetamide the baffled flask is attached to a vacuum pump for 3 hours.

6.3.2 Preparation of CDMPC-coated PGC phases

PGC(1.1 g, 5 μ m particle diameter) was weighed in to a baffled flask and refluxed in THF (30 mL). CDMPC was stirred in THF until the carbamate had dissolved.

The CDMPC solution was added to the PGC, the solvents were then slowly removed *in vacuo*. The exact quantities are shown in table 6.3.

Batch coating

The carbamate solution was divided into five equal portions. One portion was added to the PGC and the solvents were removed *in vacuo*. When dryness was achieved the PGC was broken up and the next portion of CDMPC was added.

This process was repeated until all of the CDMPC solution had been added.

Single step coating

The carbamate solution is added in one portion to the PGC, the solvents are removed and the PGC processed as normal.

Table 6.3 Quantities used for the preparation of CDMPC phases

Sample	Coating method	Mass of CDMPC(g)	Mass of each portion(g)	% coating (w/w)
PGC-1	Batch	0.40	0.08	25
PGC-2	Single-step	0.40	-	25
PGC-3	Batch	0.514	0.171	30

6.3.3 Packing procedures

The coated PGC sample (1.1 g) was slurried in hexane/2-propanol (1:1 v/v, 30 mL) and was sonicated for 3 minutes. The Haskel 780-3 column packer was

purged with packing solvent (hexane/2-propanol, 80:20). The slurried solid was quickly added to the solvent reservoir (30 mL), which had been previously connected to the column packer. A HPLC column (100 mm x 4.6 mm i.d.) was connected to the top of the reservoir. The column was upward slurry packed at 8000-9000 psi. for 10 minutes or until approximately 150 mL of solvent had been passed. The column was then inverted and downward packed for the same amount of time or for the same volume of solvent. The pressure was then slowly released to atmosphere and the column could be removed from the packer. A 1-2 cm sample plug of CDMPC-PGC was retained in the solvent reservoir which can be examined to determine the effects, if any, of the packing procedure on the characteristics of the CDMPC-PGC. The columns are equilibrated with hexane/2-propanol (90:10 v/v) for 24 hours at 0.5 mL/min.

6.4 GEL PERMEATION CHROMATOGRAPHY (GPC)

GPC was carried out to establish the molecular weight distribution of the sample with reference to a known standard. The system in this case was calibrated by a series of standard Polymethylmethacrylate samples supplied by Polymer Laboratories.

The instrument used was a dual piston HPLC pump (ICI instruments LC 1110) with a refractive index detector (ICI instruments LC 1240). The guard column used was a Polymer Laboratories 5 μ m (5.0 x 7.5 mm) and a main column of Polymer Laboratories mixed E phase 3 μ m (300 x 7.5 mm). The samples were prepared in THF with 0.1 % toluene as a flow marker. The results are shown in Chapter 2, Table 2.0.1.

6.5 DETERMINATION OF PARTICLE SIZE

As discussed in Chapter 2 particle size was determined by both laser light scattering and scanning electron microscopy.

Laser light scattering was carried out using a Malvern Mastersizer X. A control measurement was taken using HPLC grade methanol. The sample was sonicated in HPLC grade methanol with sodium diphosphate added as a dispersant. The optimum concentration of sample was found to be 3 mg/mL. The slurry was pipetted into the test cell until the obscuration measurement was in the normal range and a measurement was taken. The results can be seen in table 6.4.

Table 6.4 Results from laser light scattering

Sample	Carbamate loading (% w/w)	Mean particle size (μm)	Observed particle size distribution
CDMPC-PGC-1	25 (Batch coating)	13.35	bimodal, very wide distribution
CDMPC-PGC-2	25 (Single-step coating)	20.70	bimodal, less broad distribution than CDMPC-PCG-1

Scanning electron microscopy(SEM)

The work here was carried out in the Department of Physics, University of Warwick, using a Cambridge Instruments Stereoscan S250 Mk3. The sample was held on an aluminium sample stub and was sputter coated with gold to improve detection.

The results can be seen in chapter 2, section 2.1.4.

6.6 CHROMATOGRAPHIC EVALUATION OF CDMPC-COATED PHASES

All separations in this thesis was carried out on a system consisting of a Waters 510 pump, a Pye Unicam UV detector, Rheodyne 7125 injector with a 10 μ l loop and a J Instruments CR650 chart recorder.

All the separations were carried out at ambient temperature using the conditions decreased with each experiment. A suitable wavelength was chosen for the detection of each analyte. This was usually 254 nm, unless an alternative wavelength was chosen. The mobile phase was filtered through a porous glass filter (grade 2) then degassed by sonicating under vacuum for 5 minutes before use. The dead time (t_0) of the column was determined by addition of 1,3,5-tri-*tert*-butylbenzene in normal phase and acetone in reversed-phase conditions.

6.7 SYNTHESIS OF POLY-L-LEUCINE

L-leucine used was purchased from Lancaster, δ_H (250 MHz; D₂O; NaOD) 1.19-1.23 (6 H, m, 2-CH₃), 1.69-2.02 (4 H, m, 2-CH and CH₂), 3.67-3.72 (1H, m, NH₂).

Anhydrous conditions

When anhydrous conditions are required the reaction was carried out using a Schlenk line attached to nitrogen and vacuum. The glassware used was flame dried under alternate vacuum then nitrogen atmosphere to remove all surface bound water and oxygen.

6.7.1 Synthesis of *N*-carboxy anhydride L-leucine (NCA L-leucine)

This procedure was described by Katakai and Iizuka⁸².

This reaction was carried out under anhydrous conditions. The reaction was put under an inert atmosphere which all excesses gases being passed through water.

The whole apparatus was set up in a fume cupboard.

L-leucine (6.1 g, 0.054 mol) and activated charcoal (0.2 g) were suspended in THF (60 mL). To the suspension was added trichloromethyl chloroformate (TCF) (15 g, 0.076 mol, 40 % excess). The reaction temperature was gently increased to 55 °C. When this temperature was reached the amino acid dissolved to produce a yellow/green solution. The solution was left at this temperature and stirred for 2 hours. Remaining in the fume cupboard, the solution was then filtered through celite. The filtrate was reduced *in vacuo* at 30 °C to a yellow oil. The product was obtained from this oil as the ice-cold hexane(60 mL) insoluble fraction. L-leucine NCA was recrystallised twice from diethyl ether/hexane (1:1, 20 mL), this yielded a highly crystalline white product (7.1 g, 0.0496 mol, 91.9 %). mp = 76.7 °C (lit., = 76-77 °C); IR(KBr) $\nu_{\text{max}}/\text{cm}^{-1}$ 3297.6, 1831.6, 1754.1, 1458.6; δ_{H} (250MHz, CDCl₃) 0.96 (6H, t, 2-CH₃), 1.74 (4H, m, CH and CH₂), 4.35 (1H, m, NH).

6.7.2 Polymerisation of L-leucine NCA using the humidity cabinet

The humidity cabinet used in this process was a modified desiccator. The base of the desiccator was filled with distilled water. The top of the desiccator was connected to a supply of compressed air with had been previously bubbled through water.

L-leucine NCA (7.1 g, 0.0496 mol) was placed on a watch glass then placed in the modified desiccator for 3 days. Poly-L-leucine was recovered as a white powder (6.5 g). The poly-L-leucine was then washed with diethyl ether (40 mL) to remove any unreacted L-leucine NCA, this yielded poly-L-leucine (6.3 g). mp = > 250°C decomp., IR(KBr) $\nu_{\text{max}}/\text{cm}^{-1}$ 3287.0, 1655.3, 1461.5; Found: C, 61.68; H, 9.63; N, 11.98. Calc. for $(\text{C}_6\text{N}_1\text{O}_1\text{H}_{11})_x$: C, 63.12; N, 12.38; H, 9.73; δ_{H} (250MHz, CDCl_3) 1.19-0.95 (m, br, CH_3), 1.82-1.73 (m, br, CH_2 and CH) 4.58-4.87 (m, br, NH).

6.7.3 Polymerisation of L-leucine NCA *via* amine initiation

This reaction was carried out in a fume cupboard using anhydrous conditions. L-leucine NCA (2.50 g, 15.92 mmol) was stirred in anhydrous dichloromethane. In another flask ethylenediamine (8.89 mL, 0.133 mmol) and triethylaluminium (0.07 mL, 0.133 mmol) were mixed in anhydrous toluene (10 mL). The L-leucine NCA solution was slowly added to the initiator/catalyst solution, on addition the solution became opaque white. The reaction was stirred overnight. The solvents were removed *in vacuo* to yield a white solid. Poly-L-leucine was washed with toluene (3 x 10 mL), then dried over P_2O_5 overnight. Poly-L-leucine was recovered as a white powder (1.98 g). mp = > 250 °C decomp. Found: C, 63.21; H, 9.62; N, 12.26. Calc. for $(\text{C}_6\text{N}_1\text{O}_1\text{H}_{11})_x$: C, 63.12; N, 12.38; H, 9.73; δ_{H} (250MHz, CDCl_3) 0.83-0.95 (m, br, CH_3), 1.18-1.32 (m, br, CH_2), 1.55-1.58 (m, br, CH) 3.46-3.74 (m, br, NH).

6.7.4 Polymerisation of L-leucine

LiCl (1.0 g) and poly-vinylpyrrolidone (1.0 g, molecular weight = 3.6×10^5) were dissolved in *N*-methyl pyrrolidine (30 mL). L-leucine (1.13 g, 0.01 mol) and triphenylphosphite (3.1 g, 0.01 mol) were added to this solution with stirring. The solution was heated to 80°C and left to stir for 8 hours. The solvent was removed *in vacuo* to yield poly-L-leucine as a pale yellow solid. Poly-L-leucine was washed in boiling methanol/water (1:1 v/v, 50 mL) for 1 hour, this was followed by 1 hour washing in boiling water (50 mL). The polymer was recovered by centrifugation as a white/yellow solid product (0.96 g), mp = >250 °C, Found: C, 63.21; H, 9.62; N, 12.26. Calc. for $(C_6N_1O_1H_{11})_x$: C, 61.12; N, 10.18; H, 9.33; δ_H (250MHz, CDCl₃) 0.80-0.89 (m, br, CH₃), 1.05-1.12 (m, br, CH₂), 1.32-1.40 (m, br, CH) 3.76-3.94 (m, br, NH).

6.7.6 Continuous extraction of poly-L-leucine

Poly-L-leucine (2.0 g) (section 6.7.2) was extracted using the soxhlet extraction technique. The solvent used was DMF/ethanol (5:1 v/v, 150 mL). The sample was extracted for 48 hours. The solvent was dried *in vacuo* to yield a solid white product (0.4912 g). The extracted sample was a fine white powder (1.48 9g, 74.5 % yield by weight). Found: C, 63.70; H, 9.71; N, 12.39. Calc. for $(C_6N_1O_1H_{11})_x$: C, 63.12; N, 12.38; H, 9.73.

6.8 SOLID PHASE SYNTHESIS OF H.LEU₁₅.OH

When anhydrous conditions were required the glassware was oven dried at 250°C, then purged with argon. An inert atmosphere of argon was maintained throughout the reaction.

All reagents were purchased from Novabiochem and were used without further purification, with the exception of hydroxybenzotriazole (HOBt). HOBt was purchased from Lancaster and was recrystallised to constant

6.8.1 Functionalisation of the resin

This reaction was carried out under inert conditions.

Fmoc.Leu.OH (0.565 g, 1.6 mmol) was dissolved in anhydrous dichloromethane (20 mL) and dimethylformamide(DMF) (1.0 mL). This solution was added to 2-chlorotrityl chloride resin(2.011 g) with diisopropylethyl amine(DIEA) (3.44 g, 0.46 mL, 1.32 mmol) in anhydrous dichloromethane (20 mL). The reaction was left to stir for 5 minutes. Diisopropylethyl amine in dichloromethane(CH_2Cl_2) (1:1 v/v, 0.92 mL) was added to the reaction, resulting in the liberation of white fumes of HCl. The reaction was left to stir for a further 20 minutes. Excess methanol (4 mL) was added and the reaction was left to stand for a further 10 minutes.

6.8.2 Washing procedure

This procedure is used after every coupling step and uses alternate solvents which swell the resin then cause it to contract (Table 6.8.2). This promotes thorough washing of the resin and removal of all excess reagents.

The resin is washed with the following solvents, after each washing step the solvent is removed with vacuum.

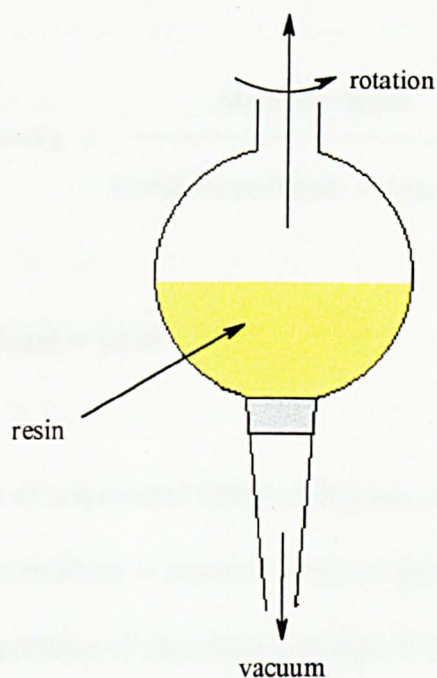
Table 6.8.2 Standard washing procedure

Solvent	Repetitions	Volume per repetitions (mL)
dichloromethane	3	10
dimethylformamide	2	10
2-propanol	2	5
dimethylformamide	2	5
2-propanol	2	5
methanol	2	5
diethyl ether	2	5

6.8.3 Equipment used in SPPS

The glassware used in these reactions was designed to allow all the processes to be carried out without the resin having to be transferred between vessels. The glassware shown in figure 6.8.3 was designed by Dr B Ridge and was made in-house in the Department of Chemistry, University of Exeter.

Figure 6.8.3 Glassware used in SPPS



6.8.4 Ultra-violet monitoring of Fmoc residue

Three silica UV-cells were used to record the UV absorbance of the sample at $\lambda = 290\text{nm}$ (Table 6.8.4).

Table 6.8.4 UV monitor for Fmoc residue

UV cell	1	2	3
Contents	Blank	1mg of resin	1 mg of resin

Washed resin (1 mg) is placed in a clean, dry silica UV cell. A solution of 20% piperidine in anhydrous dimethylformamide (3 mL) is added to each cell. The UV absorbance at 290nm was recorded. Using equation 6.8.4.1 the absorbance data

can be used to calculate the concentration (mmol/g) of Fmoc residues present and therefore assay the level of derivatisation.

Equation 6.8.4.1 Assay of Fmoc derivatisation

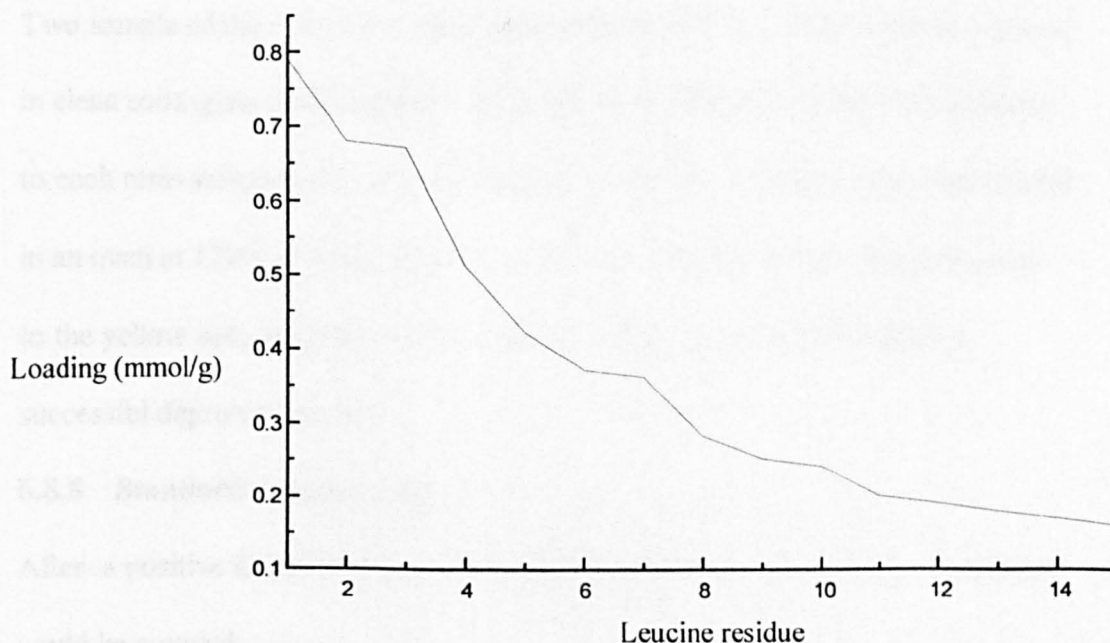
$$[\text{Fmoc residues}] \text{ mmol/g} = \frac{\text{Mean absorbance}}{\text{Extinction coefficient} \times \text{Mean mass of sample(g)}}$$

where Extinction coefficient = 1650

6.8.5 Loading profile of sequential SPPS of H.Leu₁₅.OH

Using the assay of Fmoc residues to monitor every coupling step a graph can be plotted to show the progression of the reaction (Graph 6.8.5).

Graph 6.8.5 Fmoc assay of sequential synthesis of H.Leu₁₅.OH



As is expected the loading decreases as the reaction proceed. This is due to incomplete coupling or deprotection steps which are inevitable.

6.8.6 Deprotection of tethered peptide to produce free amine residue

After the first coupling the resin was dried at 50°C overnight, however this is the only coupling which required this step. A solution of 5% piperidine in DMF/ CH_2Cl_2 (1:1 v/v, 20 mL) was added to the resin and mixed for 20 minutes. The resin was filtered to remove the solution. A solution of 20% piperidine in DMF (20 mL) was added to the resin and mixed for 10 minutes then removed. This step was repeated, the resin was then washed. To test that this deprotection step was successful a sample of the resin was tested using the Kaiser test.

6.8.7 Kaiser test

Three stock solutions were produced; Ninhydrin in ethanol (5 g in 100 mL), phenol in ethanol (80 g in 20 mL) and aqueous potassium cyanide (2 mL, 0.001 M in 100 mL).

Two sample of the resin were taken (approximately 10-20 grains each) and placed in clean soda-glass ignition tubes. Three drops of each stock solution was added to each resin sample and to a empty tube as a control. All three tubes were placed in an oven at 120°C for five minutes. A dark blue/purple colour change relative to the yellow colour of the control indicates a positive test and therefore a successful deprotection step.

6.8.8 Standard coupling step

After a positive Kaiser test had been observed the second Fmoc.Leu.OH residue could be coupled.

Fmoc.Leu.OH (1.61 g, 4.56 mmol) was dissolved in DMF(5 mL), this solution was added to a solution of 1-hydroxybenzotriazole (HOBt)(0.615 g, 4.56 mmol) and 2-(1H-benzotriazole-1-yl)-1,1,3,3-tetramethyluronium hexafluorophosphate

(HBTU)(1.73 g, 4.56 mmol) in DMF (10 mL). DIEA (1.59 mL, 9.12 mmol) is added to activate the mixture. This reaction is left stirring for 3.5 hours at ambient temperature.

6.8.9 Problem coupling steps

Coupling of the seventh residue

Fmoc.Leu.OH (5.43 g, 15.4 mmol) in DMF (5 mL) was added to a solution of HBTU (5.399 g, 14.2 mmol) and HOBt (2.067 g, 15.3 mmol) in DMF (20 mL). DIEA (5.29 mL, 40.9 mmol) was added to the reaction. The reaction was allowed to proceed for 3.5 hours. The Kaiser test was positive. The reaction was heated to 35°C and left to stir overnight. The resin was then filtered and washed. The Kaiser test was negative.

Coupling of the tenth residue

Standard coupling procedure was carried out, however a positive Kaiser test suggested that the coupling of the tenth residue was unsuccessful. The standard coupling procedure was repeated at 40°C for 12 hours. The Kaiser test was however, still positive.

Fmoc.Leu.OH (5.43 g, 15.4 mmol) in DMF (20 mL) was added to a solution of HOBt (2.07 g, 15.3 mmol) and HBTU (5.77 g, 15.3 mmol) in DMF (20 mL). This solution was activated by the addition of DIEA (5.30 mL, 40.1 mmol). The reaction was heated to 40°C and left stirring for 12 hours. The Kaiser test of this resin was negative.

Coupling of the eleventh residue

Standard coupling procedure was attempted this however, yielded a positive Kaiser test. O-(7-aza-benzotriazole-1-yl)-1,1,3,3-bis(tetramethylene) uronium hexafluorophosphate (HAPyU) (0.66 g, 1.52 mmol) in DMF (10 mL) was added to the resin. DIEA (0.146 mL, 0.84 mmol) was added to the reaction. The reaction was heated to 35°C and left to stir for 12 hours. The Kaiser test was slightly positive.

The reaction liquor was very dark brown in colour, the resin was filtered to remove the discoloured supernatant. Fmoc.Leu.OH (594 mg, 1.68 mmol) in DMF (2 mL) was added to a solution of HBTU (637 mg, 1.68 mmol) and HOBt (227 mg, 1.68 mmol) in DMF (10 mL). DIEA (0.29 mL, 1.68 mmol) and HAPyU (265 mg, 1.68 mmol) were added to the final solution. The reaction was left to stir for 12 hours. The resin was washed twice using the standard washing procedure and gave a negative Kaiser test.

The remaining coupling steps were carried out using the standard coupling procedure described in section 6.8.8. In each step the amounts of reagents used had been corrected for the UV assay obtained for the eleventh residue;

Fmoc.Leu.OH (602 mg, 1.68 mmol), HBTU (637 mg, 1.68 mmol), HOBt (227 mg, 1.68 mmol) and DIEA (0.29 mL, 1.68 mmol).

6.8.10 Cleavage of the peptide from the resin

After the coupling of the fifteenth residue had been confirmed by a negative Kaiser test result the resin was washed using the standard washing procedure.

The resin was placed in a vacuum oven at 50°C for 12 hours. The dry resin (2.853 g) was deprotected in the usual way (section 6.8.6). The resin (2.853 g)

was placed in a clean dry flask to which was added anhydrous CH_2Cl_2 /trifluoroethanol/acetic acid (3:1:1 v/v, 20 mL). The reaction was left to stir at ambient temperature for two hours. The resin was filtered and the filtrate was reserved. The resin was then washed with fresh anhydrous CH_2Cl_2 /trifluoroethanol/acetic acid (3:1:1 v/v, 10 mL) which was also collected. Water (HPLC grade, 10 mL) was added to the combined filtrates. The CH_2Cl_2 was removed *in vacuo*. Poly-L-leucine was formed as a white precipitate. Water (2 mL) and trifluoroacetic acid (3 mL) were added and the precipitate was taken into solution. The sample was lyophilised to yield poly-L-leucine as a fine white powder (0.985 g); ESI-MS, 1715.3, 1371.9, 1149.7

6.9 SYNTHESIS OF H.LEU₁₅.OH USING PENTA-PEPTIDE COUPLING

6.9.1 Synthesis of penta-peptide

The synthesis of the penta-peptide was carried out using the same methods as described for the sequential synthesis. After the initial derivatisation of the resin (2.0 g) with the first Fmoc.Leu.OH (0.565 g, 1.6 mmol) residue the loading was determined to be 0.59 mmol/g. Fmoc.Leu.OH (1.25 g, 3.54 mmol) was dissolved in DMF (5 mL). This solution was added to HOBt (0.478 g, 3.54 mmol) and HBTU (1.34 g, 3.54 mmol) in DMF (10 mL). DIEA (1.23 mL, 7.08 mmol) was added to the final solution, which was allowed to stir at ambient temperature for 3.5 hours. After the successful coupling of the fifth residue the resin was dried in a vacuum oven at 65°C for 12 hours to yield dry resin (2.93 g).

6.9.2 Cleavage of the penta-peptide from the resin

DMF/trifluoroethanol/acetic acid (3:1:1 v/v, 40 mL) was added to the dry resin (2.51 g) in a clean dry flask. The reaction was vigorously stirred for 45 minutes.

The resin was then filtered and washed thoroughly with DMF/trifluoroethanol/acetic acid (3:1:1 v/v, 20 mL). Water (HPLC grade, 30 mL) was added to the combined filtrate. The filtrate was lyophilised to yield a fine white powder, Fmoc.leu₅.OH (709 mg, 0.88 mmol,); ESI-MS (H⁺), *m/z* 584.7 (M⁺, 100 %), 433.6 (23); MALDI-TOF-MS (Na⁺), *m/z* 606.7 (M⁺, 96%).

6.9.3 Thin layer chromatography (TLC) of Fmoc.leu₅.OH

Of all the peptides synthesised only Fmoc.leu₅.OH is sufficiently soluble to be examined using TLC.

The sample was eluted using *N*-butanol/pyridine/distilled water (20:10:1, 10mL).

Two spots were observed, however, it was established that only spot A was peptide and spot B was DIEA contamination (Table 6.9.3)

Table 6.9.3 TLC analysis of Fmoc.leu₅.OH

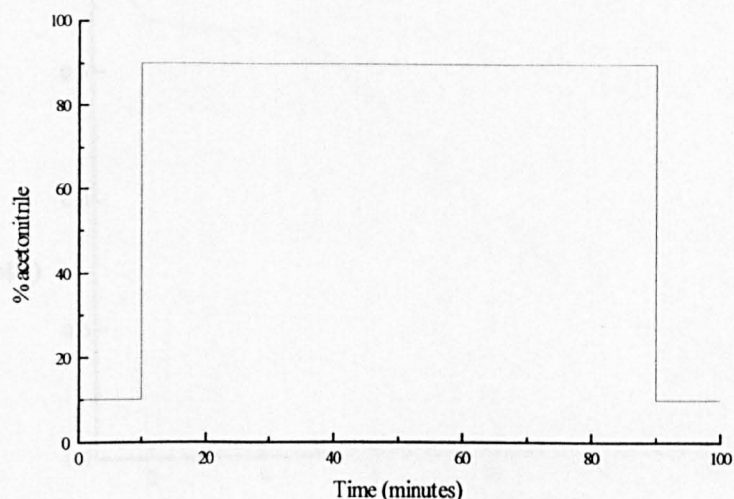
Spot	R _f value	Visualising method
A	0.81	Cl chamber followed by starch/KI spray
B	0.06	ninhydrin

Purity of Fmoc.leu₅.OH by TLC = 100%

6.9.4 Analysis of Fmoc.leu₅.OH by reversed-phase HPLC

The sample was eluted using a reversed-phase gradient. Figure 6.9.4 shows the change in percentage acetonitrile changing with time. The total mobile phase was acetonitrile/water (x%, 100 - x%) + 0.1% trifluoroacetic acid.

Figure 6.9.4 Schematic describing gradient elution for Fmoc.leu₅.OH



Column: Hypersil 5 μ C₁₈ BDS, 250 x 4.6mm.

Flow rate : 0.5ml/min

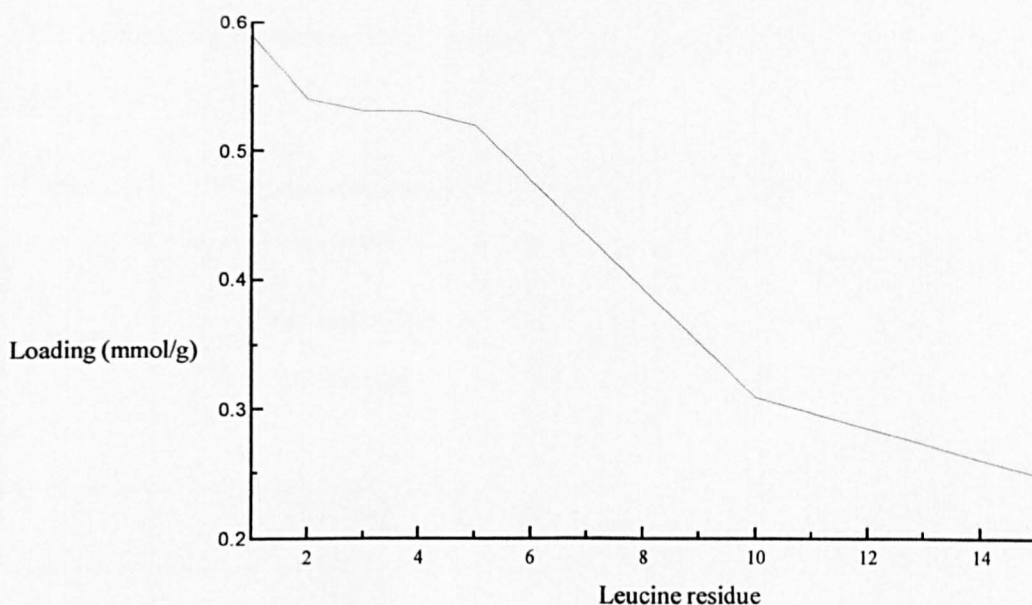
Retention time : 57.3 mins

Fmoc.leu₅.OH was found to be 89% pure by HPLC.

6.9.5 Coupling of penta-peptides

Resin (0.165 g) was swollen using DMF (10 mL). Fmoc.Leu₅.OH (354 mg, 0.44 mmol) was dissolved in DMF (5 mL). This solution was added to HOBT (59 mg, 0.44 mmol) and HBTU (167 mg, 0.44 mol) in DMF (10 mL). DIEA (0.076 mL, 0.88 mmol) was added to the final solution. The reaction was allowed to stir at ambient temperature for 3.5 hours. The resin gave a negative Kaiser test. The resin was prepared for the next coupling in the usual manner. The third penta peptide was coupled to the tethered peptide using the same method described earlier in this section.

6.9.6 Fmoc assay of block coupling synthesis of H.Leu₁₅.OH



9.6.7 Preparation of H.Leu₁₅.OH from the resin

The peptide was deprotected in the usual manner. The resin (2.67 g) was dried overnight in a vacuum oven at 50 °C. The dry resin (2.34 g) was cleaved from the resin using the standard procedure as previously described. After lyophilisation the peptide (0.562 g) is obtained as a fine white powder; Found, C, 63.04; H, 9.75; N 12.26. Calc. for C₉₀N₁₅O₁₆H₁₆₇ : C, 63.02; N, 12.26; H, 9.75. Purification of this peptide was attempted using Sephadex LH-20 and Biobeads. The differences between the peptides was not great enough to effect any significant separation. It was therefore, not possible to carry out an efficient preparative separation. The peptides were used unpurified.

9.6.8 Circular dichroism (CD)

This analysis was carried out on a Jasco J-150 spectropolarimeter under the supervision of Dr A Rodger, University of Warwick. The instrument was set-up using the parameters shown in table 9.6.8.

column was equilibrated for 24 hours at 0.5 mL/min(acetonitrile:water, 90:10 v/v)

The component masses used to produce a particular column as shown in Figure 6.7.

Figure 6.7 Poly-L-leucine on PGC packing materials

Column	Mass of Poly-L-leucine(g)	Mass of PGC (g)	Column length (mm)
A	0.1084*	1.1	100
B	0.2510*	1.1	100
C	0.7558*	3.05	250
D	0.2561 [⊗]	1.07	100
E	0.272*	1.09	100

* denotes poly-L-leucine synthesised through amine initiation (section 6.7.3)

* denotes poly-L-leucine synthesised from L-leucine NCA in humidity cabinet (section 6.7.2)

[⊗] denotes poly-L-leucine synthesised from L-leucine NCA in humidity cabinet after continuous extraction (section 6.7.6)

* denotes H.Leu₁₅.OH (section 6.9)

6.7.1 Microanalysis of PGC-Poly-L-leucine phases

Microanalysis allows us to make an assessment of the loading of poly-L-leucine (Table 6.7.1).

Table 6.7.1 Microanalysis of PGC-Poly-L-leucine phases

Column	%Carbon	%Hydrogen	%Nitrogen	% w/w loading
PGC	99.84	-	-	-
A	87.84	0.95	1.15	10
B	84.93	2.02	2.61	20
C	85.05	2.03	2.59	20
D	84.99	1.94	2.39	20
E	85.10	1.95	2.43	20

6.7.2 Synthesis of racemic epoxides

Toluene (4.7 mL/mmol of substrate) was added to a solution of NaOH (12 equiv.) in distilled water (0.5 mL/mmol of substrate) at 0°C. EDTA (0.0025 equiv.), the enone (1 equiv.) and Aliquat 336 (0.1 equiv.) were added to the mixture. 30% aqueous H₂O₂ (21 equiv.) was added dropwise to the mixture with stirring at ambient temperature. The reaction was followed using TLC (ethanol/chloroform/pet. ether, 2:5:93v/v) which was visualised using phosphomolybdic acid in ethanol (20% v/v). The final reaction was diluted with diethyl ether (10 mL) and the aqueous phase was extracted with diethyl ether (3 x 10 mL). The combined organic phase was washed with water (10 mL), brine (10 mL) then dried over magnesium sulphate. The solution was reduced *in vacuo*, then further purified by recrystallisation from diethyl ether/hexane (50:50 v/v).

(±)-2,3-epoxycyclohexanone⁷⁹

2-Methyl 1,4-naphthoquinone (1.23 g, 7.5 mmol), 30% H₂O₂ (5.36 g, 0.158 mol), reaction time = 72 hours, (±)-2,3-epoxycyclohexanone (0.95 g, 5.05 mmol, 67.3

% yield); mp 95.8 °C (from diethyl ether/hexane) (lit., 96 °C); δ_{H} (250MHz, CDCl_3) 8.00 - 7.72 (4H, m, phenyl), 3.85 (1H, s, CH), 1.72 (3H, s, CH_3).

***trans*-4-phenylbut-2-ene-1,4-dione¹⁰³**

trans-1,2-dibenzoyl-ethylene (3.0 g, 12.7 mmol), 30% H_2O_2 (9.07 g, 0.267 mol), reaction time = 72 hours, (1.92 g, 7.61 mmol, 59.9 %); mp 121.2 °C (from diethyl ether/hexane) (lit., 121-123 °C); δ_{H} (250MHz, CDCl_3) 7.28-7.38 (10H, m, phenyl), 4.5 (1H, d, J 1.6, 1-*H*); δ_{C} (62.9MHz, CDCl_3) 136.1 (2-CO), 129.3 (phenyl), 129.0(phenyl), 126.3(phenyl), 124.1(phenyl), 67.3 (CH).

6.7.3 Synthesis of bis-(3-phenyl-oxiranyl)-methanone¹⁰⁴

This reaction was carried out using standard anhydrous conditions.

Dibenzylideneacetone (1.0 g, 4.3 mmol) was dissolved in anhydrous THF (20 mL). Urea. H_2O_2 (0.956 g, 10.16 mmol) and 1,8-diazabicyclo[5.4.0]octane (DBU) (1.28 mL, 8.6 mmol) were dissolved in anhydrous THF (20 mL) and added to the dibenzylideneacetone solution. The solution was stirred under an inert atmosphere at ambient temperature for 48 hours. The reaction was followed using TLC (ethanol/chloroform/pet. ether, 2:5:93 v/v) which was visualised using phosphomolybdic acid in ethanol (20% v/v); R_f = 0.17. Distilled water (10 mL) was added to the reaction mixture. The reaction was extracted by toluene (3 x 10 mL). The organic extract was dried over magnesium sulphate and reduced *in vacuo* to yield an oil. The oil was placed in the refrigerator overnight. The resulting crystals were washed with ice cold ethanol (2 x 5 mL) to yield a

crystalline product (0.681 g, 2.5 mmol, 60.5% yield); mp 119 °C; δ_{H} (250MHz, CDCl_3) 7.28-7.38 (10H, m, phenyl), 4.18 (1H in minor product, d, J 1.59, 1- H), 4.1 (1H, d, J 1.5, 1- H), 3.72 (1H in minor product, d, J 1.60, 1- H), 3.81 (1H, d, J 1.5, 1- H); δ_{C} (62.9MHz, CDCl_3) 134.9 (CO), 129.6 (phenyl), 129.1(phenyl), 126.1(phenyl), 124.2(phenyl), 61.3 (CH), 59.36 (CH).

References

- 1 L.Pasteur, *Comptes Rendus de l'Academie des Sciences*, 1848, **26**, 535.
- 2 J.H. Van't Hoff, *Arch. Netherlands Sci. Extracts et Naturelles*, 1874, **9**, 445.
- 3 S.J. Angyal, *Angewantde Chemie*, 1969, **8**,157.
- 4 R.B. Herbert, *Natural Product Reports*, 1992, **9**, 507.
- 5 G. Blaschke, H.P. Kraft, K. Fickentscher and F. Kohler, *Arzeim.-Forsch.*,1979, **29**, 1640.
- 6 R.S. Cahn, Sir C. Ingold and V. Prelog, *Angew. Chem. Int. Ed. Engl.*, 1966, **5**, 385.
- 7 A. Piutti, *C.R. Hebd. Seances Acad. Sci.*, 1886,**103**,134.
- 8 E.L. Eliel and S. H. Wilen, *Stereochemistry of Organic Compounds*, Chapter 6-4, Wiley, 1994.
- 9 G. Blashke, H.P. Kraft, H. Markgraf, *Chem. Ber.*, 1980, **113** , 2318.
- 10 R.J. Baczuk, G.K. Landram, R.J. Dubois and H. C. Dehm, *J. Chromatogr.*, 1971, **60**, 351.
- 11 S. Loftler, R. Stadler, N. Nagakura and M.H. Zenk, *J. Chem. Soc., Chem. Commun.*, 1987, 1160.
- 12 R.H. Mazur, J.M. Schlatter and A.H. Goldkamp, *J. Am. Chem. Soc.*, 1969, **91**, 2684.
- 13 T.G. Burlingame and W.H. Pirkle, *J. Am. Chem. Soc.*, 1966, **88**, 4294.
- 14 G.M. Whitesides and D. W. Lewis, *J. Am. Chem. Soc.*, 1970, **92**, 6979.
- 15 M.S. Tswett, *Bull. Lab. Bot. Gen., Univ. Geneve.*, 1896, **1**, 123.
- 16 R. Kuhn and E. Lederer, *Ber. Deut. Chem. Ges.*,1931, **61**, 1349.
- 17 J.J.Kirkland and L.R. Snyder, *Introduction to Modern Liquid Chromatography*, 2nd Ed., New York: Wiley, 1979.
- 18 K.K. Unger, Porous Silica, *J. Chromatogr. Library*, **16**, Elsevier, 1979.
- 19 M.T. Gilbert, J.H. Knox and B. Kaur, *Chromatogr.*, 1982, **16**, 138.
- 20 Mr Paul Ross, Hypersil, oral communication and company literature

- 21 J. Hermansson, K. Strom and R. Sandberg, *J. Chromatogr.*, 1987, **407**, 217.
- 22 J. Zukowski, D. Sybilska, J. Bojarski and J. Szejtli, *J. Chromatogr.*, 1988, **436**, 381.
- 23 C.E. Dalglish, *J. Biochem.*, 1952, **52**, 3.
- 24 C.E. Dalglish, *J. Chem. Soc.*, 1952, 3940.
- 25 G. Karagounis and G. Coumoulos, *Nature*, 1938, **142**, 162.
- 26 G.M. Henderson and H.G. Rule, *Nature*, 1938, **141**, 917.
- 27 W.H. Pirkle and T.C. Pochapsky, *Chem. Rev.*, 1989, **89**, 347.
- 28 V.A. Davankov, *Adv. Chromatogr.*, 1980, **18**, 139.
- 29 E. Gil-Av, F. Mikes and G. Boshart, *J. Chromatogr.*, 1988, **450**, 205.
- 30 W.H. Pirkle and J.R. Hauske, *J. Org. Chem.*, 1976, **41**, 801.
- 31 W.H. Pirkle and M.H. Hyun, *J. Org. Chem.*, 1984, **49**, 3043.
- 32 W.H. Pirkle and M.H. Hyun, *J. Chromatogr.*, 1985, **322**, 287.
- 33 G. Dotsevi, Y. Sogah and D.J. Cram, *J. Am. Chem. Soc.*, 1975, **97**, 1259.
- 34 D.W. Armstrong and W. DeMond, *J. Chromatogr. Sci.*, 1984, **22**, 411.
- 35 S. Thelohan, P. Jadaud and I.W. Wainer, *Chromatographia*, 1989, **28**, 551.
- 36 Y. Okamoto, S. Honda, K. Hatada and H. Yuki, *J. Chromatogr.*, 1985, **350**, 127.
- 37 G. Blaschke, W. Broker and W. Fraenkel, *Angew. Chem. Int. Ed.*, 1986, **25**, 830.
- 38 M. Huffer and P. Schreier, *J. Chromatogr.*, 1989, **469**, 137.
- 39 I.W. Wainer and Y.Q. Chu, *J. Chromatogr.*, 1988, **455**, 316.
- 40 G. Schill, I.W. Wainer and S. Barkan, *J. Chromatogr.*, 1986, **365**, 73.
- 41 D.M. Johns, *Chiral Liquid Chromatography*, Blackie and Sons, Glasgow, 1989.
- 42 G. Hesse and R. Hagel, *Chromatographia*, 1973, **6**, 277.

- 43 G. Hesse and R. Hagel, *Liebigs Ann. Chem.*, 1976, 966.
- 44 Y. Okamoto, M. Kawashima, K. Hatada and K. Yamamoto, *Chem. Lett.*, 1984, 739.
- 45 Y. Okamoto, R. Aburatani, R. Kawashima, M. Hatada and N. Okamura, *Chem. Lett.*, 1987, **386**, 95.
- 46 T. Shibata, I. Okamoto and K. Ishii, *J. Liq. Chromatogr.*, 1986, **9**, 313.
- 47 I.W. Wainer and M.C. Alembik, *J. Chromatogr.*, 1986, **358**, 85.
- 48 I.W. Wainer, E. Smith and M.C. Alembik, *J. Chromatogr.*, 1987, **388**, 65.
- 49 E. Francotte and R.M. Wolf, *J. Chromatogr.*, 1992, **595**, 63.
- 50 Y. Okamoto, R. Aburatani, R. Kawashima, K. Hatada and N. Okamura, *Chem. Lett.*, 1986, 1767.
- 51 Y. Okamoto, H. Fukaya and E. Yashima, *J. Chromatogr.*, 1994, **677**, 11.
- 52 Y. Okamoto, R. Aburatani and K. Hatada, *J. Chromatogr.*, 1987, **389**, 95.
- 53 E. Yashima, M. Yamada, Y. Kaida and Y. Okamoto, *J. Chromatogr.*, 1995, **694**, 347.
- 54 U. Zogt and P. Zugenmaier, *Ber. Bunsenges. Phys. Chem.*, 1985, **89**, 1217.
- 55 S.J. Grieb, S.A. Matlin, A.M. Belenguer, H.J. Richie and P. Ross, *J. Chromatogr.*, 1995, **697**, 271.
- 56 T.D. Booth, W.J. Lough, M. Saeed, T.A.G. Noctor and I.W. Wainer, *Chirality*, 1997, **9**, 173.
- 57 T.D. Booth, D. Wahnnon and I.W. Wainer, *Chirality*, 1997, **9**, 96.
- 58 Q.H. Wan, P.N. Shaw, M.C. Davies and D.A. Barrett, *J. Chromatogr.*, 1995, **697**, 219.
- 59 J.H. Knox, B. Kaur and G.R. Millward, *J. Chromatogr.*, 1986, **352**, 3.
- 60 B.J. Bassler, R. Kaliszan and R.A. Hartwick, *J. Chromatogr.*, 1989, **461**, 139.
- 61 J.H. Knox and Q.H. Wan, *Chromatographia*, 1995, **40**, 9.
- 62 M. Jofesson, B. Carlsson and B. Norlander, *J. Chromatogr.*, 1994, **684**, 23.
- 63 A. Karlsson and C. Pettersson, *Chirality*, 1992, **4**, 323.

- 64 A. Karlsson and C. Pettersson, *J. Chromatogr.*, 1991, **543**, 287.
- 65 S.J. Grieb, PhD Thesis, University of Warwick, 1995.
- 66 S.M. Wilkins, D.R. Taylor and R.J. Smith, *J. Chromatogr.*, 1995, **697**, 587.
- 67 Y. Okamoto, M. Kawashima, R. Aburatani, K. Hatada, T. Nishiyama and M. Masuda, *Chem. Lett.*, 1986, 1237.
- 68 Y. Okamoto, R. Aburatani, K. Hatada, and Y. Kaida, *Chem. Lett.*, 1988, 1125.
- 69 C.K. Lim, *Biomedical Chromatography*, 1989, **3**, 1989.
- 70 C. Elfakir and M. Dreux, Institut de Chimie Organique et Analytique, Universite d'Orleans, France, Poster presentation, HPLC'97, Birmingham, UK.
- 71 W. Lindner, *Chemical Derivatisation in Analytical Chemistry*, **2**, 1982.
- 72 K.B. Sharpless, 1985, *Chem. Scr.*, **25**, Special Noble symposium 60 issue.
- 73 T. Katsuki and K.B. Sharpless, *J. Am. Chem. Soc.*, 1980, **102**, 5974.
- 74 S. Akabori, S. Sakuri, Y. Izumi and Y. Fijii, *Nature*, 1956, **178**, 323.
- 75 R.L. Beamer, R.H. Belding and C.S. Fickling, *J. Pharm. Sci.*, 1969, **58**, 1142.
- 76 S. Inoue, N. Ito and J. Oku, *Makromol. Chem.*, 1979, **180**, 1089.
- 77 S. Julia, J. Guixer, J. Masana, J. Rocas, S. Colonna, R. Annuziata and H. Molinari, *J. Chem. Soc. Perkin Trans I*, 1982, 1317.
- 78 H. Wynberg and J. S. Wiering, *Tetrahedron Lett.*, 1976, **21**, 1831.
- 79 S. Julia, S. Colonna, S. Banfi, J. Masana, A. Alvarez and H. Molinari, *Tetrahedron Lett.*, 1983, **39**, 1635.
- 80 J.R. Flisak, K.J. Gombatz, M.M. Holmes, A.A. Jarmas, I. Lantos, W.L. Mendelson, V.J. Novack, J.J. Remich and L. Snyder, *J. Org. Chem.*, 1993, **58**, 6247.
- 81 S.M. Roberts, W. Kroutil, P. Mayon, M.E. Lasterra-Sanchez, S.J. Maddrell, S. R. Thornton, C.J. Todd and M. Tuter, *Chem. Commun.*, 1996, 845.
- 82 R. Katakai and Y. Iizuka, *J. Org. Chem.*, 1985, **50**, 715.
- 83 F. Hagashi, K. Sano and H. Kakinoki, *J. Polym. Sci.*, 1980, **18**, 1841.
- 84 F. Hillenkamp, M. Karas, *Anal. Chem.*, 1988, **60**, 2229.

- 85 K. Tanaka, H. Waki, Y. Ido, S. Akita and Y. Yoshida, *Rapid Commun. Mass Spectrom.*, 1988, **2**, 51.
- 86 R. S. Brown and J.J. Lennon, *Anal. Chem.*, 1995, **67**, 3990.
- 87 M. Karas, U. Bahr and U. Gießmann, *Mass Spectrometry Reviews*, 1991, **10**, 335.
- 88 M. Dole, R.L. Hines, L.L. Mack, R.C. Modley, L.D. Ferguson and M.B. Alice, *J. Chem. Phys.*, 1968, **49**, 2240.
- 89 R.B. Merrifield, *J. Am. Chem. Soc.*, 1963, **85**, 2149.
- 90 K.S Lam, S.E. Salmon, E.M. Hersh, V.J. Hurby, W.M. Kazmierski and R.J. Knapp, *Nature*, 1991, **354**, 82.
- 91 L.A. Carpino and G.Y. Han, *J. Org. Chem.*, 1972, **37**, 3404.
- 92 S.S. Wang, *J. Am. Chem. Soc.*, 1973, **95**, 1328.
- 93 K. Barlos, O. Chatzi, D. Gatos and G. Stavropoulos, 1991, *Int. J. Pept. Protein Res.*, **37**, 513.
- 94 D.H. Rich, S.K. Gurwara, *J. Am. Chem. Soc.*, 1975, **97**, 1575.
- 95 E. Kaiser, R.L. Colescott, C.D. Bossinger and P.I. Cook, *Anal. Biochem.*, 1970, **34**, 595.
- 96 B. Ridge and M. Palmer, private discussion
- 97 A. Chakrabatty and R. Baldwin, *Adv. Protein Chem.*, 1995, **46**, 27.
- 98 B.H. Zimm and J.K. Bragg, *J. Chem. Phys.*, 1959, **31**, 526.
- 99 R. Lifson and A. Roig, *J. Chem. Phys.*, 1961, **34**, 1963.
- 100 C. Hirayama, H. Ihara and K. Tanaka, *J. Chromatogr.*, 1988, **450**, 271.
- 101 S. Itsuno, M. Sakakura and K. Ito, *J. Org. Chem.*, 1990, **55**, 6047.
- 102 P.A. Bentley, S. Bergergon, M.W. Cappi, D.E. Hibbs, M.B. Hursthouse, T.C Nugent, R. Pulido, S.M. Roberts and L.E. Wu, *Chem. Commun.*, 1997, 740.
- 103 W. Kroutil, M.E. Lasterra-Sanchez, S. J. Maddrell, P. Mayon, P. Morgan, S.M. Roberts, S.R. Thornton, C.J. Todd and M. Tuter, *J. Chem. Soc., Perkins Trans. 1*, 1996, 2837.

- 104 R. Annuziata, M. Benaglia, M. Cinquini, F. Cozzi and L. Raimondi,
Tetrahedron Lett., 35, 50,1994, 9481
- 105 R.E. Lutz and F.N. Wilder, *J. Am. Chem. Soc.*, 56, 1934, 1987